Periodic Pulsed Controllability with Applications to NMR

Thesis advisor

Navin Khaneja

Author

Philip D. Owrutsky

Periodic Pulsed Controllability with Applications to NMR

Abstract

In this thesis we study a class of problems that require simultaneously controlling a large number of dynamical systems, with varying system dynamics, using the same control signal. We call such problems *ensemble control problems,* as the goal is to simultaneously steer the entire ensemble of systems. These problems are motivated by many physical systems and we will be particularly interested in the manipulation of nuclear spins in Nuclear Magnetic Resonance (NMR) experiments. System dispersions arise from imprecise magnets for controls, or from disruptive intermolecular interactions. In all cases, the aim is to attenuate the aspects of the dynamics that correspond to noise or errors, while preserving the aspects that contain the quantities of interest. In liquid NMR experiments this could correspond to preserving Larmor frequency in the presence of inhomogeneities of the strength of the applied radio frequency (RF) field. In solid state NMR, reducing or eliminating orientation dependent magnetic fields is of key concern, so that a precise spectrum can be observed.

We approach the problem from the standpoint of mathematical control theory in which the challenge is to simultaneously steer a continuum of systems between points of interest with the same control signal. At the heart of this problem is finding ways for the nonlinearity of the system to be used to our advantage, so that while all members of the ensemble will be driven with the same controls, their final orientations can be orchestrated to arbitrary precision.

This thesis develops the methods necessary for two such ensemble control problems

arising in NMR, RF (control) amplitude inhomogeneity and systems with periodic drifts that exhibit dispersions in their amplitude and phase. In both cases, robust controls will rely on the non-commutativity of the system's dynamics enabling the generation of alternative and more robust control elements.

Contents

List of Figures

Acknowledgments

I would like to thank the members of my thesis committee, Professors Navin Khaneja, Roger Brockett and Todd Zickler. In particular, I thank Professor Khaneja for introducing me to the problems considered in this thesis and working with me to develop the methods presented herein, and Professor Brockett for providing a much needed push to get me started writing this dissertation.

I would also like to thank my fellow labmates, Van Do, Jamin Sheriff and Paul Coote, who were always willing to lend a thoughtful ear and provide constructive advice throughout.

While many students find thesis writing and research a solo charge, I am very fortunate to have an incredible group of friends, who have supported me in too many ways to name–everything from a pleasantly distracting conversation to work parties, where we dug in our heels and pushed onwards until the sun had long past risen.

A special thanks to my brother, Dennis Owrutsky, for constantly reminding me of my own intellectual curiosity by displaying his, and, of course, his help editing; Dr. Alison Forsyth for bringing her adventurer mentality with her to Cambridge; Ryan Wisnesky for his patience coaching me on so many things computer related; Richard Snyder for well timed vintage video game breaks; and Dr. Mackenzie Smith for her warm heart and power to soften my rough edges.

Last, but certainly not least, I would like to thank my father for his love and support throughout my now two decade long educational journey; his certainty in me made this thesis possible.

Dedicated to my father Neil,
and my brother Dennis.

Citations to Previously Published Work

Large portions of Chapter 2 have been published in Physical Review A:

> "Control of Inhomogeneous Ensembles on the Bloch Sphere", P. Owrutsky and N. Khaneja, Phys. Review A, vol. 86, p. 022315, 2012

Chapter 3 appears in its entirety as

> "Control of Inhomogeneous Ensembles in the Presence of a Random Periodic Drift", P. Owrutsky and N. Khaneja, Proceedings of the American Control Conference 2012

Chapter 1

Introduction

In this thesis, we develop methods to control an ensemble of varying dynamical systems by using the same control signal. Ensembles of dynamical systems are collections of systems whose member-system's parameters governing their dynamics, vary across the collection. Problems involving the control of such systems are called *control of inhomogeneous ensembles*. The ensemble viewpoint is applicable for two generic types of experiments: the first is when there physically exists a collection of systems exhibiting variations in the member systems dynamics, and the second is when there is physically only a finite number of systems (or perhaps only one), but the parameters of its dynamics are not precisely known. In both cases, developing controls suitable for the ensemble will likewise be appropriate for the experiment.

The motivation for looking at this class of problems arises naturally from the manipulation of nuclear spins in Nuclear Magnetic Resonance (NMR) spectroscopy and imaging. In practice, experiments are performed on a very large number of spins, which exhibit variations in system dynamics due to spatial location or orientation.

Similarly, imprecision in the control field is well captured by considering an ensemble of systems with control strength lying in a range of values corresponding to the maximum variation in control strength possible in the experimental setup.

A canonical problem in the control of quantum ensembles is to develop external excitations (control laws) that simultaneously steer an ensemble of dynamical systems from an initial state to a desired final state, where the initial and final states may depend on the dispersion parameters. In NMR spectroscopy, such control laws are called compensating pulse sequences, as they can compensate for the dispersions in the system dynamics. From the standpoint of mathematical control theory, the challenge is to simultaneously steer a continuum of systems between points or functions of interest by using the same control signal. Typical applications are the design of excitation and inversion pulses in NMR spectroscopy in the presence of RF inhomogeneity [1, 2, 3, 4, 5, 6, 7, 8, 9, 10] or periodic drifts arising from magic angle spinning (MAS) in solid state experiments [11, 12].

The primary focus of this thesis is on such systems undergoing magic angle spinning, which (we will show later in this chapter) have the following system dynamics

$$\frac{d}{dt}\begin{bmatrix} M_x \\ M_y \\ M_z \end{bmatrix} = \begin{bmatrix} 0 & -(\omega+\omega_p(t)) & u(t) \\ \omega+\omega_p(t) & 0 & -v(t) \\ -u(t) & v(t) & 0 \end{bmatrix}\begin{bmatrix} M_x \\ M_y \\ M_z \end{bmatrix} \tag{1.1}$$

where $\vec{M}$ is the state vector, u, v are the available controls, and $\omega_p(t)$ is a zero mean, periodic function, with known period τ_r, but unknown amplitude and phase. The goal will be to simultaneously steer the system to an arbitrary function of ω, independent of the unknown periodic component $\omega_p(t)$.

We will formalize definitions in Chapter 2, and begin with a review of NMR basics to motivate the study of ensemble control problems in this area. We then introduce various sources of dispersions and inhomogeneities in the control of spin ensembles for NMR spectroscopy, emphasizing those that are relevant to this thesis.

1.1 Motivating Remarks

NMR imaging or Magnetic Resonance Imaging (MRI) is a noninvasive technique for imaging optically nontransparent objects. Many objects can be penetrated by radio-frequency (RF) waves including: plants, food, many synthetic materials and, most notably, biological tissue. NMR can be used to generate multi-dimensional images by using linear gradients to introduce a spatially varying frequency. This intentional inhomogeneity is then exploited to sequentially isolate and image small slices of the object under investigation.

NMR imaging has become an invaluable diagnostic tool in biomedicine, offering superior image contrast to previously developed X-ray tomography. NMR is also commonly used in spectroscopy to determine the molecular composition and structure of molecules, such as proteins.

A major challenge in performing NMR spectroscopy and NMR imaging is reliably performing NMR experiments in inherently inhomogeneous fields. In recent years, there have been great advancements in the subjects of efficient data collection and inhomogeneity compensation routines to overcome these obstacles [1, 2, 3, 4, 5, 6, 8, 9].

The motivation for these studies is twofold. First, techniques that compensate for inhomogeneities enable clearer images and more precise spectroscopy using exist-

ing apparatuses. More sophisticated techniques enable the analysis of increasingly complex molecules that are beyond current methods. Second, current performance standards could be obtained with less sophisticated spectrometers, greatly reducing costs, both upfront and maintenance. These spectrometers would also have the advantage of being smaller and more portable, increasing global access to an important diagnostic tool.

1.2 NMR Background

Nuclear Magnetic Resonance (NMR) utilizes the magnetic properties of atomic nuclei that have spin for imaging and spectroscopy. NMR experiments use a strong static magnetic field in the z direction to polarize the nuclear magnetic moments, in conjunction with time dependent radio-frequency (RF) magnetic fields to illicit a spectroscopic response. We present a brief introduction to NMR, motivating the models studied in this thesis.

1.2.1 Non-interacting Spin-$\frac{1}{2}$ Nuclei

The magnetic properties of atomic nuclei lie at the core of NMR methods [13]. Several nuclei, among them the hydrogen nucleus, possess angular momentum $\vec{I}$, which is responsible for the magnetic moment $\vec{\mu}$ exhibited by these nuclei. The two quantities are related by

$$\vec{\mu} = \gamma \vec{I} \tag{1.2}$$

where γ is a constant for a particular nuclear species and is called the gyromagnetic ratio. From quantum mechanics we know that angular momentum and the nuclear magnetic moment are quantized, and that measurement values are the associated eigenvalues of the angular momentum in the direction of observation. As is convention in NMR, we consider the angular momentum in the z direction, which takes the values

$$I_z = \hbar m \tag{1.3}$$

where m is the magnetic quantum number. For an arbitrary spin I element, the allowed values for m are

$$m = -I, -I+1, ..., I-1, I \tag{1.4}$$

for a total of $2I+1$ allowed eigenstates. For a spin$-\frac{1}{2}$ species, which includes hydrogen nuclei of significant interest due to the abundance of water in biological applications, the eigenstates are $I_z = \{\frac{1}{2}, -\frac{1}{2}\}$, which are called spin-up and spin-down respectively. The energy E of a magnetic moment $\vec{\mu}$ in a magnetic field $\vec{B}$ is

$$E = -\vec{\mu} \cdot \vec{B}. \tag{1.5}$$

In the case of a uniform magnetic field in the z direction $\vec{B} = B_0\hat{z}$ and the energy reduces to

$$E = -\gamma\hbar m B_0. \tag{1.6}$$

Accordingly a larger energy is associated with the spin down eigenstate than with the spin up state, which results in a tendency for the magnetic moments to be found in the spin up state. The Larmor frequency for a nucleus is defined as $\omega_0 = -\gamma B_0$, and the associated energy difference between the spin up and spin down states is $\Delta E = \hbar\omega_0$.

1.2.2 The Bloch Equations

On a macroscopic scale, the bulk magnetic moment $\vec{M}$ and the bulk angular momentum $\vec{J}$ are the vector sum of the individual nuclei's $\vec{\mu}$ and $\vec{I}$. For a sample at thermal equilibrium in the presence of a static field $B_0\hat{z}$, there is no coherence in the transverse components of $\vec{\mu}$ and $\vec{I}$ for different nuclei, and therefore the transverse magnetization sums to zero across the sample. However, the spin up eigenstate of a spin$-\frac{1}{2}$ nucleus has lower energy than its spin down counterpart, so there will be a tendency for systems to adopt the spin up state at equilibrium, with populations distributed according to the Boltzmann Distribution. This causes a population excess in the spin up state, and produces a bulk magnetization aligned parallel to the static z-field.

Analogously to the individual magnetic moments, the bulk magnetization is related to the bulk angular momentum $\vec{J}$ by

$$\vec{M} = \gamma \vec{J}. \tag{1.7}$$

After a static z-field has produced a net polarization in the sample, the magnetization $\vec{M}$ can be controlled using a time dependent RF magnetic field $B_{RF} = (B_x(t), B_y(t))$ in the transverse plane. The total magnetic field is then $\vec{B} = B_x(t)\hat{x} + B_y(t)\hat{y} + B_0\hat{z}$, and it exerts a torque on the system

$$\vec{T} = \vec{M} \times \vec{B}. \tag{1.8}$$

Combining with Newton's second law we find

$$\frac{d}{dt}\vec{M} = \gamma \vec{M} \times \vec{B} \tag{1.9}$$

which can be expressed as

$$\frac{d}{dt}\begin{bmatrix} M_x \\ M_y \\ M_z \end{bmatrix} = \begin{bmatrix} 0 & -\omega_0 & \gamma B_y(t) \\ \omega_0 & 0 & -\gamma B_x(t) \\ -\gamma B_y(t) & \gamma B_x(t) & 0 \end{bmatrix} \begin{bmatrix} M_x \\ M_y \\ M_z \end{bmatrix}. \tag{1.10}$$

Defining $(u(t), v(t)) = (\gamma B_x(t), \gamma B_y(t))$, we arrive at the celebrated Bloch Equation,

$$\frac{d}{dt}\begin{bmatrix} M_x \\ M_y \\ M_z \end{bmatrix} = \begin{bmatrix} 0 & -\omega_0 & u(t) \\ \omega_0 & 0 & -v(t) \\ -u(t) & v(t) & 0 \end{bmatrix} \begin{bmatrix} M_x \\ M_y \\ M_z \end{bmatrix}. \tag{1.11}$$

The system can also be expressed in terms of the generators of rotations in three dimensions as

$$\frac{d}{dt}M(t) = [\omega_0\Omega_z + u(t)\Omega_x + v(t)\Omega_y]M(t) \tag{1.12}$$

where $M(t) = [M_x, M_y, M_z]^T$ and

$$\Omega_x = \begin{bmatrix} 0 & 0 & 0 \\ 0 & 0 & -1 \\ 0 & 1 & 0 \end{bmatrix} \qquad \Omega_y = \begin{bmatrix} 0 & 0 & 1 \\ 0 & 0 & 0 \\ -1 & 0 & 0 \end{bmatrix} \qquad \Omega_z = \begin{bmatrix} 0 & -1 & 0 \\ 1 & 0 & 0 \\ 0 & 0 & 0 \end{bmatrix}. \tag{1.13}$$

The evolution of the system is norm preserving, and without loss of generality, we normalize the magnetization vector to have magnitude 1, so that it evolves on the unit (Bloch) sphere.

1.2.3 Signal Acquisition

The previous section described how a collection of spin-$\frac{1}{2}$ nuclei evolve under an applied field $\vec{B}$. The use of the RF-magnetic fields enables a direct method for

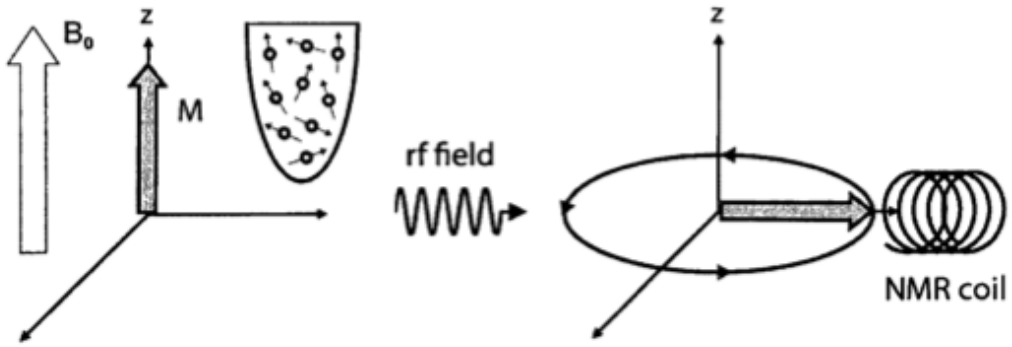

Figure 1.1: Basic NMR experiment in which RF field controls are used to produce a precessing transverse bulk magnetization, which is then observed as a current in a nearby coil.

observation of the Larmor frequency ω_0. As depicted in figure 1.1, first a large static $B_0\hat{z}$ is applied to a sample, which causes the bulk magnetization to be oriented along the z-axis. Then the RF fields are used to tip the magnetization into the transverse plane. Once in the plane, the RF fields are shut off and the magnetic moments experience a torque from the static field that is perpendicular to the bulk magnetization. This causes $M(t)$ to precess about the z-axis. According to Faraday's law, an EMF is induced in a nearby coil, and this enables observation of the bulk magnetization. The frequency of the signal depends on the known static field strength and the magnetic properties of the sample, enabling the determination of the latter.

1.3 RF Dispersion

Up to this point, we have assumed an ideal system in which all experimental parameters are precisely controlled and known. In practice, the RF controls exhibit distortion that leads to modified system dynamics with typical deviations on the order

of 5%; however, values as high as 50% can occur in toroidal coils. These distortions are well modeled by a constant multiplicative error term in the control fields, so that $(u(t), v(t)) = (\epsilon u_0(t), \epsilon v_0(t))$, $\epsilon \in (1-\delta, 1+\delta)$ and $0 < \delta < 1$. This results in the updated Bloch equations

$$\frac{d}{dt}\begin{bmatrix} M_x \\ M_y \\ M_z \end{bmatrix} = \begin{bmatrix} 0 & -\omega_0 & \epsilon u(t) \\ \omega_0 & 0 & -\epsilon v(t) \\ -\epsilon u(t) & \epsilon v(t) & 0 \end{bmatrix} \begin{bmatrix} M_x \\ M_y \\ M_z \end{bmatrix}. \tag{1.14}$$

Developing methods to compensate for the dispersion in the control strength is the primary focus of Chapter 2. It will be shown that the ϵ dependence can be made arbitrarily small, resulting in robust rotations. Alternatively, ϵ dependent rotations are also possible and are also described in the next chapter.

1.4 Orientation Dependent Effects

We have discussed how an idealized collection of non-interacting spin-$\frac{1}{2}$ nuclei leads to the Bloch Equation given in eq. (1.11). The non-interaction assumption is reasonable for liquid NMR experiments in which natural, rapid reorientation leads to virtually no anisotropic effects from intermolecular interactions. However, many spectrometry applications involve powders for which the orientation of molecules are both random and fixed, leading to significant orientation dependent effects through chemical shielding and dipolar coupling. These effects cause spectral peak broadening and corrupt spectrum acquisition.

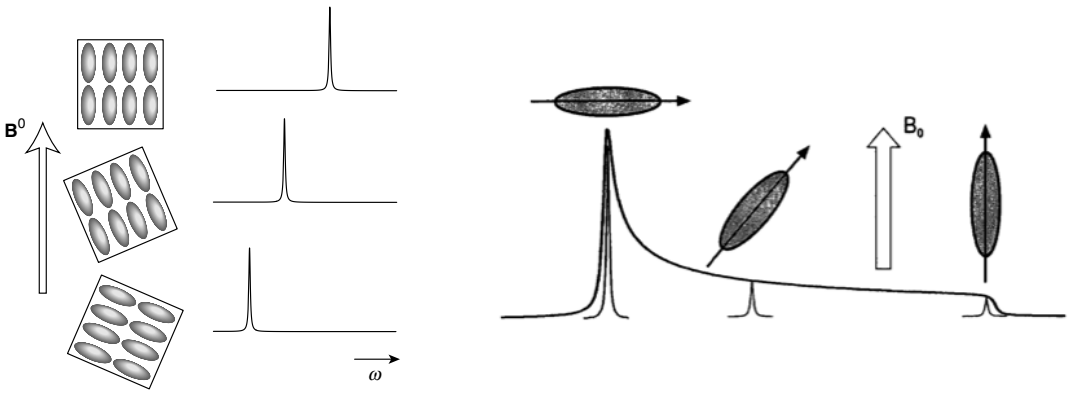

Figure 1.2: Asymmetric spectral broadening due to orientation dependent chemical shielding in a static B_0 field.

1.4.1 Chemical Shielding

Like an atomic nucleus, electrons are charged and exhibit spin giving rise to magnetic properties of their own. The charge and spin exhibited by electrons causes small magnetic fields that distort the magnetic field at the nucleus the electrons orbit. These distortions are called chemical shielding or chemical shift anisotropy [13, 14]. The tendency is for the secondary field to reinforce the static magnetic field, resulting in an increased effective field at the nucleus. The size of the shielding depends on the orientation of the molecule within the static B_0 field. The electron distribution that surrounds a nucleus within a molecule is rarely spherically symmetric, which causes an orientation dependent component. In typical applications, the isotropic chemical shielding component is of interest, since it contains information about the structure of a molecule. However, the anisotropic component is often of no interest and only serves to hinder the observation of the isotropic spectrum.

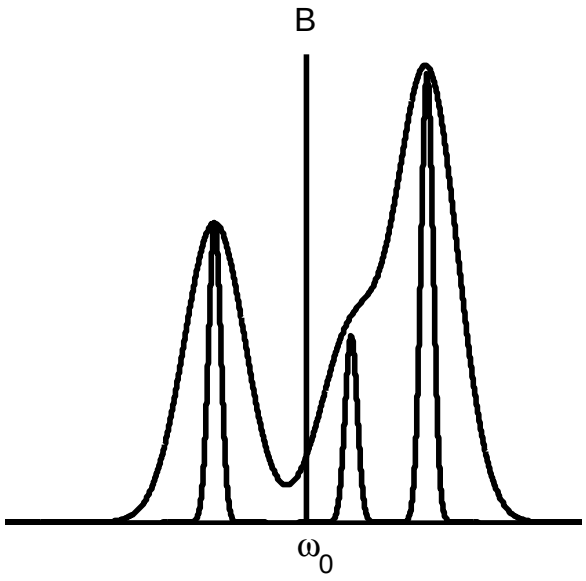

Figure 1.3: Spectral broadening due to dipolar coupling in a powder sample.

1.4.2 Dipolar Coupling

Dipolar coupling is the interaction of the applied magnetic field with the secondary field produced by nearby nuclei [13, 14]. In many applications, this effect is not of interest and results in spectrum deterioration. The dipole-dipole interaction produces a magnetic field $\Delta B_{dipolar}$ that is orientation dependent with a scaling factor that is proportional to

$$\Delta B_{dipolar} \propto 3\cos^2(\theta) - 1 \tag{1.15}$$

where θ is the angle between the internuclear axis and the direction of the static B_0 field. In a powder sample molecules can have all possible orientations, which causes significant peak broadening and makes spectrum resolution difficult or impossible.

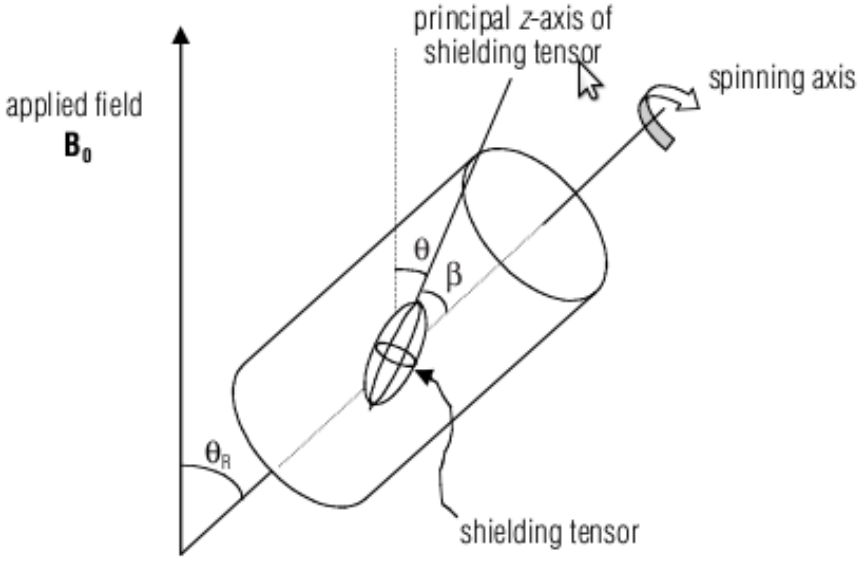

Figure 1.4: Diagram of the magic angle spinning experiment used to attenuate orientation dependent effects.

1.5 Magic Angle Spinning

To combat the static nature of solid-state spectroscopy and the resulting peak broadening from chemical shielding anisotropies and dipolar interactions, samples are spun rapidly to regain isotropy by simulating the tumbling in liquids.

It can be shown that the orientation dependent effects in (1.11) become time dependent under spinning and on average [13, 14]

$$\Delta B = \langle 3\cos^2(\theta(t)) - 1\rangle = \frac{1}{2}(3\cos^2(\theta_R) - 1)(3\cos^2(\beta) - 1) \tag{1.16}$$

where θ_R is the angle between the rotor axis and the B_0 field and β is an orientation dependent parameter. Selecting

$$3\cos^2(\theta_R) - 1 = 0 \quad \Rightarrow \quad \theta_R = \cos^{-1}\frac{1}{\sqrt{3}} \approx 54.7^\circ \tag{1.17}$$

will average the anisotropic interactions to zero; this is known as Magic Angle Spin-

ning (MAS). MAS results in more defined spectral peaks and increases NMR spectral resolution.

However, spinning rates are finite and while MAS attenuates anisotropic effects, it is often necessary to analyze the complete system with time dependence in order to successfully resolve the spectrum. The time dependent magnetic field causes a time dependent effective Larmor frequency [13]

$$\begin{aligned} \omega &= \omega_0 - \omega_0\{\sigma_{iso} + A_1\cos(\omega_r t + \gamma) + B_1\cos(\omega_r t + \gamma) \\ &\quad + A_2\cos(2\omega_r t + 2\gamma) + B_2\cos(2\omega_r t + 2\gamma)\} \end{aligned} \tag{1.18}$$

where A_1, A_2, B_1, B_2 and γ are unknown orientation dependent constants and ω_r is the rotor frequency. Letting $\omega_p(t)$ represent the periodic portion, we arrive at equation (1.1), the Bloch Equation for a system undergoing Magic Angle Spinning

$$\frac{d}{dt}\begin{bmatrix} M_x \\ M_y \\ M_z \end{bmatrix} = \begin{bmatrix} 0 & -(\omega + \omega_p(t)) & u(t) \\ \omega + \omega_p(t) & 0 & -v(t) \\ -u(t) & v(t) & 0 \end{bmatrix}\begin{bmatrix} M_x \\ M_y \\ M_z \end{bmatrix}. \tag{1.19}$$

Developing methods to adequately attenuate the effects of the periodic drift in (1.1) is the subject of chapters 3 and 4. Chapter 3 addresses the problem in the high field limit in which the control amplitudes are assumed to be large compared to the natural dynamics of the system. Chapter 4 extends these results to the low field limit, where the controls are no longer assumed to be large relative to the other system parameters, and, in fact, can be arbitrarily small.

1.6 Structure of this thesis

The thesis is organized as follows:

- In Chapter 2, we consider the ensemble control problem of producing robust pulse sequences under inhomogeneous control amplitude as described by equation (1.14). The main result is a control design algorithm that can compensate arbitrarily well for such dispersions. As with all compensating pulse sequences, pulse duration must be increased in order to obtain the associated robustness of the pulse. However, the design method described will be shown to have favorable duration to compensation characteristics compared to existing methods, specifically the so called Fourier Synthesis Method (FSM).

- In Chapter 3, we begin our study of Bloch Equations with a periodic drift, as described by equation (1.1). Such a system arises in solid state NMR in which samples are spun to average out orientation dependent dispersions, resulting in a periodic drift of known frequency. However, both the amplitude and phase of the periodic drift are not known as these remain orientation dependent and lead to unwanted spectrum broadening. The main result of the chapter is that by applying rapid pulses at integral multiples of the drift period, the system is well described by the average Hamiltonian enabling compensation for the unknown amplitude and phase.

- In Chapter 4, we continue our study of systems with periodic drift, but now consider the regime in which the control amplitudes are small relative to the other time scales of the problem. We show how equation (1.1) can be controlled

with pulses applied at multiples of the drift period with amplitudes arbitrarily weak. The construction utilizes a discretization of a series of adiabatic passages to produce broadband inversions, which when combined with the methods developed in chapter 3, enables robust control of the system, independent of both the periodic drift's amplitude, and phase.

- Chapter 5 summarizes the results of the thesis and discusses possible future applications, including multi-level spin systems such as quadrupolar nuclei, and verification of the rotating wave approximation for long duration pulse sequences.

Chapter 2

RF Compensation

2.1 Abstract

This chapter focuses on developing novel pulse elements for robust controls that compensate for control amplitude errors in the Bloch equations (1.14). The use of composite pulses for compensating for such dispersions in system dynamics is widely known and applied. In this chapter, we introduce new pulse elements for correcting pulse errors. These design methods have the advantage that they are analytical and can be used to prove arbitrarily good robust performance. Furthermore, the time-to-compensation is superior to existing Fourier Synthesis Methods, which is critical for minimizing errors due to relaxation effects.

2.2 Introduction

Many applications in control of quantum systems involve controlling a large ensemble by using the same control field. In practice, the elements of the ensemble could show variation in the parameters that govern the dynamics of the system. For example, in magnetic resonance experiments, the spins of an ensemble may have large dispersion in their natural frequencies (Larmor dispersion), strength of applied RF-field (RF-inhomogeneity) and the relaxation rates of the spins [1] to name a few. In solid state NMR spectroscopy of powders, the random distribution of orientations of inter-nuclear vectors of coupled spins within an ensemble leads to a distribution of coupling strengths [14]. A canonical problem in control of quantum ensembles is to develop external excitations that can simultaneously steer the ensemble of systems with variation in their internal parameters from an initial state to a desired final state. These are called compensating pulse sequences as they can compensate for the dispersion in the system dynamics. From the standpoint of mathematical control theory, the challenge is to simultaneously steer a continuum of systems between points of interest with the same control signal. Typical applications are the design of excitation and inversion pulses in NMR spectroscopy in the presence of larmor dispersion and RF-inhomogeneity [1, 2, 3, 4, 5, 6, 7, 8, 9, 10] or the transfer of coherence or polarization in a coupled spin ensemble with variations in the coupling strengths [15]. In many cases of practical interest, one wants to find a control field that prepares the final state as some desired function of the parameter. For example, slice selective excitation and inversion pulses in magnetic resonance imaging [16, 17, 18, 19]. The problem of designing excitations that can compensate for dispersion in the dy-

namics is a well studied subject in NMR spectroscopy and extensive literature exists on the subject of composite pulses that correct for dispersion in system dynamics [1, 2, 3, 4, 5, 6, 7]. Composite pulses have recently been used in quantum information processing to correct for systematic errors in single and two qubit operations [20, 21, 22, 23, 24, 25].

The focus of this chapter is to present novel pulse elements for compensating errors arising from uncertainties or imperfections in the pulse amplitude. The constructions presented here have the advantage that they are analytical and exhibit favorable performance compared to the existing analytical Fourier Synthesis Method [26]. Namely, the same level of RF robustness is obtained with reduced pulse length and power, which is critical for minimizing errors due to relaxation.

To fix ideas, consider an ensemble of noninteracting spin $\frac{1}{2}$ particles in a static field B_0 along the z axis and a transverse RF-field, $(A(t)\cos(\phi(t)), A(t)\sin(\phi(t)))$, in the $x-y$ plane. Let x, y, z represent the coordinates of the unit vector in the direction of the net magnetization vector of the ensemble. The dispersion in the amplitude of the RF-field is given by a dispersion parameter ϵ such that $A(t) = \epsilon A_0(t)$ where $\epsilon \in [1-\delta, 1+\delta]$, for $\delta > 0$. The Bloch equations for the ensemble take the form

$$\frac{d}{dt}\begin{bmatrix} x \\ y \\ z \end{bmatrix} = \begin{bmatrix} 0 & -\omega & \epsilon u(t) \\ \omega & 0 & -\epsilon v(t) \\ -\epsilon u(t) & \epsilon v(t) & 0 \end{bmatrix}\begin{bmatrix} x \\ y \\ z \end{bmatrix}, \tag{2.1}$$

where

$$(u(t), v(t)) = \gamma(A_0(t)\cos(\phi(t)), A_0(t)\sin(\phi(t))).$$

Let $X(t)$ denote the unit vector $(x(t), y(t), z(t))$. Consider now the problem of de-

signing controls $u(t)$ and $v(t)$ that simultaneously steer an ensemble of such systems with dispersion in the strength of their RF-field from an initial state $X(0) = (0, 0, 1)$ to a final state $X_F = (1, 0, 0)$ [8]. This problem raises interesting questions about controllability, i.e., showing that in spite of bounds on the strength of the rf-field, $\sqrt{u^2(t) + v^2(t)} \leq A_{max}$, there exist excitations $(u(t), v(t))$, which simultaneously steer all the systems with dispersion in ϵ, to a ball of desired radius r around the final state $(1, 0, 0)$ in a finite time (which may depend on A_{max}, B, δ, and r). Besides steering the ensemble between two points, we can ask for a control field that steers an initial distribution of the ensemble to a final distribution, i.e., different elements of the ensemble now have different initial and final states depending on the value of the their dispersion parameter ϵ. The initial and final state of the ensemble are described by functions $X_0(\epsilon)$ and $X_F(\epsilon)$ respectively. Consider the problem of steering an initial distribution $X_0(\epsilon)$ to within a desired distance r of a target function $X_F(\epsilon)$ by appropriate choice of controls in equation (2.1). We use the L2 norm as our error metric

$$E = \sqrt{\int_{1-\delta}^{1+\delta} ||X_F(\epsilon) - X_{target}(\epsilon)||^2 d\epsilon}. \tag{2.2}$$

If a system with dispersion in its parameters can be steered between states that have dependency on the dispersion parameter arbitrarily well, then we say that the system is ensemble controllable with respect to those parameters.

We present novel pulse elements that compensate for inhomogeneity or uncertainty in the amplitude of the RF-field. The presented method extends known techniques for pulse sequences that are robust to RF inhomogeneity. The methods presented may also find applications in anisotropy compensating pulse design or in solid state

NMR experiments [27].

2.3 Novel Pulse Elements for Compensating Rf-Inhomogeneity

In this section we present two methods for producing ϵ robust rotations. The first is the previously known Fourier Synthesis Methods [26] and the second is a new modified method using δ modulation that we call Modified Fourier Synthesis. The later will be shown to have favorable pulse duration to compensation properties.

2.3.1 Fourier Synthesis Method

To fix ideas, we begin by considering the Bloch equations in a rotating frame with only RF-inhomogeneity and no Larmor dispersion.

$$\dot{X} = \epsilon(u(t)\Omega_y + v(t)\Omega_x)X, \tag{2.3}$$

where

$$\Omega_x = \begin{bmatrix} 0 & 0 & 0 \\ 0 & 0 & -1 \\ 0 & 1 & 0 \end{bmatrix}, \quad \Omega_y = \begin{bmatrix} 0 & 0 & 1 \\ 0 & 0 & 0 \\ -1 & 0 & 0 \end{bmatrix}, \Omega_z = \begin{bmatrix} 0 & -1 & 0 \\ 1 & 0 & 0 \\ 0 & 0 & 0 \end{bmatrix}$$

are the generators of rotation around x, y and z axis, respectively.

We define the pulse elements [26]

$$U_1(\beta_k, \gamma_k) = \exp(-\gamma_k \epsilon \Omega_x) \exp(\frac{\beta_k}{2} \epsilon \Omega_y) \exp(\gamma_k \epsilon \Omega_x), \tag{2.4}$$

$$U_2(\beta_k, \gamma_k) = \exp(\gamma_k \epsilon \Omega_x) \exp(\frac{\beta_k}{2} \epsilon \Omega_y) \exp(-\gamma_k \epsilon \Omega_x), \tag{2.5}$$

which correspond to directly accessible evolutions.

For suitably small β_k , we have

$$V_k = U_2 U_1 \sim \exp(\epsilon \beta_k \cos(\gamma_k \epsilon)\Omega_y). \tag{2.6}$$

To effect a larger amplitude rotation, we consider the sequence of transformations

$$\Phi_1 \equiv \prod_k (V_k)^{n_k} \sim \exp\left(\epsilon \sum_k \alpha_k \cos(\gamma_k \epsilon)\Omega_y\right), \tag{2.7}$$

where $\alpha_k = n\beta_k$. In practice, $\beta_k < \frac{\pi}{10}$ is suitably small and results in an error that is less than 1% in the L2 sense in (2.6). Now, the coefficients α_k can be chosen so that

$$\epsilon \sum_k \alpha_k \cos(\gamma_k \epsilon) \approx \theta \tag{2.8}$$

for $1 - \delta \leq \epsilon \leq 1 + \delta$, with $0 < \delta < 1$.

Therefore,

$$\Phi_1 \sim \exp(\theta \Omega_y) \tag{2.9}$$

approximately independent of ϵ. The dependence on ϵ can be made arbitrarily small by increasing the pulse length and extending the number of terms in the summation, leading to pulses that are immune to dispersions in the RF amplitude as claimed.

2.3.2 Modified Fourier Synthesis Using δ Modulation

In this section we develop a modified Fourier Synthesis Method that will be shown to have favorable time-robustness properties to the original Fourier Synthesis technique. To this end we consider the following system

$$\dot{Y} = (\epsilon u(t)\Omega_x + v(t)\Omega_z)Y \tag{2.10}$$

which corresponds to a system with one pure control by way of $v(t)$ and one control with dispersion, $\epsilon u(t)$. We will apply a similar Fourier Synthesis Method (FSM) analysis on the system and show that this results in a modified Hamiltonian to that of the previous section, the advantages of which will be discussed in subsequent sections. We then show how the previous system with both controls exhibiting dispersion (2.3) can be transformed into (2.10) by an appropriate change of coordinates.

Consider the modified transformations

$$\tilde{U}_1 = \exp(-\gamma_k \epsilon \Omega_x) \exp(\frac{\beta_k}{2} \Omega_z) \exp(\gamma_k \epsilon \Omega_x) \tag{2.11}$$

$$\tilde{U}_2 = \exp(\gamma_k \epsilon \Omega_x) \exp(-\frac{\beta_k}{2} \Omega_z) \exp(-\gamma_k \epsilon \Omega_x) \tag{2.12}$$

By again choosing β_k sufficiently small, we have

$$\tilde{V}_k = \tilde{U}_2 \tilde{U}_1 \sim \exp(\beta_k \sin(\gamma_k \epsilon) \Omega_y). \tag{2.13}$$

Applying a sequence of such transformations

$$\Phi_2 \equiv \prod_k (\tilde{V}_k)^{n_k} \sim \exp\left(\sum_k \alpha_k \sin(\gamma_k \epsilon) \Omega_y \right), \tag{2.14}$$

where again $\alpha_k = n\beta_k$ is used to control the error from the approximation in (2.13). Now, the coefficients α_k and γ_k can be chosen so that

$$\sum_k \alpha_k \sin(\gamma_k \epsilon) \approx \theta, \tag{2.15}$$

over the range of ϵ of interest $1 - \delta \leq \epsilon \leq 1 + \delta$ resulting in a robust rotation. We point out that (2.15) resembles (2.8), but no longer contains an ϵ factor external to the trigonometric argument and that cos has been replaced with sin.

To see how (2.10) can be generated from (2.3), we return to (2.3) and let $A = \gamma A_0$,

$$\dot{X} = \epsilon A(\cos \underbrace{(\phi_1(t) + \phi_2(t))}_{\phi(t)} \Omega_x + \sin \underbrace{(\phi_1(t) + \phi_2(t))}_{\phi(t)} \Omega_y) X$$

and move into the frame,

$$Y = \exp(-\phi_2(t)\Omega_z)X \tag{2.16}$$

$$\dot{Y} = [\epsilon A(t)(\ \cos\phi_1(t)\Omega_x + \sin\phi_1(t)\Omega_y\ ) - \dot{\phi_2}(t)\Omega_z]Y \tag{2.17}$$

which corresponds to (2.10) once the appropriate identifications are made.

This means that $\tilde{V}_k$ can be directly produced by implementing $\phi_1(t)$ as 0, π, π and 0 over Δt time intervals such that $A\Delta t = \gamma_k$, and with $-\dot{\phi}_2$ a delta pulse with area $\frac{\alpha_k}{2}$, and $-\frac{\alpha_k}{2}$ at time Δt and $3\Delta t$ respectively in (2.3). As $\phi_2(4\Delta t) = 0$, $X(4\Delta t) = Y(4\Delta t)$ and the lab frame and Y frame coincide after each pulse sequence, completing the δ Modulated Pulse Design Method.

2.3.3 Remarks

The previous sections presented a constructive means to produce the following rotations

$$\Phi_1(\vec{\alpha},\vec{\gamma}) = \prod_k V(\beta_k,\gamma_k)^{n_k} = \exp\left(\overbrace{\sum_k \epsilon\alpha_k\cos(\epsilon\gamma_k)}^{H_1(\epsilon,\vec{\alpha},\vec{\gamma})}\Omega_y\right) \tag{2.18}$$

$$\Phi_2(\vec{\alpha},\vec{\gamma}) = \prod_k \tilde{V}(\beta_k,\gamma_k)^{n_k} = \exp\left(\underbrace{\sum_k \alpha_k\sin(\epsilon\gamma_k)}_{H_2(\epsilon,\vec{\alpha},\vec{\gamma})}\Omega_y\right) \tag{2.19}$$

$$\beta_k = \frac{\alpha_k}{n_k} \tag{2.20}$$

using corresponding pulse elements consisting of directly accessible rotations

$$V(\beta_k, \gamma_k) = \exp(\gamma_k \epsilon \Omega_x) \exp(\frac{\beta_k}{2} \epsilon \Omega_y) \exp(-2\gamma_k \epsilon \Omega_x) \exp(\frac{\beta_k}{2} \epsilon \Omega_y) \exp(\gamma_k \epsilon \Omega_x) \quad (2.21)$$

$$\tilde{V}(\beta_k, \gamma_k) = \exp(\gamma_k \epsilon \Omega_x) \exp(-2\gamma_k \epsilon \Omega_\phi) \exp(\gamma_k \epsilon \Omega_x) \quad (2.22)$$

$$\Omega_\phi = \cos(\frac{\beta_k}{2}) \Omega_x - \sin(\frac{\beta_k}{2}) \Omega_y. \quad (2.23)$$

By completeness of a Fourier Sine Series, H_2 can be made to approximate any odd function with arbitrary accuracy. Similarly, H_1/ϵ can approximate any even function. As we are only interested in positive values of ϵ, H_1 and H_2 can be made to approximate any $f(\epsilon)\Omega_y$ rotation, where $f(\epsilon)$ is a continuous function of ϵ. We will show in the next section that keeping only the first few terms in the series is often sufficient in practice. Moreover, interchanging Ω_x and Ω_y will produce analogous rotations about the x-axis so that, any rotation,

$$\begin{aligned} &\exp(\theta(\epsilon)(\cos\beta(\epsilon)\Omega_y + \sin\beta(\epsilon)\cos\phi(\epsilon)\Omega_z + \sin\beta(\epsilon)\sin\phi(\epsilon)\Omega_x) \\ &= \exp(\phi(\epsilon)\Omega_y) \exp(\beta(\epsilon)\Omega_x) \exp(\theta(\epsilon)\Omega_y) \exp(-\beta(\epsilon)\Omega_x) \exp(-\phi(\epsilon)\Omega_y) \end{aligned} \quad (2.24)$$

where θ, ϕ and β are continuous functions of ϵ, can be produced.

This effectively reduces the problem of RF compensation to one of function fitting through selection of $\vec{\alpha}$ and $\vec{\gamma}$. Selecting $f(\epsilon) = \theta$, a constant, corresponds to robust rotations, which are the primary focus of this thesis.

An important consideration in robust RF pulse design is the total required flip angle to achieve a level of compensation as this is a measure of the time required to implement a pulse. Long duration pulses are undesirable as relaxation effects can become non-negligible.

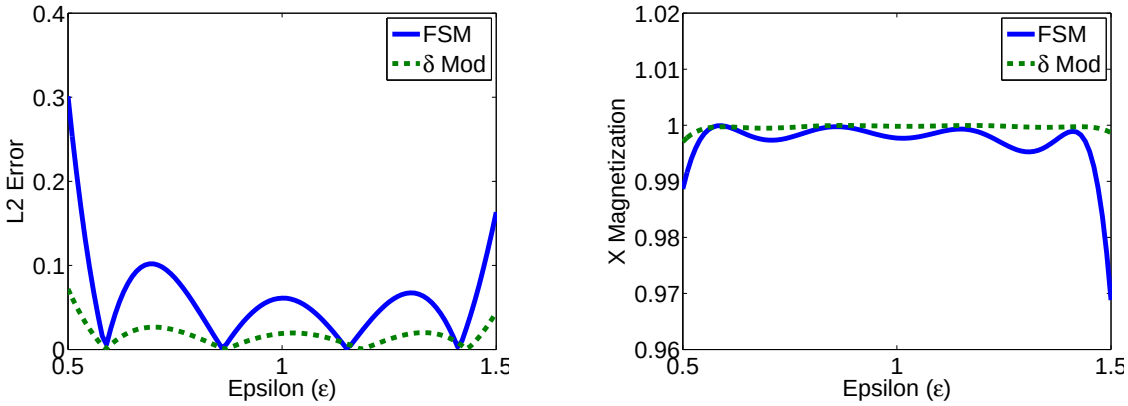

Figure 2.1: Left: L2 error with respect to the desired final magnetization $[1, 0, 0]'$ for 2 term expansions in Φ_1 and Φ_2 as a function of the dispersion parameter ϵ. Frequencies were selected using gradient descent. Right: Corresponding final X-magnetization for the 2 term sequences for both Fourier Synthesis and δ Modulation. δ modulation has a favorable magnetization profile while requiring a shorter pulse duration.

While we defer an in depth comparison of the methods to the following section, it is clear that eq. (2.18) and eq. (2.19) represent different possible bases for expansion. Consequently, series truncation is expected to result in differing levels of error for a given target function. In the case of a robust rotation, $f(\epsilon) = \theta$, the basis from δ modulation will be found to be preferable, requiring fewer terms in the expansion for a given level of error. As a result, δ modulated pulses will be shorter for a given level of robustness. Figure 2.1 shows this graphically for the case of a 2 term expansion.

2.4 Simulations and Error Performance of F. Synthesis and δ Modulation

The previous section reduced the problem of RF dispersion compensation to parameter selection, γ_k and α_k. Given the inhomogeneity parameter, $\epsilon \in [1-\delta_0, 1+\delta_0]$,

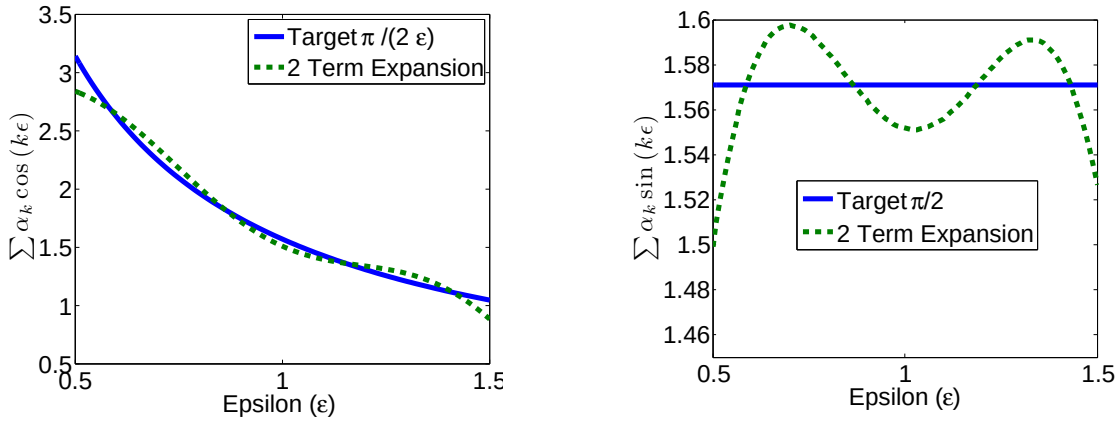

Figure 2.2: Left: 2 Term Fourier Synthesis Method approximation for $\frac{\pi}{2\epsilon}$ using gradient descent for frequency selection. Right: 2 Term δ Modulation approximation for $\frac{\pi}{2}$ using gradient descent for frequency selection.

we compute the error performance of synthesizing the effective rotations

$$\Phi_1 = \exp\left(\epsilon \sum_k \alpha_k^1 \cos(\epsilon\gamma_k^1)\Omega_y\right) \tag{2.25}$$

$$\Phi_2 = \exp\left(\sum_k \alpha_k^2 \sin(\epsilon\gamma_k^2)\Omega_y\right) \tag{2.26}$$

to approximate

$$\Phi = \exp(\theta\Omega_y).$$

We note that the $\{\alpha_k^1\}$ can be directly calculated given the $\{\gamma_k^1\}$ as

$$\vec{\alpha}^1 = M^{-1}V; \quad \langle f, g\rangle = \int_{1-\delta}^{1+\delta} f(\epsilon)g(\epsilon)d\epsilon \tag{2.27}$$

$$M_{ij} = \langle \cos(\gamma_i^1\epsilon), \cos(\gamma_j^1\epsilon)\rangle; \quad V_i = \langle \cos(\gamma_i^1\epsilon), \frac{\theta}{\epsilon}\rangle \tag{2.28}$$

and similarly the $\{\alpha_k^2\}$ can be calculated as

$$\vec{\alpha}^2 = M^{-1}V; \quad \langle f, g\rangle = \int_{1-\delta}^{1+\delta} f(\epsilon)g(\epsilon)d\epsilon \tag{2.29}$$

$$M_{ij} = \langle \sin(\gamma_i^2\epsilon), \sin(\gamma_j^2\epsilon)\rangle; \quad V_i = \langle \sin(\gamma_i^2\epsilon), \theta\rangle \tag{2.30}$$

Heuristic				**Greedy**				**Gradient**			
	$n=2$	$n=3$	$n=4$		$n=2$	$n=3$	$n=4$		$n=2$	$n=3$	$n=4$
Error FSM	0.06831	0.06523	0.06473	Error FSM	0.04031	0.01506	0.00941	Error FSM	0.07339	0.01874	0.00423
Error δ Mod	0.02012	0.00290	0.00044	Error δ Mod	0.02029	0.00422	0.00247	Error δ Mod	0.01940	0.00280	0.00044
Flip $\angle$ FSM	127.120	187.200	199.600	Flip $\angle$ FSM	130.497	179.062	229.101	Flip $\angle$ FSM	120.519	225.780	347.41
Flip $\angle$ δ Mod	115.230	172.001	216.138	Flip $\angle$ δ Mod	110.952	165.178	216.177	Flip $\angle$ δ Mod	113.341	170.134	216.137

Table 2.1: Performance of Fourier Synthesis and δ Modulation for heuristic, greedy and gradient descent based frequency selection. In all cases, δ modulation outperforms the Fourier Synthesis method in terms of L2 Error for a given pulse duration, which is important for minimizing relaxation effects. L2 error is calculated with respect to the desired final magnetization $[1, 0, 0]'$.

so that the problem reduces to selecting the optimal frequencies.

We report performance for three frequency selection methods, heuristically, greedy selection and gradient descent and show that δ modulation outperforms Fourier Synthesis Methods for all frequency selection methods. Unless stated otherwise, the notion of optimal is with respect to L2 error for a given pulse duration. L2 error is calculated with respect to the desired final magnetization $[1, 0, 0]$ and pulse duration is reported in total flip angle.

As a starting point, we consider the problem of selecting the optimal amplitudes given known frequencies which we will choose heuristically. As sine obtains its maximum at $\pi/2$ and is relatively horizontal about this point, a natural selection for the frequencies in (2.15) is $\gamma_k = \frac{(2k-1)\pi}{2}$. Similarly, selecting γ_k in (8) to maximize flatness about $\epsilon = 1$ corresponds to

$$\left[\frac{d}{d\epsilon}\epsilon\cos(\gamma_k\epsilon)\right]\Bigg|_{\epsilon=1} = \cos(\gamma_k) - \gamma_k\sin(\gamma_k) = 0. \tag{2.31}$$

Numerically solving gives the first several $\gamma_k = [0.860, 3.426, 6.437]$.

The amplitude coefficients $\vec{\alpha}$ were then calculated according to (2.27)-(2.30). The

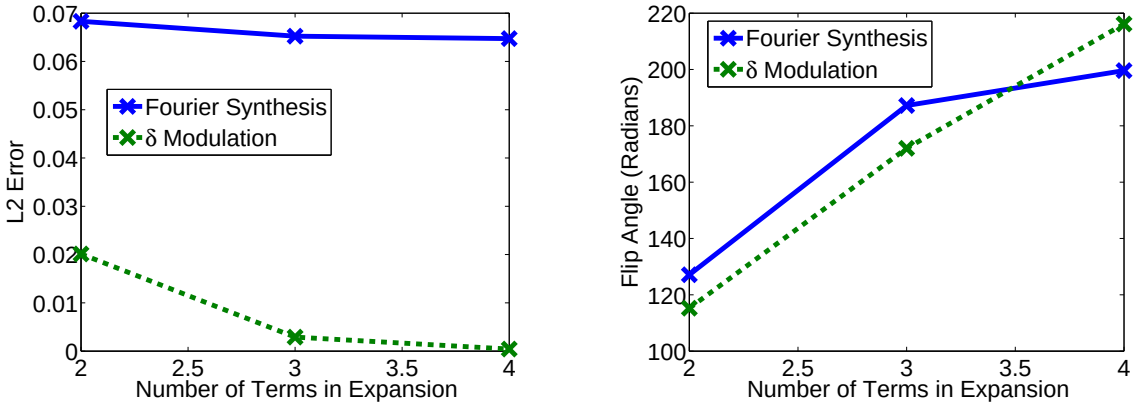

Figure 2.3: L2 error (Left) and total flip angle (Right) for heuristic frequency selection for Fourier Synthesis and δ Modulation. Error for a fixed pulse duration is smaller with δ Modulation.

comparative performance of standard FSM, Φ_1, to δ modulation, Φ_2, is tabulated in table 1 and a complete description of the pulses is given in Appendix B.

An alternative algorithm is to sequentially select the frequencies employing a greedy algorithm, in which already determined frequencies are held fixed, and only the newest frequency is optimized over. Explicitly we sequentially minimize the cost functions with respect to $\gamma_k^{1/2}$

$$F_1(\gamma_k^1, ..., \gamma_1^1) = \int_{1-\delta}^{1+\delta} \left|\left| \sum \alpha_k \cos(\epsilon \gamma_k^1) - \frac{\theta}{\epsilon} \right|\right| d\epsilon \tag{2.32}$$

$$F_2(\gamma_k^2, ..., \gamma_1^2) = \int_{1-\delta}^{1+\delta} \left|\left| \sum \alpha_k \sin(\epsilon \gamma_k^2) - \theta \right|\right| d\epsilon \tag{2.33}$$

again using (2.27)-(2.30) to calculate the $\vec{\alpha}$. This was done using gradient descent and numerically calculating the necessary derivatives. Table 1 shows that the δ modulation outperforms standard FSM.

The most general method we applied (and best performing) was simultaneously optimizing F_1 and F_2 with respect to all frequencies using gradient descent, where derivatives were again calculated numerically. As with all descent schemes, there is

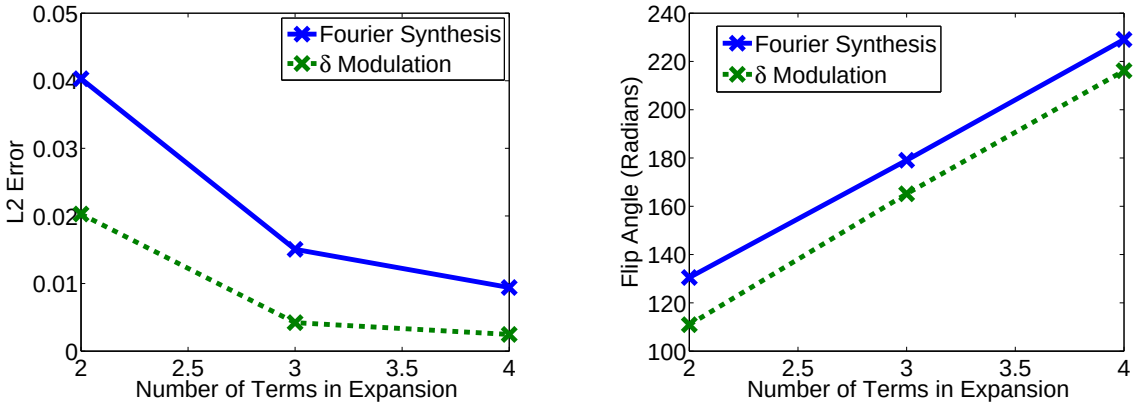

Figure 2.4: L2 error (Left) and total flip angle (Right) for greedy frequency selection for Fourier Synthesis and δ Modulation. Both duration and error are smaller for δ Modulation.

concern that one merely obtains a local minima. Moreover, the problem of unspecified frequencies is how to project onto an overrepresented subspace which is known to have local minima. To combat such issues we chose the optimal result after numerous starting points and note that the performance exceeds the other methods and the results are tabulated in table 1.

As an example we consider the resulting parameters from optimizing a two term δ modulated pulse using gradient descent

$$\gamma^2 = [88.6^\circ, 265.1^\circ]; \qquad \alpha^2 = [105.5^\circ, 16.6^\circ].$$

These are converted into a pulse sequence by first dividing large amplitudes of α_k^2 into repeated sequences with smaller amplitudes according to (14) using a threshold value of 9°, which yields the modified parameters

$$\begin{aligned} \gamma^{2'} &= [\underbrace{88.6^\circ, ..., 88.6^\circ}_{12 \text{ times}}, \underbrace{265.1^\circ, ..., 265.1^\circ}_{2 \text{ times}}] \\ \beta^2 &= [\underbrace{8.8^\circ, ..., 8.8^\circ}_{12 \text{ times}}, \underbrace{8.4^\circ, ..., 8.4^\circ}_{2 \text{ times}}] \end{aligned}$$

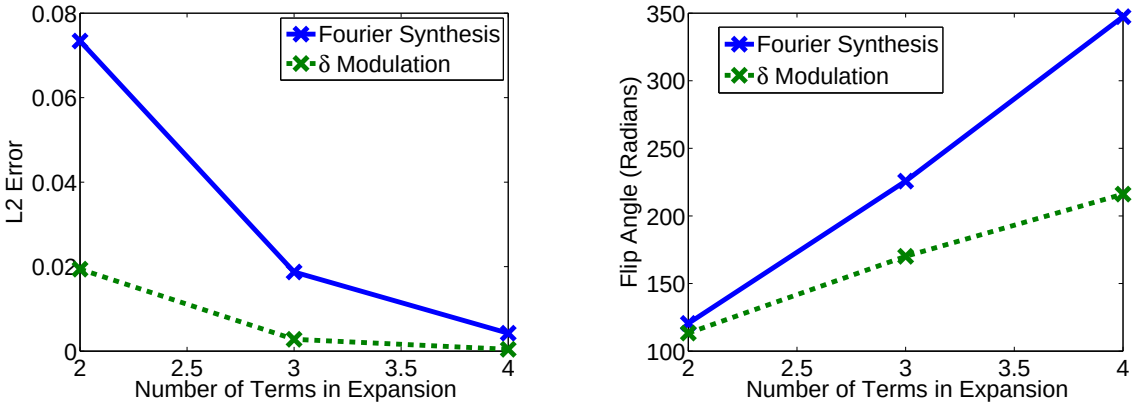

Figure 2.5: L2 error (Left) and total flip angle (Right) for gradient descent frequency selection for Fourier Synthesis and δ Modulation. Both duration and error are smaller for δ Modulation.

Pulses are calculated as described in section II.B where pulse elements are

$$[(\gamma_k)_0(2\gamma_k)_{180^\circ-\beta_k/2}(\gamma_k)_0]$$

with numbers inside the parentheses representing the flip angle and the subscripts, the phase. Applying to the parameters above yields the pulse sequence

$$[(88.6)_0(177.1)_{175.6}(88.6)_0]^{\times 12}\,[(265.1)_0(530.1)_{175.9}(265.1)_0]^{\times 2}\,.$$

The performance is displayed in Figure 2.1. The more terms kept in the series, the longer the sequence and overall pulse, but the more ϵ-robust.

2.5 General Modulation Schemes

In many ways δ modulation is the most natural choice as it has a nice correspondence with existing FSM's. However, other modulation schemes are possible and their analysis is warranted for the sake of completeness or in the event that abrupt

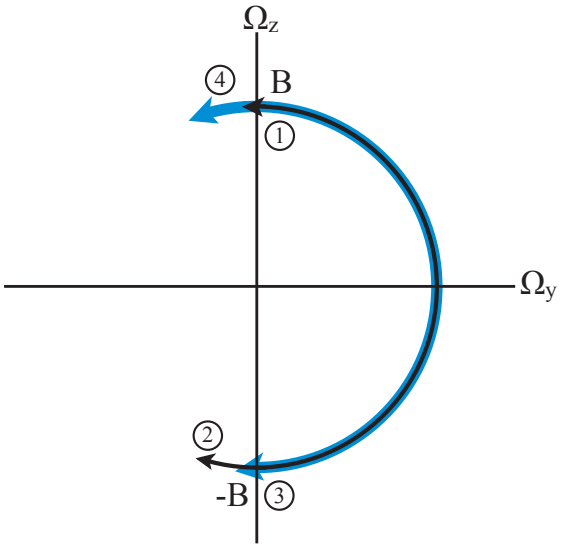

Figure 2.6: Trajectory in the interaction frame for linearly modulated controls. The trajectory is the black path from 1-2 and back to 1, followed by the blue path from 3-4 and back to 3.

phase adjustments in the RF-fields are not available. We begin by considering linear modulation.

Linear Modulation

Returning to equation (2.10) with $\Delta t = \frac{\pi}{A}$ and

$$\phi_1 = \begin{cases} 0 & 0 < t \leq \Delta t \\ \pi & \Delta t < t \leq 3\Delta t \\ 0 & 3\Delta t < t \leq 4\Delta t \end{cases} \tag{2.34}$$

$$\dot{Y} = (A\epsilon \cos\phi_1(t)\Omega_x - \dot{\phi}_2\Omega_z)Y \tag{2.35}$$

Moving into the interaction frame

$$Z \equiv \exp(-\int_0^t \epsilon A \cos\phi_1(\tau)d\tau\ \Omega_x)Y \tag{2.36}$$

$$\dot{Z} = -\dot{\phi}_2\left(\cos\epsilon\int_0^t A\cos\phi_1(\tau)d\tau\ \Omega_z + \sin\epsilon\int_0^t A\cos\phi_1(\tau)d\tau\ \Omega_y\right)Z \tag{2.37}$$

We note that under the assumptions

$$\int_0^T \cos\phi_1(t)dt = \int_0^T \dot{\phi}_2(t)dt = 0 \tag{2.38}$$

the Z frame will agree with the Y frame which will agree with the lab frame at time T, so that it is sufficient to analyze the system in the interaction frame. Letting $\phi_2(t)$ be a linear modulation of the form

$$\dot{\phi}_2 = \begin{cases} -B & 0 \le t < 2\Delta t \\ B & 2\Delta t \le t \le 4\Delta t \end{cases} \tag{2.39}$$

we can analyze the resulting rotation with the Peano-Baker Series

$$\begin{aligned}
\Phi &= I + \int_0^{\frac{4\pi}{A}} H(t)dt + \int_0^{\frac{4\pi}{A}} H(t)\int_0^t H(\sigma_1)d\sigma_1 dt + ... \\
&= I + \int_0^{\frac{4\pi}{A}} H(t)dt + O\left(\frac{B}{A}\right)^2 \\
&= I + 4B\int_0^{\frac{\pi}{A}} \sin(A\epsilon t)dt\Omega_y + O\left(\frac{B}{A}\right)^2 \\
&= I + \frac{4B}{A\epsilon}(1-\cos(\pi\epsilon)) + O\left(\frac{B}{A}\right)^2 \\
&= I + \frac{8B}{A}(1-\delta) + o(\delta)^2 + O\left(\frac{B}{A}\right)^2
\end{aligned} \tag{2.40}$$

which, to first order, has resulted in an evolution with the dispersion term reversed. Combining with a directly accessible evolution of $\frac{8B(1+\delta)}{A}\Omega_y$ will produce a pulse that is robust to first order in δ. Figure 2.6 displays the trajectory in the interaction frame

for the linearly modulated pulse with $\epsilon > 1$ and provides the intuition for why the dispersion term is negated.

Arbitrary Modulation Schemes

Other modulation functions are also possible. Let $|f(t)| < B$ be such a candidate modulation, then choosing

$$\dot{\phi}_2 = \begin{cases} f(t) & 0 < t \leq \Delta t \\ f(2\Delta t - t) & \Delta t < t \leq 2\Delta t \\ -f(t - 2\Delta t) & 2\Delta t < t \leq 3\Delta t \\ -f(4\Delta t - t) & 3\Delta t < t \leq 4\Delta t \end{cases} \tag{2.41}$$

will produce a rotation

$$I - 4\int_0^{\frac{\pi}{A}} f(t)\sin(A\epsilon t)dt\Omega_y + O\left(\frac{B}{A}\right)^2 \tag{2.42}$$

which can be used to produce new dispersion dependencies and thereby robust pulses as was done in the linear case.

2.6 Conclusion

We have presented a new method for pulse design in the presence of RF-inhomogeniety that extends existing Fourier Synthesis Methods. The method displays superior time-compensation properties to conventional Fourier Synthesis Methods. These methods are analytical and can be used to produce arbitrarily robust performance.

Chapter 3

Control of Inhomogeneous Ensembles in the Presence of a Random Periodic Drift

3.1 Abstract

This chapter motivates control of systems with random yet periodic drift. Numerous physical systems conform to such a model, perhaps the best known is solid state nuclear magnetic resonance experiments in which periodic sample rotation is used to average random effects. We present a control design method that allows for robust selective excitation in the presence of such random, periodic drifts.

3.2 Introduction

Many applications in the control of quantum systems involve manipulating a large ensemble by using the same control signal [28] [29] [30] [31] . The member systems of the ensemble frequently show variation in the parameters that govern the dynamics of each system. For example, in liquid nuclear magnetic resonance (NMR) experiments, the spins of an ensemble may exhibit dispersion in their natural frequencies, strength of applied RF field, and in the relaxation rates of the spins to name a few. In solid-state NMR spectroscopy of powders, the random distribution of orientations of internuclear vectors between coupled spins leads to dispersion in coupling strengths.

An important component of NMR experiments is designing selective excitation and inversion pulses, which involves driving systems within certain parameter regions to a particular location while leaving others unaffected. Developing such pulses for NMR spectroscopy in the presence of Larmor dispersion and RF inhomogeneity, or the transfer of coherence or polarization in a coupled spin ensemble with variation in the coupling strengths [11] are critical for a range of experiments and are common examples of using the same control to manipulate a range of systems. A canonical problem then, is to develop external excitations that can simultaneously steer the ensemble of systems arbitrarily close to a desired function of the system's parameters.

This chapter presents a control design law that allows for selective excitation in the presence of a periodic natural drift with random phase and amplitude, but known period. Such a system arises in solid state NMR experiments in which the sample is spun to average out unwanted intermolecular interactions. Additional information on such systems may be found in [13]'s discussion of Magic Angle Spinning (MAS).

We focus on the following dynamical system and use the notation

$$\begin{bmatrix} \dot{M}_x \\ M_y \\ M_z \end{bmatrix} = \begin{bmatrix} 0 & -(\omega + \omega_p(t)) & u(t) \\ \omega + \omega_p(t) & 0 & -v(t) \\ -u(t) & v(t) & 0 \end{bmatrix} \begin{bmatrix} M_x \\ M_y \\ M_z \end{bmatrix} \tag{3.1}$$

Here $\omega_p(t) = A\cos(\omega_r t + \gamma)$, $M(\omega, \gamma) = [M_x, M_y, M_z]'$ is the state vector, $u(t), v(t) \in R$ are our controls, ω_r is known and fixed for all systems in the ensemble, γ is an undesired dispersion parameter in the range $[0, 2\pi)$ and A is random and fixed.

We desire a control design algorithm to steer the system to any desired function of ω (independent of γ and A). Applications will include developing ω selective, excitation and inversion pulses.

This chapter is organized as follows; first we consider a natural way to control the system in the absence of $\omega_p(t)$ and show that this strategy is not effective in the presence of periodic drift. Next, we apply the Fourier synthesis method (FSM) [28] for selective excitation even in the presence of large values of A. In the next section we bound the error in the approximate commutation assumption of the FSM and show that it can be made arbitrarily small. It will be seen that this method loses controllability under certain aliasing conditions, and in the third section we describe an extension that regains controllability by suppressing this aliasing. We conclude with simulations.

3.3 Conventional Pulses

A natural starting point for analyzing the system is to consider the periodic term small and apply controls corresponding to $\omega_p(t) = 0$. We obtain these controls by

considering the non-periodic case ($A = 0$) and performing a change of coordinates into a rotating frame as follows

$$\dot{X} = (w\Omega_z + u\Omega_x + v\Omega_y)X \tag{3.2}$$

$$Y \equiv \exp(-wt\Omega_z)X \tag{3.3}$$

$$\dot{Y} = [u(t)(\cos(wt)\Omega_x - \sin(wt)\Omega_y) + v(t)(\cos(wt)\Omega_y + \sin(wt)\Omega_x)]Y \tag{3.4}$$

where $\Omega_x,\ \Omega_y$ & Ω_z are the generators of rotations defined as

$$\Omega_x = \begin{bmatrix} 0 & 0 & 0 \\ 0 & 0 & -1 \\ 0 & 1 & 0 \end{bmatrix} \qquad \Omega_y = \begin{bmatrix} 0 & 0 & 1 \\ 0 & 0 & 0 \\ -1 & 0 & 0 \end{bmatrix} \qquad \Omega_z = \begin{bmatrix} 0 & -1 & 0 \\ 1 & 0 & 0 \\ 0 & 0 & 0 \end{bmatrix}$$

Applying an on resonance pulse of the form

$$u(t) = B\cos(wt); \quad v(t) = B\sin(wt) \tag{3.5}$$

produces the static Hamiltonian in the rotating frame

$$\dot{Y} = B\Omega_x Y \tag{3.6}$$

Applying this pulse for $\pi/(2B)$ units of time will then produce a selective excitation. However, as figure 3.1 indicates, when $\omega_p(t) \neq 0$ performance deteriorates rapidly; As one might expect, ignoring the periodicity of the system dynamics proves problematic, necessitating a different approach.

3.4 Fourier Synthesis

The problem is to design $u(t)$ and $v(t)$ to effect some desired evolution of the ensemble as a function of w while compensating for the dispersion in A, γ. We can

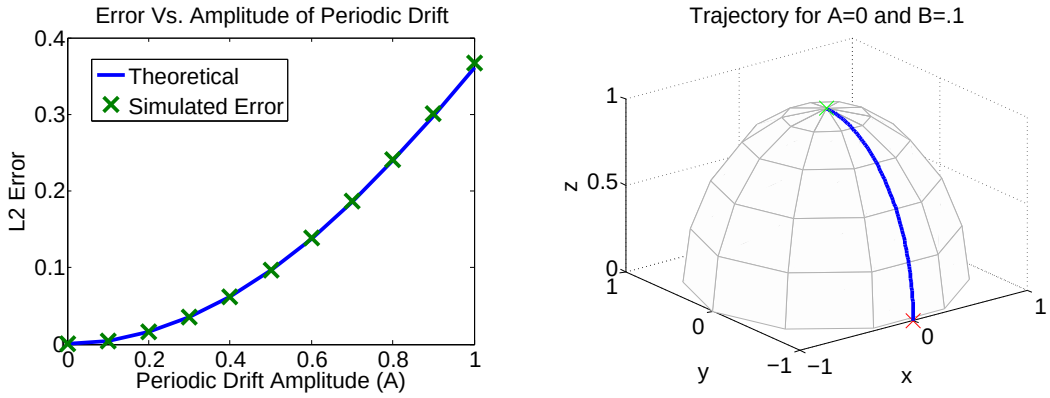

Figure 3.1: Left: L2 error for weak irradiation as a function of periodic drift amplitude A with $\omega_r = 1$ and control amplitude $B = 0.1$. Error is calculated with respect to the desired excitation $[0, -1, 0]'$. Agrees well with the first order error approximation denoted in green. Right: Weak irradiation trajectory without periodic drift (A=0).

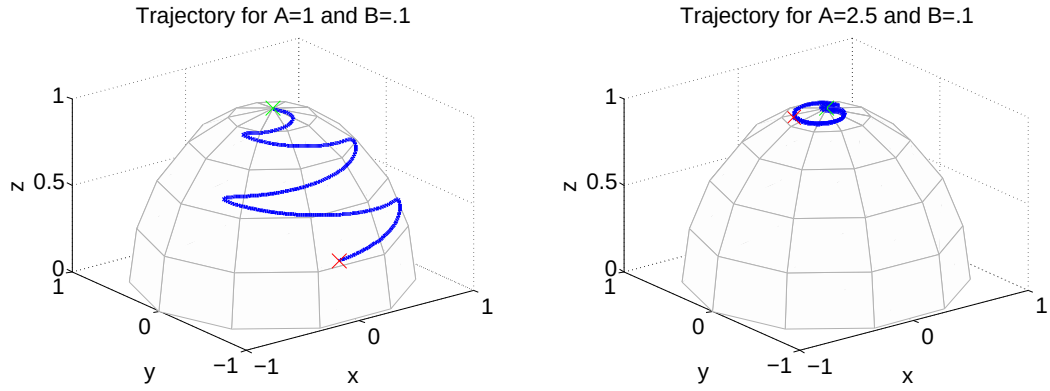

Figure 3.2: Trajectory in the rotating frame for an on resonance weak irradiation with $B = 0.1$ and $\omega_r = 1$. Left: Moderate periodic drift amplitude $A = 1$, which results in an attenuated excitation. Right: Larger periodic drift amplitude $A = 2.5$, which results in virtually no excitation.

express (3.1) in terms of the generators of rotations as

$$\dot{M} = (\ (w + A\cos(w_r t + \gamma))\Omega_z + u(t)\Omega_x + v(t)\Omega_y\ )M \tag{3.7}$$

We now show how to construct such controls in the limit when strength of u, v can be made much larger than ω and A, so called the high RF limit.

3.4.1 High RF Field Regime

Explicitly, we define the high RF limit as the regime for which the evolution due to the natural Hamiltonian during an RF rotation is negligible; mathematically

$$\frac{\max(w, A)}{RF_{max}} \equiv \epsilon << 1. \tag{3.8}$$

We additionally assume that the RF pulse duration is short relative to a rotor period. If we consider a transverse rotation of angle θ about an axis Ω and define $\Delta t = \theta / RF_{max}$ as the amount of time required to produce the θ pulse, we assume $\Delta t << \tau_r$ so that the pulse sequences we consider can comfortably be executed within a rotor period. Moving into the control frame we find

$$Z \equiv \exp\left(-\underbrace{(u\Omega_x + v\Omega_y)t}_{\phi\Omega} \right) M \tag{3.9}$$

$$\begin{aligned} \dot{Z} &= \exp(-\phi\Omega)(w + A\cos(w_r t + \gamma))\Omega_z \exp(\phi\Omega) Z \\ &= \underbrace{(w + A\cos(w_r t + \gamma))(\cos(\phi)\Omega_z - \sin(\phi)[\Omega, \Omega_z])}_{H} Z \end{aligned} \tag{3.10}$$

$$\tag{3.11}$$

Expanding the state transition matrix for H in its Peano-Baker series

$$\Phi = I + \int_0^{\Delta t} d\sigma_1 H(\sigma_1) + \int_0^{\Delta t} d\sigma_1 H(\sigma_1) \int_0^{\sigma_1} d\sigma_2 H(\sigma_2) + \cdots$$

Since

$$|H(t)| \leq (A + w)|\Omega'| \leq 3(A + \omega)$$

we can bound the nth term in the series by

$$\begin{aligned}\left|\int_0^{\Delta t} d\sigma_1 H(\sigma_1)\cdots\int_0^{d\sigma_n} d\sigma_n H(\sigma_k)\right| &\leq \int_0^{\Delta t}\cdots\int_0^{d\sigma_n}(3(A+\omega))^n d\sigma_1\cdots d\sigma_n \\ &\leq \frac{(3(A+w)\Delta t)^n}{n!} \\ &\leq \frac{(6\theta\epsilon)^n}{n!} \end{aligned} \tag{3.12}$$

so that the error due to the natural evolution during an RF rotation satisfies

$$E_\theta \leq \exp(6\theta\epsilon) - 1 \tag{3.13}$$

which we assume is so small as to be safely ignored.

3.4.2 Rotation About The x,y-Axis

The natural Hamiltonian also called the drift Hamiltonian for the system (controls identically zero) is

$$H_0 = (w + A\cos(w_r t + \gamma))\Omega_z \tag{3.14}$$

Defining $\tau_r = 2\pi/w_r$ we have

$$\int_0^{\tau_r} H_0(t)dt = \int_0^{\tau_r}(w + A\cos(w_r t + \gamma))\Omega_z dt = w\tau_r\Omega_z$$

Noting the relation (derived in appendix A)

$$\exp(\alpha\Omega_x)\exp(\beta\Omega_y)\exp(-\alpha\Omega_x) = \exp(\beta(\cos(\alpha)\Omega_y + \sin(\alpha)\Omega_z)) \tag{3.15}$$

then defining

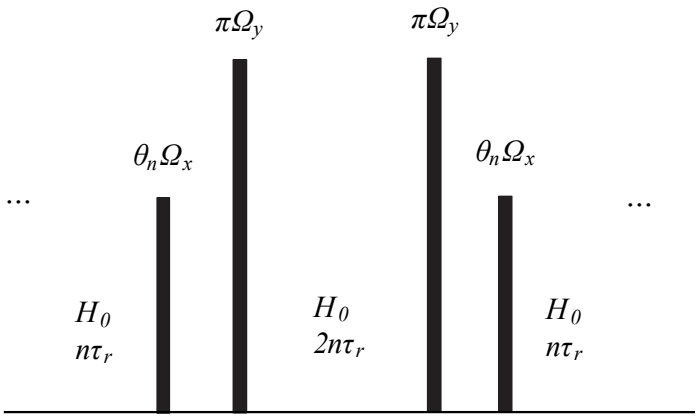

Figure 3.3: Schematic of the pulse sequence element $U_n(\theta_n)$ described in equation (3.16). The element consists of seven steps, three of which are evolving under the natural dynamics H_0 as well as four rapid rotations using $u(t)$ and $v(t)$.

$$\begin{aligned} U_n(\theta_n) &= \exp\left(\int_0^{n\tau_r} H_0(t)dt\right)\exp(\theta_n\Omega_x)\exp(\pi\Omega_y)\exp\left(\int_0^{2n\tau_r} H_0(t)dt\right) \\ &\qquad \times \exp(\pi\Omega_y)\exp(\theta_n\Omega_x)\exp\left(\int_0^{n\tau_r} H_0(t)dt\right) \\ &= \exp\left(nw\tau_r\Omega_z\right)\exp(\theta_n\Omega_x)\exp\left(-nw\tau_r\Omega_z\right) \\ &\qquad \times \exp\left(-nw\tau_r\Omega_z\right)\exp(\theta_n\Omega_x)\exp\left(nw\tau_r\Omega_z\right) \\ &= \exp(\theta_n(\cos(nw\tau_r)\Omega_x - \sin(nw\tau_r)\Omega_y)) \\ &\qquad \times \exp(\theta_n(\cos(nw\tau_r)\Omega_x + \sin(nw\tau_r)\Omega_y)) \\ &\approx \exp(2\theta_n\cos(nw\tau_r)\Omega_x) \end{aligned} \tag{3.16}$$

which is independent of both dispersion parameters A and γ [12]. The approximate equality holds for small θ_n and negation of the drift Hamiltonian is accomplished by applying a rapid π pulse. We will analyze in detail the error from the commutation assumption in section C and show that it is readily bounded and controlled.

By selecting θ_n according to Fourier expansion of our desired excitation profile $\phi(\omega)\Omega_x$

$$\begin{aligned} \theta_0 &= \frac{1}{4B}\int_{-B}^{B}\phi(\omega)d\omega \\ \theta_n &= \frac{1}{2B}\int_{-B}^{B}\phi(\omega)\cos(n\omega\tau_r)d\omega \end{aligned} \tag{3.17}$$

any rotation about the x-axis can be decomposed into a product of U_n's independent of A and γ provided there is no aliasing, i.e. $\nexists w_1, w_2$ such that $(w_2 - w_1)\tau_r = 2\pi$. Otherwise this method will not be able to control such values independently. Fortunately, in the high RF field limit this limitation can be overcome in a straightforward manner and will be described in section D. Lastly, substituting $\theta_n\Omega_y$ for $\theta_n\Omega_x$ will generate corresponding rotations around the y-axis.

3.4.3 Error Analysis

The previous pulse sequence is susceptible to error from two sources, the first is from the commutation assumption in Eq. (3.16) and the second is due to the hard RF pulse assumption from section A. To complete the analysis we will show how both can be bounded and that the error from the commutation assumption can be made arbitrarily small.

Commutation Approximation

For large θ the commutation approximation in Eq. (3.16) is invalid. Here we bound the error introduced by the approximation and show that by instead evolving N, $U_n(\theta/N)$ sequential cycles, the error can be made arbitrarily small. That is to say

we make the following substitution

$$U_n(\theta_n) \to \left[U_n\left(\frac{\theta_n}{N}\right)\right]^N \tag{3.18}$$

where N is determined by error tolerance as larger N increases pulse duration and reduces error.

To see this we use the Frobenius norm as our error metric

$$E(A,B) = ||A - B|| \tag{3.19}$$

and note that our desired trajectory is

$$\exp\left(2\alpha\frac{\theta}{N}\Omega\right) = I + 2\alpha\frac{\theta}{N} + M_1(N)$$

Then we define one such cycle from the described pulse sequence as

$$\begin{aligned}\Phi &\equiv \exp\left(\frac{\theta}{N}(\alpha-\beta)\Omega\right)\exp\left(\frac{\theta}{N}(\alpha+\beta)\Omega\right)\\ &= \left(I + \frac{\theta}{N}(\alpha-\beta)\Omega + O\left(\frac{1}{N^2}\right)\right)\left(I + \frac{\theta}{N}(\alpha+\beta)\Omega + O\left(\frac{1}{N^2}\right)\right)\\ &= I + 2\alpha\frac{\theta}{N}\Omega + M_2(N)\end{aligned}$$

where $M_1(N)$ and $M_2(N)$ are matrices with finite entries and maximum order of $1/N^2$. Therefore the difference is on the order of $\frac{1}{N^2}$ and likewise $E\left(\Phi, \exp\left(2\alpha\frac{\theta}{N}\Omega\right)\right)$ is of order $\frac{1}{N^2}$ so that

$$\begin{aligned}E_{\text{Total}} &\equiv E\left(\Phi^N, \exp\left(2\alpha\theta\Omega\right)\right)\\ &\leq NE\left(\Phi, \exp\left(2\alpha\frac{\theta}{N}\Omega\right)\right)\\ &\sim \frac{1}{N}\end{aligned} \tag{3.20}$$

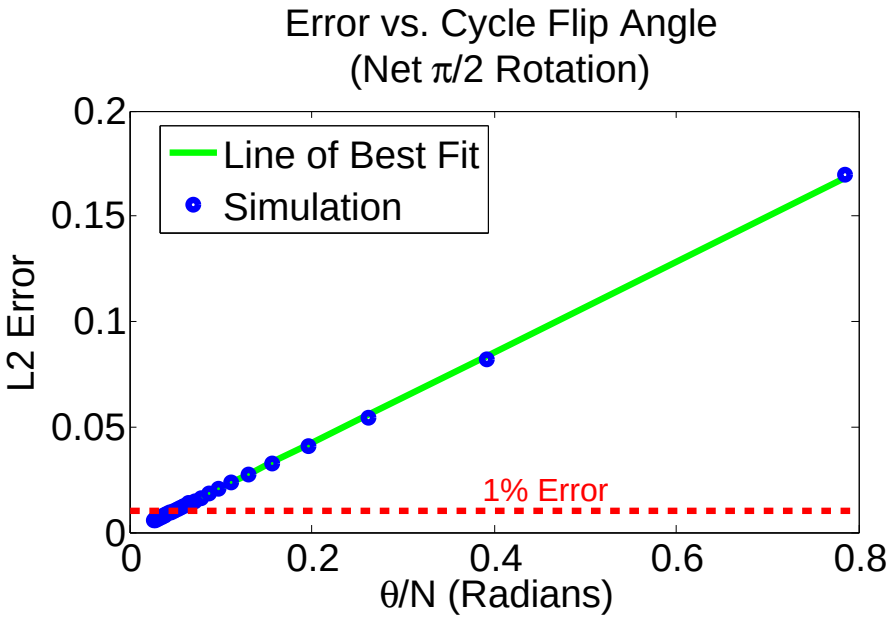

Figure 3.4: Deviation of $\left[U_1\left(\frac{\theta_1}{N}\right)\right]^N$ from $\exp(2\theta_1\cos(\omega\tau_r)\Omega_x)$ due to the commutation assumption in equation (3.16) for $\theta_1 = \frac{\pi}{4}$ and $\tau_r = 2\pi$. As calculated in equation (3.20), the error is proportional to $\frac{\theta_1}{N}$ as indicated by the adherence to the line of best fit. The red line indicates the 1% error level.

where we made use of the inequality

$$\begin{aligned}
||A^n - B^n|| &= ||A^n - A^{n-1}B + A^{n-1}B - A^{n-2}B^2 + A^{n-2}B^2 - \cdots + AB^{n-1} - B^n|| \\
&= ||A^{n-1}(A-B) + A^{n-2}B(A-B) + \cdots + B^{n-1}(A-B)|| \\
&\leq ||A^{n-1}(A-B)|| + ||A^{n-2}B^2(A-B)|| + \cdots + ||B^{n-1}(A-B)|| \\
&= ||A-B|| + ||A-B|| + \cdots + ||A-B|| \\
&= n||A-B||
\end{aligned}$$

for any rotation matrices A and B.

Therefore reducing the flip angle per cycle and applying more cycles allows for arbitrary reduction in the error due to the commuting assumption. Figure 6 displays

this pictorially and confirms the linear decay in error. We see that θ around $\pi/20$ results in $< 1\%$ error. In practice, flip angles smaller than about 10 degrees commute satisfactorily.

Hard Pulse Error

The second source of error is the accumulation of the small amount of drift that occurs during the execution of the RF pulses. In section A we showed that to first order in ϵ the error is $6\theta\epsilon$, so it suffices to show that the sum of the RF flip angles is well bounded to provide a bound on the total error. Noting that $\phi(\omega) \in [-\pi, \pi]$ for all ω since it represents a rotation and applying Parseval's Theorem to (3.17), we find

$$\frac{1}{2B}\int_{-B}^{B}\phi^2(\omega)d\omega \leq \pi^2 \tag{3.21}$$

$$\Rightarrow \quad \sum_i (2\theta_i)^2 \leq \pi^2 \tag{3.22}$$

$$\Rightarrow \quad 2\sum_i \theta_i \leq \sqrt{n}\pi \tag{3.23}$$

where the last inequality follows from noting the worst case corresponds $\theta_i = \frac{\pi}{2\sqrt{n}}$ for all i and n is the number of terms kept in the Fourier expansion. Assuming a threshold value θ_{TH} for the maximum flip angle per cycle and noting that each U_n

requires two π pulses, we conclude that the total error is bounded by

$$\begin{aligned} E_{RF} &\leq 12\epsilon \sum_i \left(\pi \left\lceil \frac{\theta_i}{\theta_{TH}} \right\rceil + \theta_i \right) \\ &\leq 12n\epsilon \left(\pi \left\lceil \frac{\theta_i}{\theta_{TH}} \right\rceil + \theta_i \right) \\ &\leq 12n\epsilon \left(\pi \frac{\theta_i}{\theta_{TH}} + \theta_i + \pi \right) \\ &\leq \epsilon \left(6\pi\sqrt{n} \left(\frac{\pi}{\theta_{TH}} + 1 \right) + 12\pi n \right). \end{aligned} \tag{3.24}$$

Again we assume that ϵ is sufficiently small so that this error term is negligible.

3.4.4 Anti-Aliasing Method

The dispersion compensation method described in section B is vulnerable to aliasing due to the time scale, τ_r required for the periodic drift to average out. Here we describe a method of overcoming this shortcoming.

Making use of the periodic nature of the drift Hamiltonian (see figure 9), we define the functional

$$I_{t_p}\{f(\cdot)\} = \int_0^{t_p} f(t)dt - \int_{t_p}^{\frac{\tau_r}{2}} f(t)dt + \int_{\frac{\tau_r}{2}}^{\frac{\tau_r}{2}+t_p} f(t)dt - \int_{\frac{\tau_r}{2}+t_p}^{\tau_r} f(t)dt \tag{3.25}$$

where $0 \leq t_p \leq \pi/w_r$. Notice that

$$\begin{aligned} I_{t_p}\{H_0\} &= w(4t_p - \tau_r)\Omega_z + I_{t_p}\{A\cos(w_r t + \gamma)\} \\ &= w(4t_p - \tau_r)\Omega_z \end{aligned} \tag{3.26}$$

also eliminates the dependence on A and γ. Explicitly, we effect the net rotation using the controls to produce rapid π pulses at times $t = \{t_p, \frac{\tau_r}{2}, \frac{\tau_r}{2} + t_p, \tau_r\}$ with the system evolving under the drift Hamiltonian at other times.

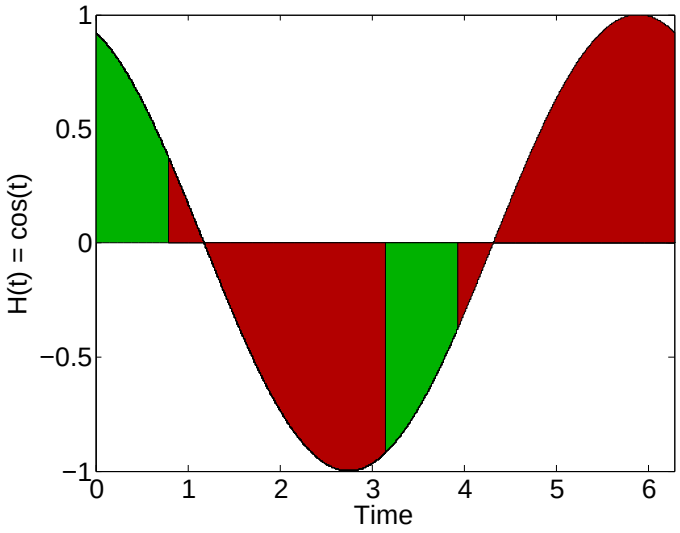

Figure 3.5: Diagram of intraperiod cancellations in $I_{t_p}\{H(t)\}$. The red area corresponds to evolving under the periodic drift, and the green represents negative drift accomplished by a rapid π pulse at the boundaries. Cancellation occurs for values separated by π radians since $\cos(\phi) = -\cos(\phi+\pi)$ resulting in no net evolution from the periodic drift (red areas and green areas cancel themselves).

Considering t_p as a design parameter motivates the definition of

$$\begin{aligned} U_n^* &= \exp\left(I_{t_p}\{H_0\}\right)^n \exp(\theta_n \Omega_x) \exp\left(-I_{t_p}\{H_0\}\right)^{2n} \\ &\quad \times \exp(\theta_n \Omega_x) \exp\left(I_{t_p}\{H_0\}\right)^n \qquad (3.27) \\ &\approx \exp(2\theta_n \cos(nw(4t_p - \tau_r))\Omega_x) \qquad (3.28) \end{aligned}$$

which is simply U_n with the H_0 evolutions replaced by $[I_{t_p}(H_0)]^n$. Since t_p and thereby $4t_p - \tau_r$ is a design parameter, we can avoid aliasing issues by appropriate selection of t_p. Specifically, we wish to avoid the aliasing condition $\exists \omega_1, \omega_2$ such that $(\omega_1 - \omega_2)(4t_p - \tau_r) = 2\pi$, which can be accomplished no matter how wide the range of ω of interest since $4t_p - \tau_r$ can be made arbitrarily small.

3.4.5 Selecting θ_n Coefficients for Frequency Dependent Rotations

We have shown how to produce rotations of the form

$$U_n^* = \exp(2\theta_n \cos(n\omega(4t_p - \tau_r))\Omega_x) \tag{3.29}$$

with arbitrary precision. By executing a sequence of such rotations we can produce a net rotation

$$U = \exp\left(\sum_n 2\theta_n \cos(n\omega(4t_p - \tau_r))\Omega_x\right) \tag{3.30}$$

which reduces the problem to finding the appropriate coefficients θ_n.

We will assume the frequency range of interest is of the form $\omega \in [-B, B]$. If $B\tau_r > \pi$, t_p is selected so that $B(4t_p - \tau_r) = \pi$; this removes aliasing as previously described. By way of direct integration we have

$$\frac{1}{B}\int_{-B}^{B} \cos(n\omega(4t_p - \tau_r)) \cos(n'\omega(4t_p - \tau_r))d\omega = \delta_{nn'} \tag{3.31}$$

Suppose we wish to produce the rotation $\phi(w)\Omega_x$. Then the coefficients are calculated as follows (combining (3.30) and (3.31))

$$\begin{aligned} \theta_0 &= \frac{1}{4B}\int_{-B}^{B} \phi(\omega)d\omega \\ \theta_n &= \frac{1}{2B}\int_{-B}^{B} \phi(\omega)\cos(n\omega(4t_p - \tau_r))d\omega \end{aligned} \tag{3.32}$$

Noting that the same analysis applies to y-axis rotations and that all rotations on the Bloch sphere can be decomposed into x and y rotations via Euler angle decomposition, this completes the design law algorithm.

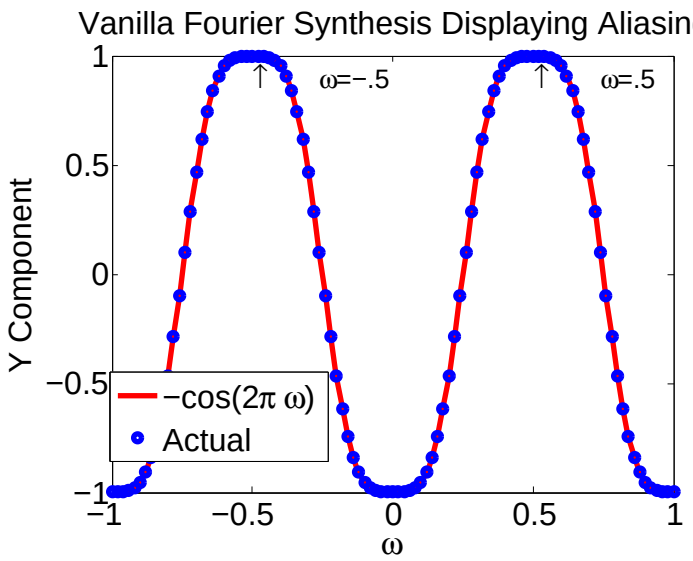

Figure 3.6: $\left[U_1\left(\frac{\pi}{20}\right)\right]^5$ with $\omega_r = 1$. Closely matches the expected rotation $\exp(\frac{\pi}{2}\cos(\omega\tau_r)\Omega_x)$ as calculated in equation (3.16). Since $\tau_r = 2\pi$, aliasing occurs for ω values separated by 1 unit.

3.5 Simulations

All simulations were performed in Matlab version 2008b and the code can be found at `http://www.people.fas.harvard.edu/~owrutsky/periodicPaper.m`.

As a concrete example we will consider frequencies in the range $\omega = [-1, 1]$ with $\omega_r = 1$. We will be interested in producing a robust selective excitation for $\omega \in [-.5, .5]$.

As a first step we apply the standard Fourier method with only U_1 and $\theta_1 = \frac{\pi}{4}$. This produces a net rotation of $\exp\left(\frac{\pi}{2}\cos(2\pi\omega t)\Omega_x\right)$. Figure 3.6 displays the results. As expected, aliasing occurs for $(\omega_1 - \omega_2)\tau_r = 2\pi$ which corresponds to ω separated by 1 unit and therefore the standard algorithm will not be able to produce the excitation profile we desire.

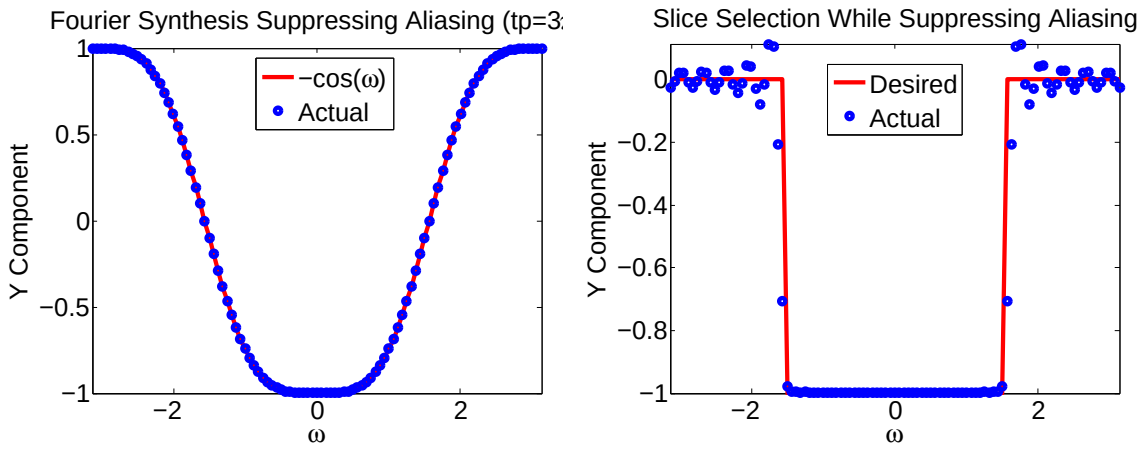

Figure 3.7: $\left[U_1^*\left(\frac{\pi}{20}\right)\right]^5$ with $\omega_r = 1$ and $t_p = 3\pi/4$ so that $(w_{\max} - \omega_{\min})(4t_p - \tau_r) = 2\pi$, which suppresses the aliasing present in $\left[U_1\left(\frac{\pi}{20}\right)\right]^5$ seen in figure 3.6.

To suppress the aliasing we select $t_p = 3/4\pi$ so that $4t_p - \tau_r = \pi$ and

$$(w_{\max} - \omega_{\min})(4t_p - \tau_r) = 2\pi$$

Figure 3.7 displays the results and shows that the aliasing has been successfully removed. By appropriate choice of $\{\theta_n\}$ selective excitation will be possible.

We calculate $\{\theta_n\}$ using (3.32)

$$\begin{aligned} \theta_0 &= \frac{1}{4}\int_{-.5}^{.5} \frac{\pi}{2} dw = \frac{\pi}{8} \\ \theta_n &= \frac{1}{2}\int_{-.5}^{.5} \frac{\pi}{2}\cos(n\pi w) = \frac{\sin(\frac{n\pi}{2})}{2n} \end{aligned} \tag{3.33}$$

Figure 3.7 shows the results of the slice selection. We kept the first 20 terms in the Fourier expansion, but in practice the number of terms should be determined by the acceptable level of side band noise and desired duration of the pulse sequence. As the figure indicates, slice selection is readily accomplished while suppressing aliasing.

3.6 Conclusion

We have presented a method to design control laws for selective excitation of the Larmor frequencies, ω in the presence of a periodic drift when both its amplitude and phase are unknown. These methods are of immediate use to solid state NMR experiments where magic angle spinning leads to a Hamiltonian with periodic drift.

Chapter 4

Periodic Drift in the Limit of Low RF-Field Strength

4.1 Abstract

This chapter continues the study of systems with a periodic drift of known frequency, but random amplitude and phase. We extend the previous chapter's results to the low RF-field limit, where the control amplitudes are no longer assumed large relative to the other parameters of the system's dynamics. We show that applying constant amplitude pulses at rotor periods makes the effect of the periodic drift negligible, which motivates restricting our candidate controls to this class of periodically pulsed sequences. The challenge is to show that the class of periodically pulsed controls with arbitrarily small amplitudes is sufficiently rich to establish controllability of the ensemble, and ultimately to develop such control pulses.

Controlling the maximum amplitude of a pulse sequence is difficult. In the ab-

sence of a periodic drift, one way to invert a broad spectrum of spins with weak RF amplitude is to use an adiabatic pulse. We show how an adiabatic pulse can be converted to a periodically pulsed sequence, effectively removing the periodic drift from the system, to produce broadband inversions with arbitrarily small control field amplitudes. Leveraging the results from the pervious chapter, these broadband inversions are then used to show controllability of the ensemble. Again, systems with such random periodic drifts arise in Magic angle spinning (MAS) magnetic resonance experiments, and applications include selective inversion of isotropic chemical shifts in solid state nuclear magnetic resonance experiments.

4.2 Introduction

In this chapter, we study the control of an ensemble of Bloch equations, containing a drift component that is random and time varying, yet still periodic. The drift averages over a period to a nonzero value, which we call the DC portion of the drift. The goal is to simultaneously steer the ensemble of spins from the north pole to a desired arbitrary point or set of points on the Bloch Sphere that have a functional dependence on this DC value.

The previous chapter reduced this problem to producing broadband, robust inversions. The focus of this chapter will be to construct such a pulse sequence in the limit of arbitrarily small RF-field power. We show how this can be accomplished by applying pulses at periodic intervals, such that over this interval, the random portion of the drift averages to zero. We do not assume that strong RF pulses are available, and the construction will have the property that the amplitude of the pulses can be

made arbitrarily small. The ability to invert spins over a broad range enables the construction of pulse sequences that are selective for specific isotropic resonances or chemical shifts.

The problem arises in selective inversion pulses in solid state nuclear magnetic resonance (NMR), whereby the goal is to selectively invert isotropic chemical shifts in the presence of large chemical shift anisotropies. In Magic angle spinning (MAS) NMR experiments, the chemical shift anisotropies manifest as time varying resonance frequencies with randomness resulting from powder dispersion of the chemical shift tensor. This leads to the following Bloch equation [13]

$$\dot{X} = \{(\omega + \omega_p(t))\Omega_z + u\Omega_x + v\Omega_y\}X, \tag{4.1}$$

where $\omega_p(t + \tau_r) = \omega_p(t)$, ω is the DC value, τ_r is the rotor period of the MAS apparatus and throughout this chapter we use

$$\Omega_x = \begin{bmatrix} 0 & 0 & 0 \\ 0 & 0 & -1 \\ 0 & 1 & 0 \end{bmatrix}, \quad \Omega_y = \begin{bmatrix} 0 & 0 & 1 \\ 0 & 0 & 0 \\ -1 & 0 & 0 \end{bmatrix}, \quad \Omega_z = \begin{bmatrix} 0 & -1 & 0 \\ 1 & 0 & 0 \\ 0 & 0 & 0 \end{bmatrix}$$

to denote the generators of rotations about their respective axes.

The main result of this chapter is the construction of pulse sequences with arbitrarily weak pulses, given at Rotor Echoes, which produce broadband and selective inversions. Further applications of the proposed construction may include broadband and selective inversion sequences in quadrupolar nuclei in the presence of anisotropic chemical and quadrupolar shifts.

In this direction, previous work has developed DANTE sequences from a parent adiabatic pulse that preserve either the fidelity or the bandwidth of the parent pulse,

but not both [33, 34]. Both properties are a necessary component of general excitation schemes [32]. Experimental results in [35] indicate that adiabatic pulses are ineffective in the presence of quadrupole shifts under MAS, further necessitating alternative techniques.

This chapter is structured as follows: First we display the limited applicability of DANTE and adiabatic sequences for systems with periodic drift. Next we show how short duration, constant amplitude pulses applied at rotor periods, effectively remove the periodic drift component from the system dynamics. The next section develops the components necessary to produce broadband inversions within this restricted class of controls. The last section presents simulations of the proposed pulse sequences.

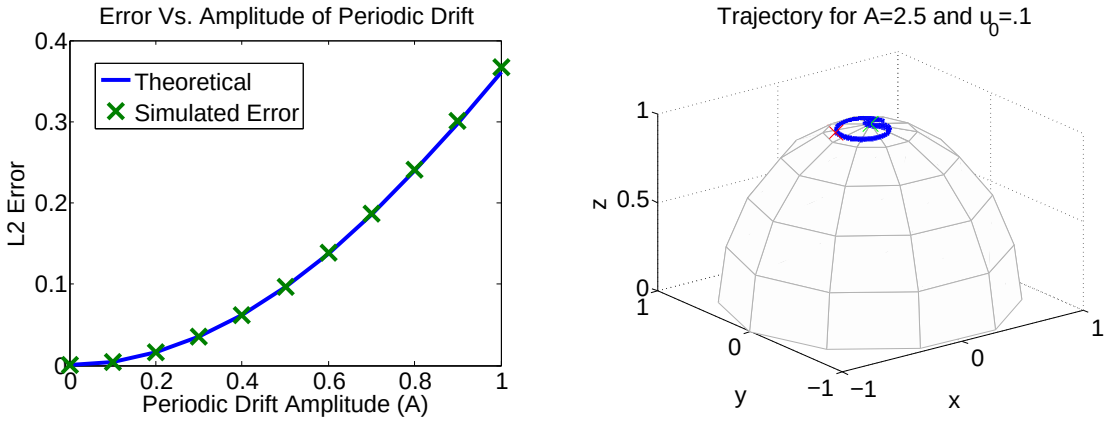

Figure 4.1: (Left) L2 error (calculated according to eq. 2.2) of weak irradiation with respect to the desired final magnetization $[0, 1, 0]'$, as a function of periodic drift amplitude A. System parameters are: $\omega = 1$, $\omega_r = 1$, control amplitude $u_0 = 0.1$, and on resonance controls, $(u(t), v(t)) = u_0(\cos(\omega t), \sin(\omega t))$. (Right) Trajectory in the rotating frame with A=2.5, resulting in virtually no excitation.

4.3 Traditional Methods Under Periodic Drift

To fix ideas, we return to eq. (4.1) and consider a periodic drift with a single harmonic

$$\dot{X} = [(\omega + A\cos(\omega_r t + \gamma))\Omega_z + u\Omega_x + v\Omega_y]X, \tag{4.2}$$

where the frequency ω_r is assumed to be precisely known, but A and γ are random fixed quantities.

In the absence of periodic drift ($A = 0$), weak irradiation is frequently used to produce selective excitations with corresponding final magnetization $[0, 1, 0]'$. However, as we have shown in chapter 3, for systems with non-zero periodic drift ($A > 0$), this results in an error that to first order is $J_0\left(\frac{A}{w_r}\right)$, where J_0 is the zeroth order Bessel function of the first kind. As figure (4.1) displays, for $\frac{A}{\omega_r}$ approaching 1, this results in significant excitation attenuation and for values of 2 and larger essentially no excitation occurs.

Another commonly employed technique is using adiabatic passages for broadband inversion. While we defer an in depth description of adiabatic passages to section 4.5.2, figure (4.2) shows that periodic drift causes unpredictable behavior for adiabatic passages even for relatively small amplitudes A.

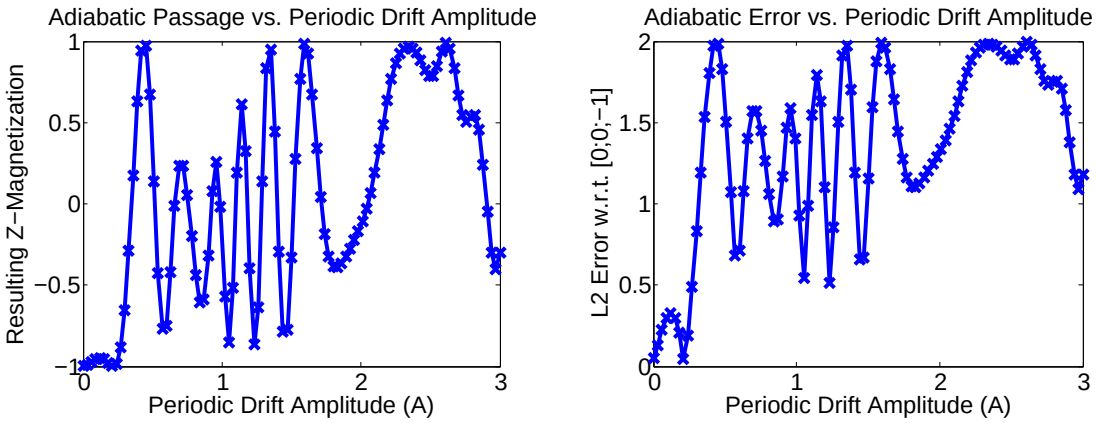

Figure 4.2: Resulting z-magnetization (Left) and L2 error with respect to the desired final magnetization $[0, 0, -1]'$ (Right), for a linearly swept adiabatic pulse as a function of periodic drift amplitude A, with system parameters $\omega = 0$, $\omega_r = 1$ and $\gamma = \frac{\pi}{2}$. Pulse Parameters are: $a = 0.001$, $u_0 = 0.1$, pulse duration $T = 2\pi/a$, modulation function $\phi(t) = -\pi t + at^2/2$ and $(u(t), v(t)) = u_0(\cos\phi(t), \sin\phi(t))$.

4.4 Periodic Pulsing of Systems with a Periodic Drift

In this section, we consider the effect of controls implemented at integral multiples of the drift period τ_r (also called rotor periods) on eq. (4.1)

$$\dot{X} = \{(\omega + \omega_p(t))\Omega_z + u\Omega_x + v\Omega_y\}X.$$

We will show that using such controls effectively removes the periodic drift and motivates considering controls within this restricted class.

Theorem 4.4.1. *Let $n' = \frac{\tau_r}{\Delta t}$ and F be the propagator under the free evolution Hamiltonian which includes isotropic chemical shift ω and time varying chemical shit*

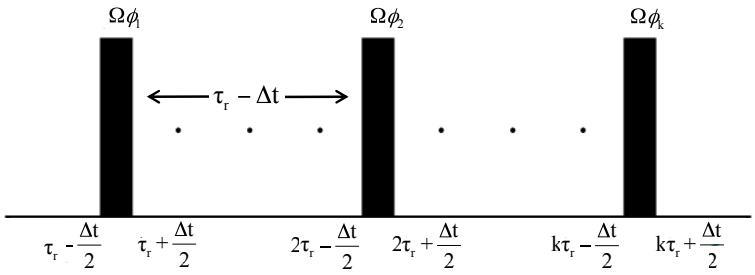

Figure 4.3: Rotor Period Pulsing.

anisotropy $\omega_p(t)$*, then*

$$F\left((n'-\frac{1}{2})\Delta t\right)\exp\left(\oint_{k\tau_r-\frac{\Delta t}{2}}^{k\tau_r+\frac{\Delta t}{2}}\underbrace{(\omega+\omega_p(t))\Omega_z}_{H_0(t)}+\underbrace{u\Omega_\phi}_{H_1}\,dt\right)F\left((n'-\frac{1}{2})\Delta t\right)$$
$$=\exp\left(n'\omega\Delta t\Omega_z\right)\exp(u\Delta t\Omega_\phi)\exp\left(n'\omega\Delta t\Omega_z\right)+O(\Delta t^3)$$

where k *indexes the free evolution periods of length* τ_r *and* $\exp\left(\oint H(t)dt\right)$ *denotes the evolution propagator under the Hamiltonian* H*.*

Proof. Applying the Zassenhaus formula and using the periodicity of $H_0(t)$, we calculate

$$\exp\left(\oint_{k\tau_r-\frac{\Delta t}{2}}^{k\tau_r}H_0(t)+H_1dt\right)=\exp\left(\oint_{-\frac{\Delta t}{2}}^{0}H_0(t)+H_1dt\right)$$
$$=\left[I+\int_{-\frac{\Delta t}{2}}^{0}[H_0(t),\int_{-\frac{\Delta t}{2}}^{t}H_1d\sigma]dt+O(\Delta t^3)\right]\exp\left(\int_{-\frac{\Delta t}{2}}^{0}H_1dt\right)\exp\left(\int_{-\frac{\Delta t}{2}}^{0}H_0(t)dt\right)$$

Similarly

$$\exp\left(\oint_{k\tau_r}^{k\tau_r+\frac{\Delta t}{2}}H_0(t)+H_1dt\right)$$
$$=\exp\left(\int_0^{\frac{\Delta t}{2}}H_0(t)dt\right)\exp\left(\int_0^{\frac{\Delta t}{2}}H_1dt\right)\left[I+\int_0^{\frac{\Delta t}{2}}[H_1,\int_0^{t}H_0(\sigma)d\sigma]dt+O(\Delta t^3)\right]$$

Evaluating to leading order we have

$$
\begin{aligned}
& \left[I + \int_0^{\frac{\Delta t}{2}} [H_1, \int_0^t H_0(\sigma) d\sigma] dt + O(\Delta t^3)\right] \left[I + \int_{-\frac{\Delta t}{2}}^0 [H_0(t), \int_{-\frac{\Delta t}{2}}^t H_1 d\sigma] dt + O(\Delta t^3)\right] \\
= & \left[\int_0^{\frac{\Delta t}{2}} [H_1, \int_0^t H_0(\sigma) d\sigma] dt\right] + \left[\int_{-\frac{\Delta t}{2}}^0 [H_0(t), \int_{-\frac{\Delta t}{2}}^t H_1 d\sigma] dt\right] + O(\Delta t^3) \\
= & \left[\int_0^{\frac{\Delta t}{2}} [u\Omega_\phi, \int_0^t (\omega + A\cos(\omega_r \sigma + \gamma))\Omega_z d\sigma] dt\right] \\
& \quad + \left[\int_{-\frac{\Delta t}{2}}^0 [(\omega + A\cos(\omega_r t + \gamma))\Omega_z, \int_{-\frac{\Delta t}{2}}^t u\Omega_\phi d\sigma] dt\right] + O(\Delta t^3) \\
= & \left[\int_0^{\frac{\Delta t}{2}} u\left(\omega t + \frac{A}{\omega_r}(\sin(\omega_r t + \gamma) - \sin(\gamma))\right)\Omega_{\phi - \pi/2} dt\right] \\
& \quad + \left[\int_{-\frac{\Delta t}{2}}^0 u\left(t + \frac{\Delta t}{2}\right)(\omega + A\cos(\omega_r t + \gamma))\Omega_{\phi + \pi/2} dt\right] + O(\Delta t^3) \\
= & \frac{1}{8}(u\omega + Au\cos(\gamma))\Delta t^2 \Omega_{\phi - \pi/2} + \frac{1}{8}(u\omega + Au\cos(\gamma))\Delta t^2 \Omega_{\phi + \pi/2} + O(\Delta t^3) \\
= & O(\Delta t^3)
\end{aligned}
$$

where we used $\Omega_{\phi+\pi} = -\Omega_\phi$. Therefore

$$
\begin{aligned}
& F\left((n' - \frac{1}{2})\Delta t\right) \exp\left(\oint_{k\tau_r - \frac{\Delta t}{2}}^{k\tau_r + \frac{\Delta t}{2}} (\omega + \omega_p(t))\Omega_z + u\Omega_\phi dt\right) F\left((n' - \frac{1}{2})\Delta t\right) \\
= & \left[F\left((n' - \frac{1}{2})\Delta t\right) \exp\left(\int_{-\frac{\Delta t}{2}}^0 H_0(t) dt\right) \exp\left(\int_{-\frac{\Delta t}{2}}^0 H_1 dt\right) + O(\Delta t^3)\right] \\
& \quad \times \left[\exp\left(\int_0^{\frac{\Delta t}{2}} H_1 dt\right) \exp\left(\int_0^{\frac{\Delta t}{2}} H_0(t) dt\right) F\left((n' - \frac{1}{2})\Delta t\right) + O(\Delta t^3)\right] \\
= & F\left(n'\Delta t\right) \exp(u\Delta t \Omega_\phi) F\left(n'\Delta t\right) + O(\Delta t^3) \\
= & \exp\left(n'\omega\Delta t\Omega_z\right) \exp(u\Delta t\Omega_\phi) \exp\left(n'\omega\Delta t\Omega_z\right) + O(\Delta t^3)
\end{aligned}
$$

as claimed. □

This theorem shows that under rotor period pulsing, the effect of the periodic

Hamiltonian is negligible. Therefore, it suffices to consider the following system

$$\dot{X} = (\omega\Omega_z + u\Omega_x + v\Omega_y)X, \tag{4.3}$$

with the additional constraints that u, v be piecewise constant controls implemented at rotor periods. The challenge is to show that this limited set of control inputs is rich enough to control the system. The following section develops a pulse from this class of controls for broadband inversion based on a parent adiabatic passage.

4.5 Broadband Inversion with Periodic Pulsing

In this section we consider a system without periodic drift and construct pulsed controls to produce a broadband inversion. The main challenge is to work around the fixed period delay in theorem 4.4.1, necessary to remove the periodic component of the drift. A brute force approach of discretizing a parent pulse and applying at rotor periods is rendered ineffective because of this delay.

We present a pulse sequence based on a parent adiabatic pulse that we show produces a broadband inversion, while only requiring short duration pulses at rotor periods. These controls have the desirable property that they maintain the parent adiabatic pulse's properties, namely large range RF field insensitivity and preserves both the bandwidth and adiabatic quality of the parent pulse. In conjunction with the previous section, this establishes a constructive method for broadband inversion in the presence of a periodic drift.

Let τ_r be a fixed period nominally set to 1. We consider frequencies $\omega \in [-\frac{B}{2}, \frac{B}{2}]$ such that $B\tau_r \in (-2\pi, 2\pi)$. Given an L2 error tolerance ϵ, a unit vector $X \in R^3$ and

the Bloch equation,

$$\dot{X} = \{\omega\Omega_z + u\Omega_x + v\Omega_y\}X,$$

the goal is to construct a bounded amplitude pulse sequence with pulses applied at discrete time intervals τ_r, i.e. $(u(t), v(t)) = u(\cos(\theta_k), \sin(\theta_k))$ with $t \in [k\tau_r - \frac{\Delta t}{2}, k\tau_r + \frac{\Delta t}{2}]$, $u < u_0$ and u zero elsewhere, such that $\int_{-\frac{B}{2}}^{\frac{B}{2}} ||X_T(\omega) - X_F||^2 d\omega \leq \epsilon$ for $X_F = [0, 0, -1]'$. We call this pulsed ensemble controllability.

The following subsection outlines the main ideas behind the construction of a pulse sequence that ensures all frequencies of interest can be inverted with arbitrarily small RF power, while at the same time enabling the error to be made arbitrarily small.

4.5.1 Methodology

1. Construct an adiabatic pulse with constant linear sweep rate a, which inverts all frequencies over the range $\omega \in [-\frac{B}{2}, \frac{B}{2}]$. Linear sweep, adiabatic pulses will be reviewed in detail in the following section.

2. Construct a piecewise constant approximation to the adiabatic pulse such that $t_{k+1} - t_k = \Delta t$, the error introduced is $||X(\omega, u, \phi(t)) - X(\omega, u, \phi_k)|| \sim O(\Delta t^3)$

3. Apply $2n + 1$ frequency shifted versions of the discretized pulse with the offset taking values $w - kB$ with $k \in \pm\{0, 1, ..., n\}$. When the offset is zero, the frequency range $\omega \in [-\frac{B}{2}, \frac{B}{2}]$ is inverted. The remaining $2n$ applications will be shown to only perturb the magnetization controllably. The result is that the frequency range $\omega \in [-\frac{(2n+1)B}{2}, \frac{(2n+1)B}{2}]$ is inverted where $(2n + 1)\Delta t = \tau_r$.

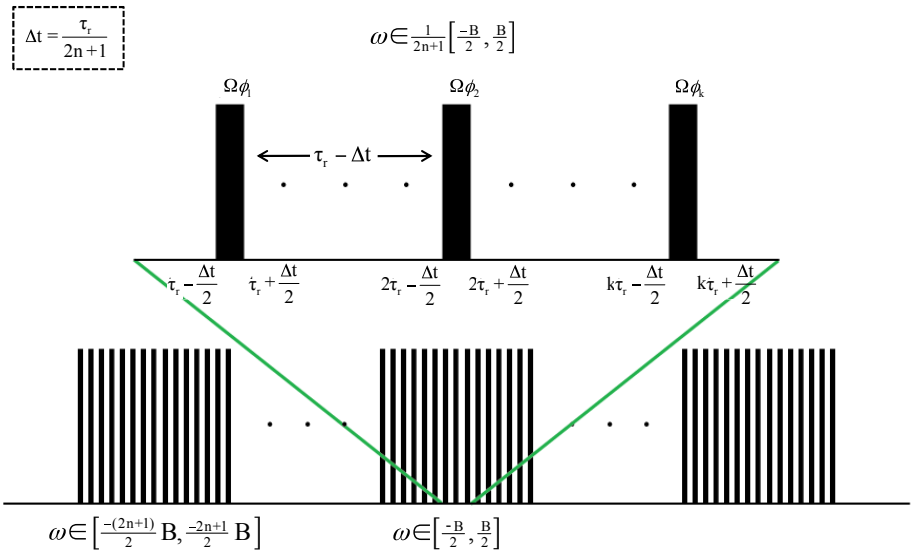

Figure 4.4: Pulse schematic for broadband inversion by periodic pulsing in the presence of a periodic drift. Adiabatic sequences are discretized and implemented at rotor periods, necessitating multiple passages due to bandwidth compression.

4. Apply the discretized pulses at rotor periods. Free evolution periods under such periodic pulsing effectively dilate time from Δt to $(2n+1)\Delta t$; this compresses the bandwidth and reverts the excitation band to the original range $\omega \in [-\frac{B}{2}, \frac{B}{2}]$.

Combining these pieces provides a constructive method for producing broadband inversion by periodic pulsing while maintaining the properties of the original adiabatic pulse. We continue by describing each step in turn.

4.5.2 Linear Sweep Adiabatic Sequence

The first ingredient is a broadband inversion pulse sequence through an adiabatic pulse. We show how this can be done using a linear sweep modulation function and can be achieved with arbitrarily small control amplitudes.

Consider $(u(t), v(t)) = u_0(\cos(\phi(t)), \sin(\phi(t)))$ with $\phi(t) = -Ct + \frac{at^2}{2}$, $C = \frac{B}{2} + \Delta B$, $\frac{u_0}{\Delta B} < \alpha$ and $0 \leq t \leq \frac{2C}{a}$. Substituting into the Bloch Equations, we have

$$\dot{X} = \{w\Omega_z + u_0 \cos\phi(t)\Omega_x + u_0 \sin\phi(t)\Omega_y\}X. \tag{4.4}$$

Provided a is sufficiently small, we will show that all systems can be steered from an initial state $X_0 = [0, 0, 1]'$ to an inverted final state $X_T = [0, 0, -1]'$. To see this, we make the change of variables $Y = \exp(-\phi(t)\Omega_z)X$. Then

$$\begin{aligned} Y &= \exp(-\phi(t)\Omega_z), & (4.5)\\ \dot{Y} &= \{\overbrace{\underbrace{(w + C - at)}_{\omega - \dot{\phi}}\Omega_{z'} + u_0\Omega_{x'}}^{\tilde{\omega}\Omega_{z''}}\}Y, & (4.6) \end{aligned}$$

where the RF phase has been relocated to an additional frequency offset. As is convention, we refer to the Y frame as the frequency modulated (FM) frame and denote it with primes in figure 4.5 . Note that a broadband inversion in the FM frame corresponds to a broadband inversion in the lab frame X, since rotations about the z-axis leave the z-axis unchanged.

The FM frame does not offer sufficient intuition as to why the system stays locked to the effective field in eq. (4.6). To understand this property, we make the further change of coordinates into the so called B_{eff} frame

$$\begin{aligned} Z &= \exp(-\theta\Omega_{y'})Y & (4.7)\\ \dot{Z} &= \{\tilde{\omega}\Omega_{z''} - \dot{\theta}\Omega_{y''}\}Z & (4.8)\\ \tilde{\omega}\Omega_{z''} &= (w + C - at)\Omega_{z'} + u_0\Omega_{x'} & (4.9) \end{aligned}$$

where

$$\tilde{w} = \sqrt{u_0^2 + (w + C - at)^2}; \qquad \tan\theta(t) = \frac{u_0}{\omega - \dot{\phi}}; \qquad \dot{\theta} = \frac{u_0 a}{u_0^2 + (w + C - at)^2} \tag{4.10}$$

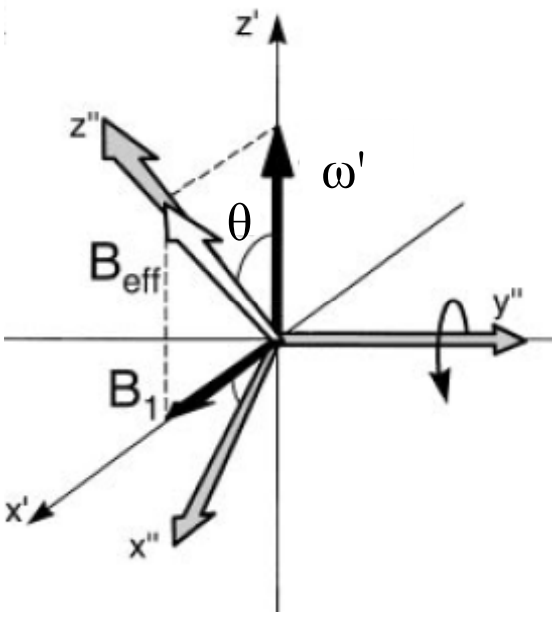

Figure 4.5: Illustration of an adiabatic passage. The singly primed frames corresponds to the FM frame, and the doubly primed, the B_{eff} frame.

and denote this frame with doubly primed axes. The motivation for the B_{eff} frame comes from considering its effect on the $\Omega_{z'}$ axis

$$\Omega_{z'} = e^{\theta\Omega_y}\Omega_{z''}e^{-\theta\Omega_y} \tag{4.11}$$

indicating that the $\Omega_{z''}$ axis rotates relative to $\Omega_{z'}$ by an angle θ, corresponding to the net sweep angle of the adiabatic passage as displayed in figure 4.5. Moreover, for $\dot{\theta} << \tilde{\omega}$ the magnetization vector will rotate about an axis almost parallel to the $\Omega_{z''}$ axis, causing a "phase locking" phenomenon. By additionally choosing $\theta(T) - \theta(0) \approx \pi$, the $\Omega_{z''}$ axis fully inverts relative to the $\Omega_{z'}$ axis, providing the intuition for adiabatic inversions.

We now calculate explicitly, let $s = \int_0^t \tilde{w}(\tau)d\tau$, then

$$\frac{dZ}{ds} = \{\Omega_{z''} - \underbrace{\frac{\dot{\theta}}{\tilde{w}(t)}}_{b(s)} \Omega_{y''}\}Z. \tag{4.12}$$

Making the final change of coordinates, $M = \exp(-s\Omega_{z''})Z$ we have

$$\frac{dM}{ds} = b(s) \underbrace{\exp(s\Omega_{z''})\Omega_{y''} \exp(-s\Omega_{z''})}_{\Omega(s)} M. \tag{4.13}$$

We now show that for $M(0) = [0, 0, 1]'$ we also have $M(2\pi) = [0, 0, 1]'$. To see this, we use the Peano Baker series in conjunction with the observation $b(s) \leq b_0 = \frac{a}{u_0^2}$

$$M(\tau) = I + \int_0^\tau b(\sigma_1)\Omega(\sigma_1)d\sigma_1 + \int_0^\tau b(\sigma_1)\Omega(\sigma_1) \int_0^{\sigma_1} b(\sigma_2)\Omega(\sigma_2)d\sigma_2 d\sigma_1 + ... \tag{4.14}$$

Now, $\Omega(s)$ is a rotation generator of the form

$$\Omega(s) = n_x(s)\Omega_x + n_y(s)\Omega_y + n_z(s)\Omega_z$$

$$n_x(s)^2 + n_y(s)^2 + n_z(s)^2 = 1.$$

Noting that $|\Omega_{x,y,z}| = \sqrt{2}$ and that Ω_x, Ω_y and Ω_z share no common non-zero elements,

$$|\Omega(s)| = \sqrt{n_x(s)^2 + n_y(s)^2 + n_z(s)^2}\sqrt{2} = \sqrt{2}.$$

Therefore $|\int_0^\tau \Omega(s)ds| \leq \sqrt{2}\tau$ where $|\cdot|$ denotes the Frobenius norm. If we consider $M(2\pi)$, for $k \geq 2$, the kth term in the Peano baker series is bounded by $(\sqrt{2}\pi b_0)^k$, so the 2nd order and above term's contribution is bounded by

$$\left| \sum_{k=2}^{\infty} (\sqrt{2}\pi b_0)^k \right| \leq (2\pi b_0)^2 \tag{4.15}$$

for $b_0 < \frac{1}{\sqrt{8}\pi}$. Therefore the higher order terms are safely neglected for sufficiently small sweep rates a.

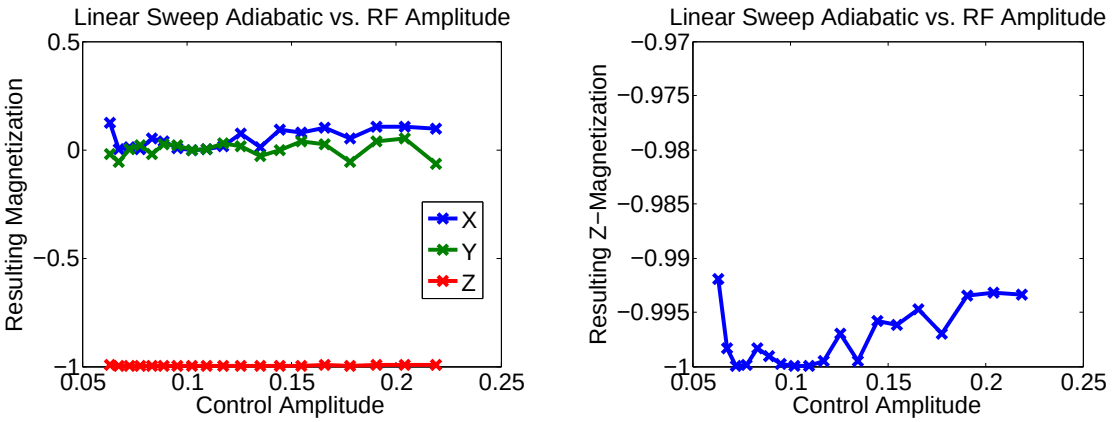

Figure 4.6: Resulting magnetization for a linearly swept adiabatic pulse as a function of RF amplitude for frequency $\omega = 0$. Pulse Parameters are: $a = 0.001$, $u_0 = 0.1$, pulse duration $T = 2\pi/a$, modulation function $\phi(t) = -\pi t + at^2/2$ and $(u(t), v(t)) = u_0(\cos\phi(t), \sin\phi(t))$. The pulse maintains 99% inversion over 2 orders of magnitude of control amplitude.

Evaluating the first order term using integration by parts and the bound on $b(s)$ we find

$$||I - M(2\pi)|| = \left|\left|\int_0^{2\pi} b(\sigma_1)\Omega(\sigma_1)d\sigma_1\right|\right| \leq 2\sqrt{2}\pi \left|\frac{db}{ds}\right|_{max}. \tag{4.16}$$

We can bound $\frac{db}{ds}$ by noting $\frac{db}{ds} = \frac{db}{dt}/\frac{ds}{dt}$ with

$$\frac{db}{dt} = \frac{d}{dt}\frac{\dot\theta}{\tilde\omega} = \frac{\ddot\theta}{\tilde\omega} - \frac{\dot\theta}{\tilde\omega^2}\dot{\tilde\omega} \tag{4.17}$$

$$\frac{\ddot\theta}{\tilde\omega} = \frac{2a^2u_0(w + C - at)}{(u_0^2 + (w + C - at)^2)^{5/2}} \tag{4.18}$$

$$\frac{\dot\theta}{\tilde\omega^2}\dot{\tilde\omega} = \frac{-a^2u_0(w + C - at)}{(u_0^2 + (w + C - at)^2)^{5/2}} \tag{4.19}$$

$$|\frac{db}{ds}| = \frac{\frac{\ddot\theta}{\tilde\omega} - \frac{\dot\theta}{\tilde\omega^2}\dot{\tilde\omega}}{\sqrt{u_0^2 + (w + C - at)^2}} \leq \frac{3a^2}{2u_0^4} \tag{4.20}$$

Combining with the bound on the higher order terms in eq. (4.15), the total error in the period $\tau = 2\pi$ is $E = \frac{3\sqrt{2}\pi a^2}{u_0^4} + (2\pi b_0)^2$. Noting that $\tilde\omega \leq C\epsilon$ where $\epsilon \leq 2 + \frac{u_0}{C}$,

the total error is

$$E_T = \frac{E}{2\pi}\int_0^T \tilde{\omega}(\tau)d\tau \leq \frac{2C^2\epsilon}{2\pi a}E = \underbrace{(3\sqrt{2}+4\pi)}_{\kappa}\frac{\epsilon a C^2}{u_0^4} = \frac{\overbrace{\epsilon\kappa}^{\epsilon_\kappa^{-1}} a C^2}{u_0^4}. \tag{4.21}$$

For a desired error tolerance E_T, we have the sweep rate condition

$$a \leq \frac{\epsilon_\kappa E_T u_0^4}{C^2}. \tag{4.22}$$

Therefore, arbitrarily complete inversion can be accomplished for a bandwidth $\omega \in [-\frac{B}{2}, \frac{B}{2}]$, using a linear adiabatic sweep. Moreover, inversion can be done with arbitrarily small control amplitudes.

4.5.3 Piecewise Constant Approximation

In the previous section, we showed that a linear sweep adiabatic passage can be used for arbitrarily complete inversion. In this section, we show that an adiabatic passage can be implemented as a piecewise constant control, with error that is proportional to $(\Delta t)^2$.

Theorem 4.5.1.

$$||X(\omega, u_0, \phi(t))) - X(\omega, u_0, \phi_k)|| \sim O(\Delta t^3)$$

over a time interval $\Delta t = t_{k+1} - t_k$, where the piecewise controls are given by

$$(u_k\Omega_x + v_k\Omega_y)\Delta t = u_0 \textstyle\int_0^{\Delta t} \cos(\phi_k + \omega_k\tau)\Omega_x + \sin(\phi_k + \omega_k\tau)\Omega_y d\tau$$

$$\phi_k = \omega_0 t_k + a t_k^2/2 \qquad\qquad \omega_k = \omega_0 + a t_k$$

Proof. We will do this by direct calculation of corresponding terms in the Peano Baker series, and note that 3rd order terms and above are bounded by $O(\Delta t^3)$ and safely ignored, so that it suffices to consider only the first and second order terms.

Directly calculating the first order term after making a change of variables

$$\begin{aligned} E_1 &= \Big| \int_0^{\Delta t} u_0(\cos(\phi_k + w_k\tau + a\tau^2/2) - \cos(\phi_k + w_k\tau))\Omega_x \\ &\qquad +u_0(\sin(\phi_k + w_k\tau + a\tau^2/2) - \sin(\phi_k + w_k\tau))\Omega_y d\tau \Big| \\ &= \Big| \int_0^{\Delta t} -u_0 \sin(\phi_k + w_k\tau)\sin(a\tau^2/2)\Omega_x + u_0\cos(\phi_k + w_k\tau)\sin(a\tau^2/2)\Omega_y d\tau \Big| \\ &\leq \frac{a u_0 \Delta t^3}{3} \end{aligned}$$

Similarly, we compute the error in the second order term in appendix D and state the result here,

$$\begin{aligned} E_2 &= \Big| \int_{t_k}^{t_{k+1}} (\omega\Omega_z + u_0\cos\phi(t)\Omega_x + \sin\phi(t)\Omega_y) \\ &\qquad \int_{t_k}^{t} (\omega\Omega_z + u_0\cos\phi(\tau)\Omega_x + \sin\phi(\tau)\Omega_y) d\tau dt \\ &\qquad -\frac{(\omega\Omega_z + u_k\Omega_x\Delta t + v_k\Omega_y\Delta t)^2}{2} \Big| \\ &= u_0(u_0+\omega)\omega_k O(\Delta t^3) \\ &\leq u_0 B^2 O(\Delta t^3) \end{aligned}$$

where the last follows from the adiabatic regime $\frac{u_0}{B} << 1$ and $\omega, \omega_k \leq B$. □

Lemma 1. *For any rotations $\{E_i\}$ and $\{F_i\}$,*

$$||\prod_{i=1}^{n} E_i - \prod_{i=1}^{n} F_i|| \leq \sum_{i=1}^{n} ||E_i - F_i||$$

Proof. The lemma follows by induction with the trivial base case

$$||\prod_{i=1}^{1} E_i - \prod_{i=1}^{1} F_i|| = ||E_1 - F_1|| \leq ||E_1 - F_1|| = \sum_{i=1}^{1} ||E_i - F_i||.$$

To show the induction hypothesis we note

$$\begin{aligned}
||\prod_{i=1}^{n} E_i - \prod_{i=1}^{n} F_i|| &= ||E_n \prod_{i=1}^{n-1} E_i - F_n \prod_{i=1}^{n-1} F_i|| \\
&= ||(E_n - F_n)\prod_{i=1}^{n-1} E_i + F_n(\prod_{i=1}^{n-1} E_i - \prod_{i=1}^{n-1} F_i)|| \\
&\leq ||(E_n - F_n)\prod_{i=1}^{n-1} E_i|| + ||F_n(\prod_{i=1}^{n-1} E_i - \prod_{i=1}^{n-1} F_i)|| \\
&= ||E_n - F_n|| + ||F_n(\prod_{i=1}^{n-1} E_i - \prod_{i=1}^{n-1} F_i)|| \\
&\overset{IH}{\leq} ||E_n - F_n|| + \sum_{i=1}^{n-1} ||E_i - F_i|| \\
&= \sum_{i=1}^{n} ||E_i - F_i||,
\end{aligned}$$

completing the proof. □

Corollary 4.5.2. *Approximating a complete adiabatic passage by such a piecewise approximation*

$$||\prod_{k=1}^{N} \Phi(\phi(t), t_k, t_{k+1}) - \prod_{k=1}^{N} \exp((\omega\Omega_z + u_k\Omega_x + v_k\Omega_y)\Delta t)|| \sim O(\Delta t^2)$$

over the range of inversion, where $N = \frac{B}{a\Delta t}$.

Proof. Follows from successive applications of theorem 4.5.1 and the previous lemma.

□

Figure 4.7 displays an example comparison of the piecewise approximation to a continuous adiabatic passage, and the deviation is well within the error bound of theorem 4.5.1.

It will prove convenient in subsequent analyses to use an approximation to u_k and v_k. We define the controls

$$u\Omega_{\tilde{\phi}_k}, \qquad \Omega_{\tilde{\phi}_k} = \cos\tilde{\phi}_k\Omega_x + \sin\tilde{\phi}_k\Omega_y$$
$$\tilde{\phi}_k = \phi_k + \tfrac{\omega_k\Delta t}{2}, \qquad \phi_k = \omega_0 t_k + a t_k^2,$$

Lemma 2.

$$|u\Omega_{\tilde{\phi}_k} - (u_k\Omega_x + v_k\Omega_y)| \sim O(\Delta t^2)$$

Proof.

$$\begin{aligned}
u_k &= \frac{u}{\Delta t}\int_0^{\Delta t}\cos(\phi_k + \omega_k\tau)d\tau \\
&= \frac{u}{\omega_k\Delta t}(\sin(\phi_k + \omega_k\Delta t) - \sin(\phi_k)) \\
&= \frac{u}{\omega_k\Delta t}(\sin(\phi_k)(\cos(\omega_k\Delta t) + \cos(\phi_k)\sin(\omega_k\Delta t))) \\
&= \frac{u}{\omega_k\Delta t}\left(\sin(\phi_k)\frac{(\omega_k\Delta t)^2}{2} + \cos(\phi_k)\left(\omega_k\Delta t - \frac{(\omega_k\Delta t)^3}{6}\right)\right) + O(\Delta t^4) \\
&= u\cos\left(\phi_k + \frac{\omega_k\Delta t}{2}\right) - \frac{1}{24}(\omega_k\Delta t)^2 \\
&= u\cos\tilde{\phi}_k + O(\Delta t^2)
\end{aligned}$$

Performing a similar calculation on v_k yields the analogous result

$$v_k = u\sin\tilde{\phi}_k + O(\Delta t^2),$$

which completes the proof. □

Corollary 4.5.3. *The piecewise constant controls $u\Omega_{\tilde{\phi}_k}$ generate an error that is $O(\Delta t)$ with respect to the parent adiabatic passage; explicitly,*

$$||\prod_{k=1}^{N}\Phi(\phi(t), t_k, t_{k+1}) - \prod_{k=1}^{N}\exp((\omega\Omega_z + u_k\Omega_x + v_k\Omega_y)\Delta t)|| \sim O(\Delta t)$$

Proof. Follows from lemma 2 and the triangle inequality. □

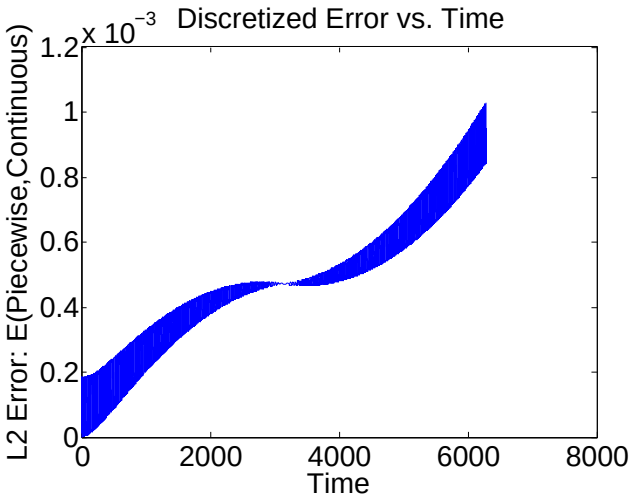

Figure 4.7: L2 error of a piecewise constant adiabatic pulse compared to its continuous counterpart over an entire pulse sequence. Pulse parameters are $\Delta t = 0.1, \omega = 0, u_0 = 0.1, a = 0.001$ and sweeps from $[-\pi, \pi]$ taking $2\pi/a$ units of time. Observed error is within the calculated bound in theorem 4.5.1.

4.5.4 Off Resonance

In this section we consider the effect of additional, off resonance adiabatic pulses and show that their effect on the magnetization is controllable and can be made arbitrarily small. This will be important in the next section to ensure that bandwidth is maintained under periodic pulsing. Specifically, we consider the effect of $2n$ off resonance adiabatic pulses with offsets taking values $\omega - kB$ and $k \in \{-n, -n+1, ..., -1, 1, ...n\}$. We begin by developing a few lemmas

Lemma 3. *Let*

$$\begin{aligned} \Theta_1 &= \exp(\theta_1 \Omega_1), \quad \Theta_2 = \exp(\theta_2 \Omega_2) \\ \Theta_3 &= \Theta_1 \Theta_2 \end{aligned}$$

with $|\theta_1|, |\theta_2| < \frac{\pi}{4}$ *and* Ω_1, Ω_2 *are arbitrary axes, then*

$$\Theta_3 = \exp(\delta_1 \Omega_z) \exp(\theta_3 \Omega_y) \exp(\delta_2 \Omega_z)$$

where $\theta_3 \leq |\theta_1| + |\theta_2|$.

That is to say, the flip angle generated by the product of two rotations is bounded by the sum of the individual flip angles.

Proof. We first consider the the case where the axes are transverse. By Euler angle decomposition, any rotation can be decomposed into 3 successive rotations using two axes as follows:

$$\exp(\theta\Omega) = \exp(\alpha_3 \Omega_z) \exp(\alpha_2 \Omega_x) \exp(\alpha_1 \Omega_z)$$

for some $\alpha_i \in (-\pi, \pi]$. Therefore

$$\Theta_1 \Theta_2 = \exp(\alpha_1 \Omega_z) \exp(\theta_1 \Omega_x) \exp(\beta \Omega_z) \exp(\theta_2 \Omega_x) \exp(\alpha_2 \Omega_z)$$

Evaluating the resulting z component of the magnetization

$$\cos(\theta_3) = \cos(\theta_2)\cos(\theta_1) - \sin(\theta_2)\sin(\theta_1)\cos(\beta)$$

where $\theta_3 \in [-\pi, \pi]$. Therefore

$$\cos(\theta_3) \geq \cos(\theta_2)\cos(\theta_1) - \sin(\theta_2)\sin(\theta_1) \geq \cos(\theta_1 + \theta_2) \geq \cos(|\theta_1| + |\theta_2|)$$

$$\Rightarrow \quad |\theta_3| \leq |\theta_1| + |\theta_2|$$

For the non-orthogonal case, we note that the transverse angle $\bar{\theta}$ generated by the rotation

$$R = \exp(\theta\Omega), \quad \Omega = n_x \Omega_x + n_y \Omega_y + n_z \Omega_z$$

is given by Rodrigues' Formula,

$$R = I\cos\theta + \sin\theta\Omega + (1-\cos\theta)\Omega^2. \tag{4.23}$$

Applying,

$$\begin{aligned} \cos\bar{\theta} &= [0,0,1]R[0,0,1]' \\ &= R(3,3) \\ &= \cos\theta + n_z^2(1-\cos\theta) \geq \cos\theta \\ \Rightarrow \quad \bar{\theta} &\leq \theta. \end{aligned}$$

Therefore, we can express the non-orthogonal rotations as

$$\Theta_1 = \exp(\alpha_1\Omega_z)\exp(\theta_1'\Omega_x)\exp(\alpha_2\Omega_z), \quad \Theta_2 = \exp(\beta_1\Omega_z)\exp(\theta_2'\Omega_x)\exp(\beta_2\Omega_z)$$

where $\theta_1' \leq \theta_1$ and $\theta_2' \leq \theta_2$, which reduces the problem to the already considered orthogonal case. □

Lemma 4.

$$\exp(\alpha\Omega_y)\exp(\beta\Omega_z)\exp(-\alpha\Omega_y) = \exp(\beta\cos\alpha\Omega_z + \beta\sin\alpha\Omega_x)$$

Proof. Follows from repeated applications of Baker-Campbell-Hausdorff and is presented in appendix A. □

Theorem 4.5.4. *The sequence of off resonant discretized adiabatic passages*

$$\begin{aligned} U(\omega) &= \prod_{\substack{m=-n \\ \omega-\omega_{m,k}\notin(-\frac{B}{2},\frac{B}{2})}}^{n}\prod_{k=1}^{N} \exp((\omega\Omega_z + u\Omega_{\tilde{\phi}_{m,k}})\Delta t) \\ &= \exp(C_1\Omega_z)\exp(\bar{\theta}\Omega_x)\exp(C_2\Omega_z), \end{aligned}$$

produces a transverse flip angle $\bar{\theta}$, that is bounded by

$$\bar{\theta} \leq c_1 \frac{u_0}{B} + c_2 \frac{\ln n}{n}, \tag{4.24}$$

where $N = \frac{B}{a\Delta t}$, $(2n+1)\Delta t = \tau_r$, $B(\tau_r + \Delta t) \leq 2\pi$, Δt is the discretization time scale and

$$\begin{aligned} \phi_k &= \omega_0 t_k + a t_k^2/2 & \omega_k &= \omega_0 + a t_k \\ \phi_{m,k} &= \phi_k + mBt_k + \phi_{m-1,N} & \omega_{m,k} &= \omega_k + mB \\ \tilde{\phi}_{m,k} &= \phi_{m,k} + \tfrac{\omega_{m,k}\Delta t}{2} & \phi_{0,N} &= 0 \end{aligned}$$

Before proving, we develop the following lemmas,

Lemma 5. *The rotation*

$$U = \exp(-\theta_2 \Omega_x) \exp(-\Delta \Omega_z) \exp(\theta_1 \Omega_x)$$

generates a transverse flip angle $\bar{\theta}$ that is bounded by

$$\bar{\theta} \leq |\theta_2 - \theta_1| + \theta_1 \Delta + O(\Delta^3). \tag{4.25}$$

Proof.

$$\begin{aligned} U &= \exp(-\theta_2 \Omega_x) \exp(-\Delta \Omega_z) \exp(\theta_1 \Omega_x) \\ &= \exp(-\theta_2 \Omega_x) \exp(\theta_1 (\cos \Delta \Omega_x - \sin \Delta \Omega_y)) \exp(-\Delta \Omega_z) \\ &= \exp(-\theta_2 \Omega_x) \exp(\theta_1 \Omega_x - 2\theta_1 \sin \frac{\Delta}{2} \underbrace{(\sin \frac{\Delta}{2} \Omega_x + \cos \frac{\Delta}{2} \Omega_y)}_{\Omega}) \exp(-\Delta \Omega_z) \\ &= \exp(-\theta_2 \Omega_x) \exp(\theta_1 \Omega_x - 2\theta_1 \sin \frac{\Delta}{2} \Omega) \exp(-\Delta \Omega_z) \\ &= \exp(-\theta_2 \Omega_x) \exp(\theta_1 \Omega_x) \Phi(1) \exp(-\Delta \Omega_z) \end{aligned}$$

We define $\Phi(t)$ by first considering

$$\dot{Y} = (\theta_1\Omega_x - 2\theta_1 \sin\frac{\Delta}{2}\Omega)Y \qquad Y(0) = I$$

moving into the frame of $\theta_1\Omega_x$ for 1 unit of time we have $Y(t) = \exp(\theta_1\Omega_x)\Phi(t)$, which has the desired form of the inner terms in U. Performing the change of coordinates

$$\begin{aligned}
\Phi &= \exp(-\theta_1\Omega_x)Y \\
\dot{\Phi}(t) &= 2\theta_1 \sin\frac{\Delta}{2} \underbrace{\exp(-\theta_1\Omega_x)\Omega(t)\exp(\theta_1\Omega_x)}_{\tilde{\Omega}(t)} \Phi(t)
\end{aligned}$$

so that

$$\Phi(1) = \lim_{\Delta t\to 0} \prod_{k=1}^{\lfloor 1/\Delta t\rfloor} \exp(2\theta_1 \sin\frac{\Delta}{2}\tilde{\Omega}(k\Delta t)).$$

Applying lemma 3, the transverse flip angle θ_Φ is bounded by

$$\begin{aligned}
\theta_\Phi &\leq \lim_{\Delta t\to 0} \sum_{k=1}^{\lfloor 1/\Delta t\rfloor} 2\theta_1 \sin\frac{\Delta}{2} \\
&= \int_0^1 2\theta_1 \sin\frac{\Delta}{2} dt \\
&= \theta_1\Delta + O(\Delta^3).
\end{aligned}$$

Therefore the total transverse flip angle $\bar{\theta}$ is bounded by

$$\bar{\theta} \leq |\theta_2 - \theta_1| + \theta_1\Delta + O(\Delta^3)$$

as claimed. □

Lemma 6.

$$\begin{aligned}
U(\omega) &\equiv \exp(\omega\Delta t\Omega_z)\exp(u\Delta t\Omega_x) \\
&= \exp(\theta(\cos\kappa\Omega_z + \sin\kappa(\cos\frac{\omega\Delta t}{2}\Omega_x + \sin\frac{\omega\Delta t}{2}\Omega_y))) \qquad (4.26)
\end{aligned}$$

where

$$\cos\frac{\theta}{2} = \cos\frac{\omega\Delta t}{2}\cos\frac{u\Delta t}{2} \tag{4.27}$$

$$\tan\kappa = \frac{\sqrt{n_x^2+n_y^2}}{n_z} = \frac{\tan\frac{u\Delta t}{2}}{\sin\frac{\omega\Delta t}{2}} \tag{4.28}$$

Proof. To see this we perform the multiplication explicitly

$$U(\omega) = \begin{bmatrix} \cos\omega\Delta t & -\cos u\Delta t\sin\omega\Delta t & \sin u\Delta t\sin\omega\Delta t \\ \sin\omega\Delta t & \cos u\Delta t\cos\omega\Delta t & -\sin u\Delta t\cos\omega\Delta t \\ 0 & \sin u\Delta t & \cos u\Delta t \end{bmatrix}$$

From the properties of Rotation Matrices, the rotation angle θ is given by

$$\begin{aligned} \mathrm{tr}(U(\omega)) &= 1+2\cos\theta = \cos u\Delta t+\cos\omega\Delta t+\cos u\Delta t\cos\omega\Delta t \\ &\Rightarrow\ 2+2\cos(\theta) = 1+\cos u\Delta t+\cos\omega\Delta t+\cos u\Delta t\cos\omega\Delta t \\ &\Rightarrow\ (2+2\cos\theta) = (1+\cos u\Delta t)(1+\cos u\Delta t) \\ &\Rightarrow\ 4\cos^2\frac{\theta}{2} = 4\cos^2 u\Delta t\cos^2 u\Delta t \\ &\Rightarrow\ \cos\frac{\theta}{2} = \cos\frac{u\Delta t}{2}\cos\frac{\omega\Delta t}{2} \end{aligned} \tag{4.29}$$

Calculating the eigenvector corresponding to the eigenvalue 1 yields the rotation axis

$$\frac{1}{\sqrt{\sin^2\frac{u\Delta t}{2}+\sin^2\frac{\omega\Delta t}{2}\cos^2\frac{u\Delta t}{2}}}\begin{bmatrix} \cos\frac{\omega\Delta t}{2}\sin\frac{u\Delta t}{2} \\ \sin\frac{\omega\Delta t}{2}\sin\frac{u\Delta t}{2} \\ \sin\frac{\omega\Delta t}{2}\cos\frac{u\Delta t}{2} \end{bmatrix} = \begin{bmatrix} \sin\kappa\cos\frac{\omega\Delta t}{2} \\ \sin\kappa\sin\frac{\omega\Delta t}{2} \\ \cos\kappa \end{bmatrix} \tag{4.30}$$

completing the lemma[1]. □

[1]Both the rotation axis and θ are only specified up to a factor of ± 1. To avoid ambiguity, we take the positive root in equation (4.30) for the rotation axis, and select $\theta \in [0,\pi]$ in equation (4.27).

Corollary 4.5.5.

$$\begin{aligned} U(\omega) &= \exp(\theta(\cos\kappa\Omega_z + \sin\kappa(\cos\frac{\omega\Delta t}{2}\Omega_x + \sin\frac{\omega\Delta t}{2}\Omega_y))) \\ &= \exp(\frac{\omega\Delta t}{2}\Omega_z)\exp(\theta(\cos\kappa\Omega_z + \sin\kappa\Omega_x))\exp(-\frac{\omega\Delta t}{2}\Omega_z) \\ &= \exp(\frac{\omega\Delta t}{2}\Omega_z)\exp(\kappa\Omega_y)\exp(\theta\Omega_z)\exp(-\kappa\Omega_y)\exp(-\frac{\omega\Delta t}{2}\Omega_z) \end{aligned}$$

Lemma 7.

$$\begin{aligned} & \exp((\omega\Omega_z + u_k\Omega_x + v_k\Omega_y)\Delta t) \\ = \quad & \exp\left(\frac{\omega\Delta t\Omega_z}{2}\right)\exp(u_k\Delta t\Omega_x + v_k\Delta t\Omega_y)\exp\left(\frac{\omega\Delta t\Omega_z}{2}\right) + O(\Delta t^3) \end{aligned}$$

This follows from expanding to 2nd order and calculating the product directly.

We are now prepared to prove theorem (4.5.4)

Proof. Recall that

$$N = \tfrac{B}{a\Delta t} \qquad (2n+1)\Delta t = \tau_r \qquad \Delta t = t_{k+1} - t_k$$

$$\phi_{m,k} = (\omega_0 + mB)t_k + a\tfrac{t_k^2}{2} + \phi_{m-1,N} \qquad \phi_{0,N} = 0$$

$$\omega_{m,k} = \omega_0 + mB + at_k \qquad \tilde{\phi}_{m,k} = \phi_{m,k} + \tfrac{\omega_{m,k}\Delta t}{2}$$

and that the off resonance rotation is given by

$$U(\omega) = \prod_{\substack{m=-n \\ \omega-\omega_{m,k}\notin(-\frac{B}{2},\frac{B}{2})}}^{n}\prod_{k=1}^{N} \exp((\omega\Omega_z + u\Omega_{\tilde{\phi}_{m,k}})\Delta t).$$

We note that under the most pessimistic assumption that all transverse flip angles add constructively, we can analyze the contributions from off resonance to the left

and right separately. We make the following natural definitions

$$\begin{aligned} U(\omega) &= U_R(\omega)U_L(\omega) \\ U_L(\omega) &= \prod_{\substack{m=-n \\ \omega-\omega_{m,k}<\frac{B}{2}}}^{n}\prod_{k=1}^{N}\exp((\omega\Omega_z + u\Omega_{\tilde{\phi}_{m,k}})\Delta t) \\ U_R(\omega) &= \prod_{\substack{m=-n \\ \omega-\omega_{m,k}>\frac{B}{2}}}^{n}\prod_{k=1}^{N}\exp((\omega\Omega_z + u\Omega_{\tilde{\phi}_{m,k}})\Delta t) \end{aligned}$$

Noting the symmetry of the pulse, it is clear that

$$U_L(\omega) = U_R(-\omega), \tag{4.31}$$

so it suffices to analyze $U_R(\omega)$. We do so as follows, neglecting terms of $O(\Delta t)$ and above,

$$\begin{aligned} U_R(\omega) &= \prod_{\substack{m=-n \\ \omega-\omega_{m,k}>\frac{B}{2}}}^{n}\prod_{k=1}^{N}\exp((\omega\Omega_z + u\Omega_{\tilde{\phi}_{m,k}})\Delta t) \\ &\overset{lem7}{=} \exp(\alpha_1\Omega_z)\left[\prod_{\substack{m=-n \\ \omega-\omega_{m,k}>\frac{B}{2}}}^{n}\prod_{k=1}^{N}\exp(\omega\Delta t\Omega_z)\exp(u\Delta t\Omega_{\tilde{\phi}_{m,k}})\right]\exp(\alpha_2\Omega_z) \\ &= \exp(\beta_1\Omega_z)\left[\prod_{\substack{m=-n \\ \omega-\omega_{m,k}>\frac{B}{2}}}^{n}\prod_{k=1}^{N}\exp((\omega\Delta t + \tilde{\phi}_{m,k} - \tilde{\phi}_{m,k+1})\Omega_z)\exp(u\Delta t\Omega_x)\right]\exp(\beta_2\Omega_z) \end{aligned}$$

Directly calculating,

$$\begin{aligned} \tilde{\phi}_{m,k+1} - \tilde{\phi}_{m,k} &= \phi_{m,k+1} - \phi_{m,k} + \frac{\omega_{m,k+1}\Delta t}{2} - \frac{\omega_{m,k}\Delta t}{2} \\ &= \phi_{k+1} - \phi_k + mB\Delta t + \frac{a\Delta t^2}{2} \\ &= (\omega_0 + mB)\Delta t + \frac{a}{2}(t_{k+1}^2 - t_k^2) + \frac{a\Delta t^2}{2} \\ &= \omega_{m,k+1}\Delta t. \end{aligned}$$

Substituting into $U_R(\omega)$ we have

$$\begin{aligned} U_R(\omega) &= \exp(\beta_1\Omega_z)\left[\prod_{\substack{m=-n \\ \omega-\omega_{m,k}>\frac{B}{2}}}^{n}\prod_{k=1}^{N}\exp((\overbrace{\omega-\omega_{m,k}}^{\tilde{\omega}_{m,k}})\Delta t)\Omega_z)\exp(u\Delta t\Omega_x)\right]\exp(\beta_2\Omega_z) \\ &\overset{corr4.5.5}{=} \exp(\gamma_1\Omega_z)\exp(\kappa_{n,N}\Omega_y) \\ &\quad\times\left[\prod_{\substack{m=-n \\ \omega-\omega_{m,k}>\frac{B}{2}}}^{n}\prod_{k=1}^{N}\exp(\theta_{m,k}\Omega_z)\exp(-\kappa_{m,k+1}\Omega_y)\exp(-\frac{\Delta\omega\Delta t}{2}\Omega_z)\exp(\kappa_{m,k}\Omega_y)\right] \\ &\quad\times\exp(\theta_{1,1}\Omega_z)\exp(-\kappa_{1,1}\Omega_y)\exp(\gamma_2\Omega_z) \end{aligned}$$

where

$$\kappa_{m,k}(\omega)=\arctan\left(\frac{\tan\frac{u\Delta t}{2}}{\sin\frac{\tilde{\omega}_{m,k}\Delta t}{2}}\right)\qquad\Delta\omega=a\Delta t.$$

Applying lemma 3, the transverse flip angle is bounded by the sum of the individual transverse flip angles in the product. We find (suppressing the explicit ω dependence)

$$\bar{\theta}_R(\omega) \leq |\kappa_{n,N}|+\sum_{m=1}^{n}\left[\sum_{k=1}^{N}|\kappa_{m,k+1}-\kappa_{m,k}|+|\kappa_{m,k}\frac{\Delta\omega\Delta t}{2}|\right]+|\kappa_{1,1}| \quad (4.32)$$

Focusing on the boundary terms first, we note

$$\begin{aligned} &\tilde{\omega}_{1,1}\leq\tilde{\omega}_{m,k}\leq\tilde{\omega}_{n,N} \\ &\tilde{\omega}_{1,1}=\frac{B}{2}+a\Delta t\geq\frac{B}{2}\quad\text{(Off Resonance Condition)} \\ &\tilde{\omega}_{n,N}\leq(2n+1)B=\frac{B\tau_r}{\Delta t}\leq\frac{2\pi}{\Delta t}-B \\ \Rightarrow\quad &\kappa_{m,k}\leq\frac{\tan\frac{u\Delta t}{2}}{\sin\frac{\tilde{\omega}_{1,1}\Delta t}{2}}\leq\frac{u\Delta t}{\frac{B\Delta t}{4}}\leq\frac{4u}{B}. \end{aligned}$$

Next we calculate the contribution from the $|\kappa_{m,k+1}-\kappa_{m,k}|$ terms, noting that there are two regimes to consider; $\tilde{\omega}_{m,k}\Delta t\in(0,\pi]$ and $\tilde{\omega}_{m,k}\Delta t\in[\pi,2\pi)$. For the first case

we calculate

$$\begin{aligned}
\kappa_{m,k} - \kappa_{m,k+1} &\leq \tan\kappa_{m,k} - \tan\kappa_{m,k+1} \\
&\leq u\Delta t\left(\left[\sin\frac{\tilde{\omega}_{m,k}\Delta t}{2}\right]^{-1} - \left[\sin\frac{\tilde{\omega}_{m,k+1}\Delta t}{2}\right]^{-1}\right) \\
&\leq u\Delta t\left(\left[\sin\frac{\tilde{\omega}_{m,k}\Delta t}{2}\right]^{-1} - \left[\sin\frac{\tilde{\omega}_{m,k}\Delta t}{2}\cos\frac{\Delta\omega\Delta t}{2} + \sin\frac{\Delta\omega\Delta t}{2}\cos\frac{\tilde{\omega}_{m,k}\Delta t}{2}\right]^{-1}\right) \\
&\leq u\Delta t\left(\left[\sin\frac{\tilde{\omega}_{m,k}\Delta t}{2}\right]^{-1} - \left[\sin\frac{\tilde{\omega}_{m,k}\Delta t}{2} + \sin\frac{\Delta\omega\Delta t}{2}\right]^{-1}\right) \\
&= \frac{u\Delta t\sin\frac{\Delta\omega\Delta t}{2}}{\sin\frac{\tilde{\omega}_{m,k}\Delta t}{2}(\sin\frac{\tilde{\omega}_{m,k}\Delta t}{2} + \sin\frac{\Delta\omega\Delta t}{2})} \\
&\leq \frac{\frac{1}{2}u\Delta\omega\Delta t^2}{\left(\frac{\tilde{\omega}_{m,k}}{4}\right)^2} \\
&= \frac{8u\Delta\omega}{\tilde{\omega}_{m,k}^2}
\end{aligned}$$

Performing an analogous calculation for $\tilde{\omega}_{m,k}\Delta t \in [\pi, 2\pi)$ after making the substitution $\frac{\nu_{m,k}\Delta t}{2} = \pi - \frac{\tilde{\omega}_{m,k}\Delta t}{2}$ yields

$$\kappa_{m,k+1} - \kappa_{m,k} \leq \tan\kappa_{m,k+1} - \tan\kappa_{m,k} \leq \frac{8u\Delta\nu}{\nu_{m,k}^2}.$$

Lastly, we consider the terms of the form $\kappa_{m,k}\frac{\Delta\omega\Delta t}{2}$, which also must be treated in 2 parts. For $\tilde{\omega}_{m,k}\Delta t \in (0, \pi]$ we find

$$\begin{aligned}
\kappa_{m,k}\frac{\Delta\omega\Delta t}{2} &\leq \tan\kappa_{m,k}\frac{\Delta\omega\Delta t}{2} \\
&\leq u\Delta t\Delta\omega\left(\frac{\Delta t}{\sin\frac{\tilde{\omega}_{m,k}\Delta t}{2}}\right) \\
&\leq \frac{4u\Delta t\Delta\omega}{\tilde{\omega}_{m,k}}.
\end{aligned}$$

For $\tilde{\omega}_{m,k}\Delta t \in (\pi, 2\pi)$ we again make the substitution $\frac{\nu_{m,k}\Delta t}{2} = \pi - \frac{\tilde{\omega}_{m,k}\Delta t}{2}$ and find

$$\left|\kappa_{m,k}\frac{\Delta\omega\Delta t}{2}\right| \leq \frac{4u\Delta t\Delta\nu}{\tilde{\nu}_{m,k}}.$$

Applying equation 4.31 we have

$$\bar{\theta}(\omega) \leq \bar{\theta}_R(\omega) + \bar{\theta}_L(\omega) = \bar{\theta}_R(\omega) + \bar{\theta}_R(-\omega).$$

We complete the bound on $\bar{\theta}$ by substituting into equation 4.32, and approximate the sum with an integral yielding,

$$\bar{\theta}(\omega) \leq \frac{16u}{B} + \int_{\frac{B}{2}}^{(n+\frac{1}{2})B} \frac{16u}{\omega^2} + \frac{8u\Delta t}{\omega} dw \leq 48\frac{u}{B} + 8u\tau_r \frac{\ln(2n+1)}{2n+1}$$

as claimed. □

Remark 1. *This theorem shows that additional off resonance pulses can be made to have arbitrarily small effect by choosing* $\frac{u}{B}$ *and* Δt *sufficiently small. The former is already chosen to be small in accordance with the standard adiabatic regime. The ability to perform additional pulses without perturbing other spins will be important in the next section, where we will show that rotor period pulsing results in bandwidth compression, and additional pulses will be used to recover the original bandwidth.*

4.5.5 Periodic Pulsing

We have shown that a piecewise constant pulse based on a parent adiabatic pulse can be used to produce a broadband inversion. We now consider the effect of applying the pulse at periodic intervals as shown in figure 4.4 and we will see that this leads to bandwidth compression. The full bandwidth is then readily recovered by applying additional off resonance pulses that will not appreciably disturb the on resonance behavior by theorem (4.5.4).

We begin by considering the on resonance behavior under periodic pulsing

Theorem 4.5.6.

$$\begin{aligned} U(\omega) &= \prod_{k=1}^{N} \exp(n\omega\Delta t)\exp((\omega\Omega_z + u\Omega_{\tilde{\phi}_k})\Delta t)\exp(n\omega\Delta t) \\ &= \exp(\gamma_1\Omega_z)\left[\prod_{k=1}\exp((\omega'\Omega_z + u\Omega_{\tilde{\phi}_k})\Delta t)\right]\exp(\gamma_2\Omega_z) + O(\Delta t^2), \end{aligned}$$

for all k such that $(\omega' - \omega_{k+1}) \in [-\frac{B}{2}, \frac{B}{2}]$, where $\omega' = (2n+1)\omega$, $\Delta t = \frac{\tau_r}{2n+1}$, $\omega_{k+1} - \omega_k = a\Delta t$, τ_r is the period of the pulsing and $\gamma_1, \gamma_2 \in [-\pi, \pi]$.

Proof.

$$\begin{aligned} U(\omega) &= \prod_{k=1}^{N} \exp(n\omega\Delta t)\exp((\omega\Omega_z + u\Omega_{\tilde{\phi}_k})\Delta t)\exp(n\omega\Delta t) \\ &\overset{lem7}{=} \prod_{k=1}^{N} \exp\left(\omega\frac{\tau_r}{2}\Omega_z\right)\exp(u\Omega_{\tilde{\phi}_k}\Delta t)\exp\left(\omega\frac{\tau_r}{2}\Omega_z\right) + O(\Delta t^3) \\ &\overset{lem1}{=} \exp\left(-\omega\frac{\tau_r}{2}\Omega_z\right)\left[\prod_{k=1}^{N}\exp\left(\omega\tau_r\Omega_z\right)\exp(u\Omega_{\tilde{\phi}_k}\Delta t)\right]\exp\left(\omega\frac{\tau_r}{2}\Omega_z\right) + O(\Delta t^2) \\ &= \exp(\alpha_1\Omega_z)\left[\prod_{k=1}^{N}\exp\left((\omega\tau_r - \omega_{k+1}\Delta t)\Omega_z\right)\exp(u\Omega_x\Delta t)\right]\exp(\alpha_2\Omega_z) + O(\Delta t^2) \\ &= \exp(\alpha_1\Omega_z)\left[\prod_{k=1}^{N}\exp\left((\omega' - \omega_{k+1})\Delta t\Omega_z\right)\exp(u\Omega_x\Delta t)\right]\exp(\alpha_2\Omega_z) + O(\Delta t^2) \\ &\overset{lem7}{=} \exp(\alpha_1\Omega_z)\left[\prod_{k=1}^{N}\exp\left((\omega' - \omega_{k+1})\Omega_z + u\Omega_x)\Delta t\right)\right] + O(\Delta t^2) \\ &= \exp(\beta_1\Omega_z)\left[\prod_{k=1}^{N}\exp\left((\omega'\Omega_z + u\Omega_{\tilde{\phi}_k})\Delta t\right)\right]\exp(\beta_2\Omega_z) + O(\Delta t^2), \end{aligned}$$

where we made use of the on resonance condition to safely apply lemma 7 in reverse.

□

Remark 2. *The product term is readily identified as the previously considered discretized adiabatic passage, which was shown to perform arbitrarily complete inversion.*

As we are interested in broadband inversions, the additional z-rotations can be ignored. Lastly, $\omega \to \omega'$, resulting in bandwidth compression.

That is to say, discretizing an adiabatic passage on the time scale Δt and applying it as Δt duration pulses at rotor periods, produces an inversion with bandwidth reduced by a factor of $(2n+1)$ to that of the original adiabatic pulse. In order to produce a broadband pulse of the same bandwidth as the parent adiabatic passage, one can apply $2n$ additional frequency shifted discretized passages, recovering the original bandwidth. By theorem (4.5.4), these additional pulses have negligible impact beyond their resonant band, and serve only to increase the bandwidth.

Given that periodic pulsing results in bandwidth compression of the adiabatic passage, the reader might be curious why we did not use a single adiabatic passage with bandwidth $(2n+1)[-\frac{B}{2}, \frac{B}{2}]$, and avoid the need to consider on resonance and off resonance behavior separately. However, the error bound described in theorem (4.5.1) for substituting a piecewise constant approximation for the continuous adiabatic passage is of the form

$$E_{\Delta t} \leq u_0 \omega \omega_{m,k} \Delta t^3$$

per time step Δt. By increasing the sweep range by a factor $(\Delta t)^{-1}$, the time, and thereby the number of time steps, also increases by a factor of $(\Delta t)^{-1}$. Moreover, $\omega_{m,k}$ is no longer bounded by B, but instead by $B(\Delta t)^{-1}$ resulting in a second reduction in order. Therefore the total error bound calculated in corollary 4.5.2 would become

$$E_T = || \prod_{k=1}^{N'} \Phi(\phi(t), t_k, t_{k+1}) - \prod_{k=1}^{N'} \exp((\omega\Omega_z + u_k\Omega_x + v_k\Omega_y)\Delta t)|| = O(Constant),$$

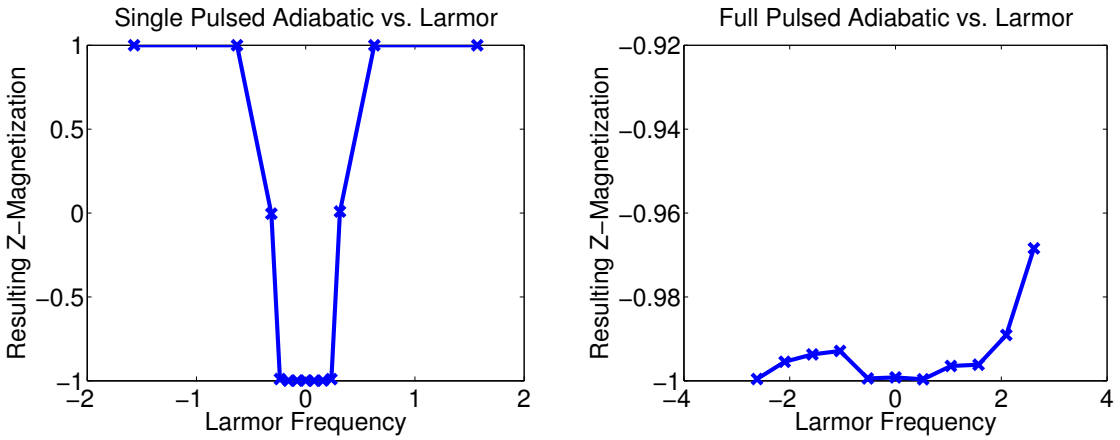

Figure 4.8: (Left) Selective inversion using a parent adiabatic pulse designed for exciting $[-\pi, \pi]$. Due to bandwidth compression selective excitation occurs for $\omega \in [-\pi/10, \pi/10]$. (Right) Broadband inversion by implementing 10 such passages to recover the entire bandwidth of the parent adiabatic pulse. Pulse parameters are: $a = 0.001$ and $u = 0.1$.

where $N' = \frac{B}{a\Delta t^2}$. Accordingly, the error could no longer be controlled by reducing Δt, necessitating the presented analysis.

4.6 Simulations

We have presented a method for constructing pulsed sequences that produce both selective and broadband inversions in the presence of a periodic drift. We now display the performance of the methods discussed to several applications commonly of interest, and show that choosing $\Delta t \leq 0.1$ is sufficient for many applications.

4.6.1 Selective Inversion

We have shown that periodic pulsing leads to a rescaling of the bandwidth of the parent adiabatic pulse. For a particular $\Delta t, \tau_r$ and the parent adiabatic's excitation

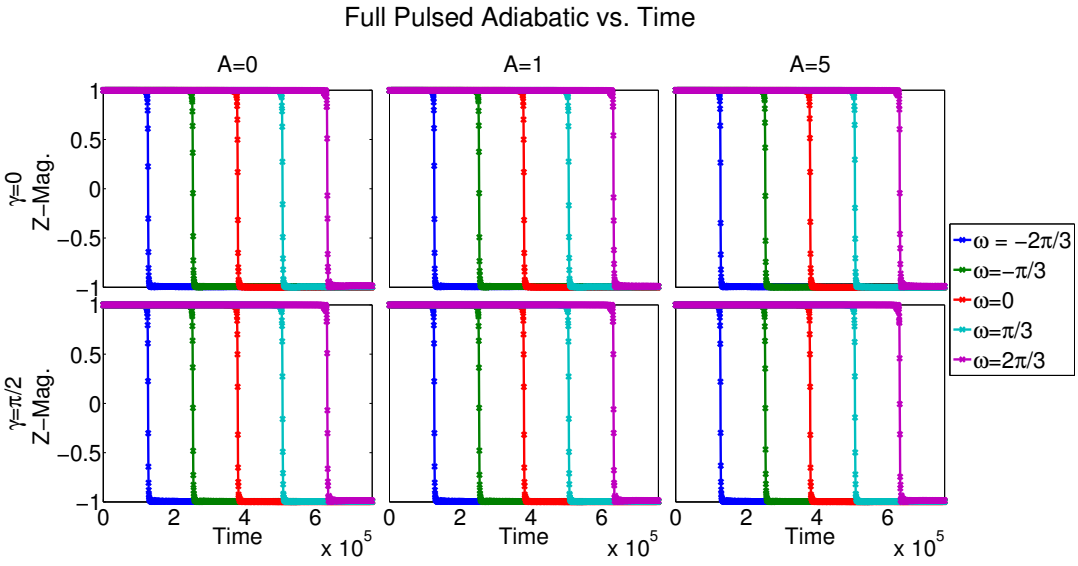

Figure 4.9: Resulting Z-magnetization for a broadband periodic pulsed sequence with $\Delta t = \frac{1}{11}$ and parent adiabatic parameters $u = 0.1, a = 0.001$ and $\omega \in [-\pi, \pi]$. Requires 11 passages to invert the entire bandwidth $[-\pi, \pi]$.

bandwidth $[-\frac{B}{2}, \frac{B}{2}]$, inversion occurs for $\omega \in \frac{\Delta t}{\tau_r}[-\frac{B}{2}, \frac{B}{2}]$. As a specific example, we consider a system with $\tau_r = 1$, and parent adiabatic passage parameters $a = 0.001, u = 0.1$ with excitation bandwidth $[-\pi, \pi]$. Consider inverting frequencies in the range $\omega \in [\frac{-\pi}{10}, \frac{\pi}{10}]$. To do so, we select $\Delta t = 0.1$, resulting in the desired bandwidth after compression. The resulting magnetization profile is displayed in figure 4.8, and we see that the frequencies of interest have been inverted while leaving the others unaffected.

4.6.2 Broadband Inversion

Broadband inversion is accomplished by implementing additional frequency shifted pulses to offset the bandwidth compression. Using a parent adiabatic passage with parameters $u = 0.1, a = 0.001$ and $\omega \in [-\pi, \pi]$ and selecting $\Delta t = \frac{1}{11}$, broadband

inversion is achieved by applying 11 passages. Figure 4.9 shows that broadband inversion is accomplished and is completely independent of the amplitude A and phase γ of the periodic drift.

4.6.3 Full Controllability

Chapter 3 reduced the problem of controllability to producing broadband π inversions by the pulse sequence elements depicted in figure 3.3 and equations 3.16 and 3.17. Substituting the periodically pulsed broadband inversions for the π pulses allows for arbitrary rotations as a function of ω.

For example, the prototypical Fourier Synthesis element with $n = 1, \theta = \pi/4$ and excitation profile $\Phi(\omega) = \exp(\cos(\pi/2\cos\omega)\Omega_x)$ given in equation (3.16) is shown in figure 4.10. In an analogous manner to chapter 3, any desired rotation can be constructed by a sequence comprised of such pulse elements.

4.7 Conclusion

We have presented a pulse design algorithm for robust inversions in the presence of a random, yet periodic drift. In the process, we have developed a method for implementing an adiabatic passage by applying short duration pulses at periodic intervals. By selecting the pulsing period to coincide with the rotor period of the system, the effect of the periodic drift term in the system's dynamics can be made arbitrarily small. These results have immediate applications for solid state NMR experiments in which sample spinning is used to attenuate orientation dependent intermolecular interactions. This enables the construction of pulse sequences that are

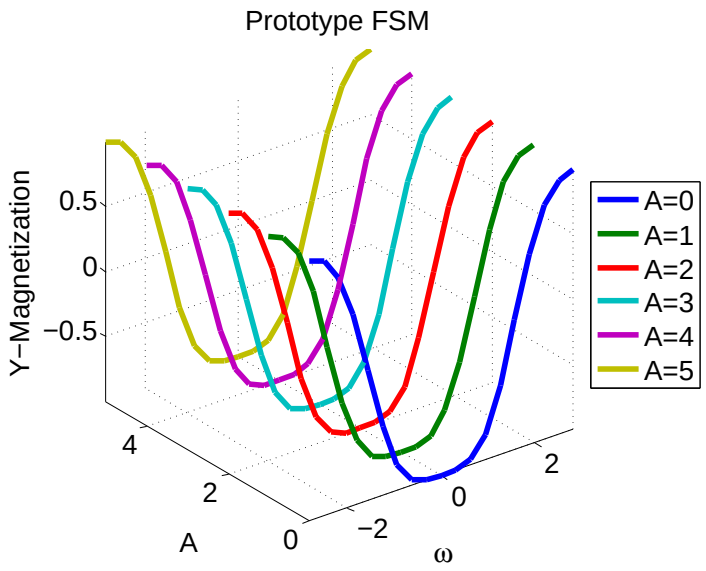

Figure 4.10: Resulting Z-magnetization for a FSM pulse element generated using periodic pulsing to generate the π rotations. The magnetization is robust to periodic drift amplitude and phase.

selective for specific isotropic resonances or chemical shifts in magic angle spinning experiments.

Chapter 5

Conclusion

5.1 Future Directions

In this thesis, we have presented novel pulse elements for simultaneous control of ensembles exhibiting variation in the member-systems' dynamics. In particular, chapter 4 developed pulsed controls for systems with periodic Hamiltonians arising in Solid State NMR experiments in which sample spinning is used to average out orientation dependent interactions. Future work should determine the applicability of pulsed controls to other systems exhibiting periodicity in their system dynamics such as quadrupolar nuclei, which we briefly outline in section 5.1.2. Pulsed controls may also provide an extension to the rotating wave approximation in the long pulse duration limit, which we consider in the next section.

5.1.1 Rotating Wave Approximation

Specifically, we started with the model

$$\dot{X} = (\omega(t)\Omega_z + u\cos(\phi(t))\Omega_x + u\sin(\phi(t))\Omega_y)X \tag{5.1}$$

where $\omega(t)$ has a static part ω and an uncertain periodic component with known frequency. The goal was to selectively invert certain ω immune to the periodic disturbance. In the previous chapter, we accomplished this goal by discretizing a broadband adiabatic passage and applying it at periodic intervals, $\tau_r = 2\pi\omega_r$. We now relax the control degrees of freedom and consider the model,

$$\dot{X} = (\omega(t)\Omega_z + u\cos(\phi(t))\Omega_x)X. \tag{5.2}$$

This model is more realistic in many experimental NMR settings. A standard approximation that is made to reduce (5.2) to (5.1) is the so called rotating wave approximation.

For the moment, let us assume we only have a static part $\omega = \omega_0 + \Delta\omega$. If we choose $\phi(t) = \omega_0 t + \phi_1(t)$ and transform into the frame $Y = \exp(-\omega_0\Omega_z t)X$ then

$$\begin{aligned}\dot{Y} = [&\Delta\omega\Omega_z + \frac{u}{2}(\cos\phi_1(t)\Omega_x + \sin\phi_1(t)\Omega_y) \\ &+\frac{u}{2}(\cos(2\omega_0 + \phi_1(t))\Omega_x + \sin(2\omega_0 + \phi_1(t))\Omega_y)]Y\end{aligned} \tag{5.3}$$

In practice, the fast oscillating component at frequency $2\omega_0$ is neglected, as it produces an error that is bounded by $\frac{u^2}{2\omega_0}T$, where T is the time of the sequence.

In the solutions presented in chapter 4, the time of the sequence can be very large, and as a result, this bound can become unusably large. Future work should attempt to show pulsed controllability without making the rotating wave approximation.

5.1.2 Periodic Disturbances with Non-Zero Average

Future work should also extend the presented methods to systems where the periodic disturbance averages to a non-zero value, which may be unknown. This problem arises in the design of pulses for study of quadrupolar nuclei, whereby the anisotropic terms are not completely averaged by sample spinning.

A model system is

$$iU'\dot{U} = \begin{bmatrix} \omega_1(t) & 0 & 0 & 0 \\ 0 & \omega_2(t) & 0 & 0 \\ 0 & 0 & \omega_3(t) & 0 \\ 0 & 0 & 0 & \omega_4(t) \end{bmatrix} + u \begin{bmatrix} 0 & 1 & 0 & 0 \\ 1 & 0 & 1 & 0 \\ 0 & 1 & 0 & 1 \\ 0 & 0 & 1 & 0 \end{bmatrix} + v \begin{bmatrix} 0 & i & 0 & 0 \\ -i & 0 & i & 0 \\ 0 & -i & 0 & i \\ 0 & 0 & -i & 0 \end{bmatrix}$$

where

$$\omega_j(t) = \omega_j + A_j(t), \qquad \int_0^{\tau_r} A_j(t) \neq 0, \qquad \nu_j = \omega_j + \tau_r^{-1} \int_0^{\tau_r} A_j(t)$$

and we have frequency separation, i.e.,

$$|\nu_1 - \nu_2|, |\nu_3 - \nu_4| >> |\nu_2 - \nu_3|.$$

The goal is to engineer pulses such that one can produce selective rotations

$$U \begin{pmatrix} 1 \\ 0 \\ 0 \\ 0 \end{pmatrix} \rightarrow \begin{pmatrix} 0 \\ 1 \\ 0 \\ 0 \end{pmatrix}$$

in spite of all the uncertainties in ν_j. Future work should address the applicability of pulsed controls on such systems.

5.2 Summary

In this thesis we have developed pulse design algorithms for ensemble control of several systems arising in NMR experiments. Chapter 2 built on existing methods to generate controls that are insensitive to errors in control amplitude for use in liquid NMR experiments. These controls have the advantage that they require less time to obtain the same amount of robustness compared to existing Fourier Synthesis Methods.

Chapters 3 and 4 considered systems with uncertainties in their periodic drift. The motivation for such problems came from control of spin dynamics in solid state NMR, where the sample is spun to average anisotropic effects. This results in a periodic Hamiltonian whose parameters have a distribution, which causes uncertainty in the precise value of the system parameters. The challenge is to control the system in the presence of this time varying uncertainty.

In many applications, one is interested is selectively exciting the system for only specific values of system parameters which are stationary, in the presence of a random periodic disturbance. A natural strategy is to control with pulsed inputs given at periodic intervals over which the uncertain Hamiltonian averages out. The challenge was to show that this limited set of control inputs is rich enough to control the system between desired points of interest. Limits on the amplitude of the pulses and the fact that system drifts during time periods when no control is applied makes control of such systems interesting.

This thesis addresses controllability of such systems. The control design methodology presented were developed in the context of Magic Angle Spinning solid state

NMR experiments, which provides a natural setting for systems with uncertain time varying periodic drift. There are a rich class of spin systems including quadrupolar nuclei that offer concrete physical settings where the presented methods may be extended and that offer further challenges for control. There are approximations, which are used in control of such systems, including the rotating wave approximation, which should be further studied in the context of pulsed inputs. Lastly, the techniques developed in this thesis might also find use outside NMR.

Bibliography

[1] M. H. Levitt, "Composite pulses," *Progress in Nuclear Magnetic Resonance Spectroscopy*, vol. 18, pp. 61–122, 1986.

[2] R. Tycko, "Broadband population inversion," *Physical Review Letters*, vol. 51, pp. 775–777, 1983.

[3] J. Baum, R. Tycko, and A. Pines, "Spatially selective nmr with broad-band radiofrequency pulses," *Journal of Chemical Physics*, vol. 105, pp. 7–14, 1986.

[4] A. J. Shaka and R. Freeman, "Composite pulses with dual compensation," *Journal of Magnetic Resonance*, vol. 55, pp. 487–493, 1983.

[5] R. Freeman, S. P. Kempsell, and M. H. Levitt, "Radiofrequency pulse sequences which compensate their own imperfections," *Journal of Magnetic Resonance*, vol. 38, pp. 453–479, 1980.

[6] M. H. Levitt and R. R. Ernst, "Composite pulses constructed by a recursive expansion procedure," *Journal of Magnetic Resonance*, vol. 55, pp. 247–254, 1983.

[7] M. Garwood and Y. Ke, "Symmetric pulses to induce arbitrary flip angles with

compensation for rf inhomogeneity and resonance offsets," *Journal of Magnetic Resonance (1969)*, vol. 94, no. 3, pp. 511 – 525, 1991.

[8] T. E. Skinner, T. O. Reiss, B. Luy, N. Khaneja, and S. J. Glaser, "Application of optimal control theory to the design of broadband excitation pulses for high-resolution nmr," *Journal of Magnetic Resonance*, vol. 163, no. 1, pp. 8 – 15, 2003.

[9] K. Kobzar, T. E. Skinner, N. Khaneja, S. J. Glaser, and B. Luy, "Exploring the limits of broadband excitation and inversion pulses," *Journal of Magnetic Resonance*, vol. 170, no. 2, pp. 236 – 243, 2004.

[10] K. Kobzar, B. Luy, N. Khaneja, and S. J. Glaser, "Pattern pulses: design of arbitrary excitation profiles as a function of pulse amplitude and offset," *Journal of Magnetic Resonance*, vol. 173, no. 2, pp. 229 – 235, 2005.

[11] R. G. J. Lin, M.J. Bayro and N. Khaneja, "Dipolar recoupling in solid state nmr by phase alternating pulse sequences," *Journal of Magnetic Resonance*, vol. 197, 2009.

[12] J.-S. Li and N. Khaneja, "Control of inhomogeneous quantum ensembles," *IEEE Transactions on Automatic Control*, vol. 54, 2009.

[13] M. J. Duer, "Solid-state nmr spectroscopy principles and applications," *Journal of Magnetic Resonance*, vol. 197, 2009.

[14] K. Schmidt-Rhor and H. W. Spiess, *Multidimensional Solid-State NMR and Polymers*. Academic Press, 1994.

[15] G. C. Chingas, A. N. garroway, R. D. Bertrand, and W. B. Moniz, "cross-polarization in liquids: A refocusing method," *Journal of Magnetic Resonance*, vol. 35, p. 283, 1979.

[16] M. S. Silver, R. I. Joseph, C.-N. Chen, V. J. Sanik, and D. I. Hoult, "Selective population inversion in nmr," *Nature*, vol. 310, pp. 681–683, 1984.

[17] D. E. Rourke. PhD thesis, 1992.

[18] M. Shinnar, S. Eleff, H. Subramanian, and J. S. Leigh, "The synthesis of pulse sequences yielding arbitrary magnetization vectors," *Magnetic Resonance in Medicine*, vol. 12, no. 1, pp. 74–80, 1989.

[19] P. L. Roux, "Exact synthesis of radio frequency waveforms," 1988.

[20] S. Wimperis, "Broadband, narrowband, and passband composite pulses for use in advanced nmr experiments," *Journal of Magnetic Resonance, Series A*, vol. 109, no. 2, pp. 221 – 231, 1994.

[21] J. Jones, "Robust ising gates for practical quantum computation," *Physical Review A*, vol. 67, p. 012317, 2003.

[22] K. Brown, A. Harrow, and I. Chuang, "Arbitrarily accurate composite pulse sequences," *Physical Review A*, vol. 70, p. 052318, 2004.

[23] I. Roos and K. Moelmer, "Quantum computing with an inhomogeneously broadened ensemble of ions," *Physical Review A*, vol. 69, p. 022321, 2004.

[24] M. Riebe, H. Haffner, C. F. Roos, W. Hansel, J. Benhelm, G. P. T. Lancaster, T. W. Korber, C. Becher, F. Schmidt-Kaler, D. F. V. James, and R. Blatt,

"Deterministic quantum teleportation with atoms," *Nature*, vol. 429, pp. 734–737, 2004.

[25] M. D. Barrett, J. Chiaverini, T. Schaetz, J. Britton, W. M. Itano, J. D. Jost, E. Knill, C. Langer, D. Leibfried, R. Ozeri, and D. J. Wineland, "Deterministic quantum teleportation of atomic qubits," *Nature*, vol. 429, pp. 737–739, 2004.

[26] B. Pryor and N. Khaneja, "Fourier decompositions and pulse sequence design algorithms for nuclear magnetic resonance in inhomogeneous fields," *Journal of Chemical Physics*, vol. 125, pp. 1–6, 2006.

[27] N. Khaneja, C. Kehlet, S. J. Glaser, and N. Nielsen, "Composite dipolar recoupling: Anisotropy compensated coherence transfer in solid-state nuclear magnetic resonance," *Journal of Chemical Physics*, vol. 124, pp. 1–7, 2006.

[28] B. Pryor, *Fourier Synthesis Methods for Identification and Control of Ensembles*. PhD thesis, Harvard University, 2007.

[29] J.-S. Li and N. Khaneja, "Control of inhomogeneous quantum ensembles," *Physical Review A*, vol. 73, 2006.

[30] J.-S. Li, *Control of Inhomogeneous Ensembles*. PhD thesis, Harvard University, 2006.

[31] J. P. P. L. R. D. Nishimura and A. Macovski, "Parameter relations for the shinnar-le roux selective excitation pulse design algorithm," *IEEE Transactions on Medical Imaging*, vol. 10, 1991.

[32] P. Owrutsky and N. Khaneja, "Control of inhomogeneous ensembles in the presence of a random periodic drift," 2012.

[33] Y. Ke, D. G. Schupp, and M. Garwood, "Adiabatic dante sequences for b1-insensitive narrowband inversion," *Journal of Magnetic Resonance*, vol. 96, pp. 663–669, 1992.

[34] N. Tsekos, M. Garwood, H. Merkle, Y. Xu, N. Wilke, and K. Ugurbil, "Myocardial tagging with b1 insensitive adiabatic dante inversion sequences," *Magnetic Resonance in Medicine*, vol. 34, pp. 395–401, 1995.

[35] E. V. Veenendaal, B. H. Meier, and M. Kentgens, "Frequency stepped adiabatic passage excitation of half-integer quadrupolar spin systems," *Molecular Physics*, vol. 93, pp. 195–213, 1998.

Appendix A

Fourier Proof

We want to show

$$\exp(\alpha\Omega_x)\exp(\beta\Omega_y)\exp(-\alpha\Omega_x) = \exp(\beta(\cos(\alpha)\Omega_y + \sin(\alpha)\Omega_z)) \tag{A.1}$$

using the Baker-Campbell-Hausdorff identity

$$e^X Y e^{-X} = Y + [X,Y] + \frac{1}{2!}[X,[X,Y]] + ... + \frac{1}{n!}\underbrace{[X,[X,...,[X}_{n\ times},Y]]...] \tag{A.2}$$

We note the following

$$\begin{aligned} e^{\beta\Omega_y} &= \sum_{i=0}^{\infty}\frac{(\beta\Omega_y)^i}{i!} \\ e^{\alpha\Omega_x}\Omega_y e^{-\alpha\Omega_x} &= \cos(\alpha)\Omega_y + \sin(\alpha)\Omega_z \end{aligned}$$

so that

$$\begin{aligned}
\exp(\alpha\Omega_x)\exp(\beta\Omega_y)\exp(-\alpha\Omega_x) &= \exp(\alpha\Omega_x)\sum_{i=0}^{\infty}\frac{(\beta\Omega_y)^i}{i!}\exp(-\alpha\Omega_x) \\
&= \sum_{i=0}^{\infty}\exp(\alpha\Omega_x)\frac{(\beta\Omega_y)^i}{i!}\exp(-\alpha\Omega_x) \\
&= \sum_{i=0}^{\infty}\frac{\beta^i}{i!}\underbrace{e^{\alpha\Omega_x}\Omega_y e^{-\alpha\Omega_x}e^{\alpha\Omega_x}\Omega_y\ldots e^{\alpha\Omega_x}\Omega_y e^{-\alpha\Omega_x}}_{n\ times} \\
&= \sum_{i=0}^{\infty}\frac{\beta^i}{i!}(\cos(\alpha)\Omega_y+\sin(\alpha)\Omega_z)^i \\
&= e^{\beta(\cos(\alpha)\Omega_y+\sin(\alpha)\Omega_z)}
\end{aligned}$$

Appendix B

Chap 1 Pulse Parameters

Heuristic FSM, n=2

$$\alpha = [187.3, 33.8]$$

$$\gamma = [49.3, 196.5]$$

$$Pulse: \quad [(49.3)_0(4.5)_{90}(98.5)_{180}(4.5)_{90}(49.3)_0]^{\times 21}[(196.5)_0(4.2)_{90}(393.0)_{180}(4.2)_{90}(196.5)_0]^{\times 4}$$

Heuristic FSM, n=3

$$\alpha = [201.1, 49.2, 7.3]$$

$$\gamma = [49.3, 196.5, 369.0]$$

$$Pulse: \quad [(49.3)_0(4.4)_{90}(98.5)_{180}(4.4)_{90}(49.3)_0]^{\times 23}$$
$$[(196.5)_0(4.1)_{90}(393.0)_{180}(4.1)_{90}(196.5)_0]^{\times 6}[(369.0)_0(3.6)_{90}(738.0)_{180}(3.6)_{90}(369.0)_0]^{\times 1}$$

Heuristic FSM, n=4

$$\alpha = [175.2903, 18.3977, -10.8059, -5.67454]$$

$$\gamma = [49.3, 196.5, 369.0, 546.0]$$

$$Pulse: \quad [(49.3)_0(4.4)_{90}(98.5)_{180}(4.4)_{90}(49.3)_0]^{\times 20}[(196.5)_0(3.1)_{90}(393.0)_{180}(3.1)_{90}(196.5)_0]^{\times 3}$$
$$[(369.0)_0(-2.7)_{90}(738.0)_{180}(-2.7)_{90}(369.0)_0]^{\times 2}[(546.0)_0(-2.8)_{90}(1092.1)_{180}(-2.8)_{90}(546.0)_0]^{\times 1}$$

Heuristic δ Mod, n=2

$$\begin{aligned} \alpha &= [105.5, 16.7] \\ \gamma &= [90, 270] \\ Pulse: &\quad [(90.0)_0(180.0)_{175.6}(90.0)_0]^{\times 12}[(270.0)_0(540.0)_{175.8}(270.0)_0]^{\times 2} \end{aligned}$$

Heuristic δ Mod, n=3

$$\begin{aligned} \alpha &= [108.3, 22.4, 4.3] \\ \gamma &= [90, 270, 450] \\ Pulse: &\quad [(90.0)_0(180.0)_{175.8}(90.0)_0]^{\times 13}[(270.0)_0(540.0)_{176.3}(270.0)_0]^{\times 3}[(450.0)_0(900.0)_{177.9}(450.0)_0]^{\times 1} \end{aligned}$$

Heuristic δ Mod, n=4

$$\begin{aligned} \alpha &= [109.8, 25.7, 7.1, 1.2] \\ \gamma &= [90, 270, 450, 630] \\ Pulse: &\quad [(90.0)_0(180.0)_{175.8}(90.0)_0]^{\times 13}[(270.0)_0(540.0)_{175.7}(270.0)_0]^{\times 3} \\ &\qquad [(450.0)_0(900.0)_{176.4}(450.0)_0]^{\times 1}[(630.0)_0(1260.0)_{179.4}(630.0)_0]^{\times 1} \end{aligned}$$

Greedy FSM, n=2

$$\alpha = [191.9, 35.9]$$

$$\gamma = [49.9, 192.7]$$

$$Pulse: \quad [(49.9)_0(4.4)_{90}(99.9)_{180}(4.4)_{90}(49.9)_0]^{\times 22}[(192.7)_0(4.5)_{90}(385.4)_{180}(4.5)_{90}(192.7)_0]^{\times 4}$$

Greedy FSM, n=3

$$\alpha = [197.4, 40.9, -3.8]$$

$$\gamma = [49.9, 192.7, 502.9]$$

$$Pulse: \quad [(49.9)_0(4.5)_{90}(99.9)_{180}(4.5)_{90}(49.9)_0]^{\times 22}[(192.7)_0(4.1)_{90}(385.4)_{180}(4.1)_{90}(192.7)_0]^{\times 5}$$
$$[(502.9)_0(-1.9)_{90}(1005.8)_{180}(-1.9)_{90}(502.9)_0]^{\times 1}$$

Greedy FSM, n=4

$$\alpha = [200.7, 43.7, -5.9, -1.9]$$

$$\gamma = [49.9, 192.7, 502.9, 666.8]$$

$$Pulse: \quad [(49.9)_0(4.4)_{90}(99.9)_{180}(4.4)_{90}(49.9)_0]^{\times 23}[(192.7)_0(4.4)_{90}(385.4)_{180}(4.4)_{90}(192.7)_0]^{\times 5}$$
$$[(502.9)_0(-3.0)_{90}(1005.8)_{180}(-3.0)_{90}(502.9)_0]^{\times 1}[(666.8)_0(-0.9)_{90}(1333.7)_{180}(-0.9)_{90}(666.8)_0]^{\times 1}$$

Greedy δ Mod, n=2

$$\begin{aligned} \alpha &= [105.5, 16.6] \\ \gamma &= [86.7, 259.1] \\ Pulse: &\quad [(86.7)_0(173.4)_{175.6}(86.7)_0]^{\times 12}[(259.1)_0(518.1)_{175.8}(259.1)_0]^{\times 2} \end{aligned}$$

Greedy δ Mod, n=3

$$\begin{aligned} \alpha &= [108.2, 22.2, 4.1] \\ \gamma &= [86.7, 259.1, 427.8] \\ Pulse: &\quad [(86.7)_0(173.4)_{175.8}(86.7)_0]^{\times 13}[(259.1)_0(518.1)_{176.3}(259.1)_0]^{\times 3}[(427.8)_0(855.7)_{177.9}(427.8)_0]^{\times 1} \end{aligned}$$

Greedy δ Mod, n=4

$$\begin{aligned} \alpha &= [108.5, 22.9, 4.6, -.3] \\ \gamma &= [86.7, 259.1, 427.8, 730.2] \\ Pulse: &\quad [(86.7)_0(173.4)_{175.8}(86.7)_0]^{\times 13}[(259.1)_0(518.1)_{176.2}(259.1)_0]^{\times 3} \\ &\qquad [(427.8)_0(855.7)_{177.7}(427.8)_0]^{\times 1}[(730.2)_0(1460.5)_{180.2}(730.2)_0]^{\times 1} \end{aligned}$$

Gradient Descent FSM, n=2

$$\alpha = [163.4, -15.7]$$

$$\gamma = [51.5, 373.7]$$

$$Pulse: \quad [(51.5)_0(4.3)_{90}(103.0)_{180}(4.3)_{90}(51.5)_0]^{\times 19}[(373.7)_0(-3.9)_{90}(747.4)_{180}(-3.9)_{90}(373.7)_0]^{\times 2}$$

Gradient Descent FSM, n=3

$$\alpha = [169.6, -23.9, -10.3]$$

$$\gamma = [52.4, 379.1, 550.3]$$

$$Pulse: \quad [(52.4)_0(4.5)_{90}(104.9)_{180}(4.5)_{90}(52.4)_0]^{\times 19}[(379.1)_0(-4.0)_{90}(758.2)_{180}(-4.0)_{90}(379.1)_0]^{\times 3}$$
$$[(550.3)_0(-2.6)_{90}(1100.6)_{180}(-2.6)_{90}(550.3)_0]^{\times 2}$$

Gradient Descent FSM, n=4

$$\alpha = [174.4, -30.6, -19.0, -5.1]$$

$$\gamma = [53.1, 381.4, 554.0, 727.9]$$

$$Pulse: \quad [(53.1)_0(4.4)_{90}(106.1)_{180}(4.4)_{90}(53.1)_0]^{\times 20}[(381.4)_0(-3.8)_{90}(762.7)_{180}(-3.8)_{90}(381.4)_0]^{\times 4}$$
$$[(554.0)_0(-3.2)_{90}(1108.0)_{180}(-3.2)_{90}(554.0)_0]^{\times 3}[(727.9)_0(-2.6)_{90}(1455.8)_{180}(-2.6)_{90}(727.9)_0]^{\times 1}$$

Gradient Descent δ Mod, n=2

$$\begin{aligned} \alpha &= [105.5, 16.6] \\ \gamma &= [88.6, 265.1] \\ Pulse: &\quad [(88.6)_0(177.1)_{175.6}(88.6)_0]^{\times 12}[(265.1)_0(530.1)_{175.9}(265.1)_0]^{\times 2} \end{aligned}$$

Gradient Descent δ Mod, n=3

$$\begin{aligned} \alpha &= [108.3, 22.4, 4.3] \\ \gamma &= [89.1, 267.0, 444.5] \\ Pulse: &\quad [(89.1)_0(178.1)_{175.8}(89.1)_0]^{\times 13}[(267.0)_0(534.1)_{176.3}(267.0)_0]^{\times 3}[(444.5)_0(889.0)_{177.9}(444.5)_0]^{\times 1} \end{aligned}$$

Gradient Descent δ Mod, n=4

$$\begin{aligned} \alpha &= [109.8, 25.7, 7.1, 1.2] \\ \gamma &= [90.0, 270.0, 450.0, 630] \\ Pulse: &\quad [(90.0)_0(180.0)_{175.8}(90.0)_0]^{\times 13}[(270.0)_0(540.0)_{175.7}(270.0)_0]^{\times 3} \\ &\quad\quad [(450.0)_0(900.0)_{176.4}(450.0)_0]^{\times 1}[(630.0)_0(1260.0)_{179.4}(630.0)_0]^{\times 1} \end{aligned}$$

Appendix C

Full MAS Hamiltonian in Chap 2

For ease of presentation a somewhat simplified model was presented in chapter 2 for the dynamics resulting from chemical shift due to Magic Angle Spinning (MAS). The complete drift Hamiltonian is actually

$$\begin{aligned} H(t) &= [w + A_1\cos(w_r t + \gamma) + B_1\cos(w_r t + \gamma) \\ &\quad + A_2\cos(2w_r t + 2\gamma) + B_2\sin(2w_r t + 2\gamma)]\Omega_z \end{aligned}$$

which we will now explicitly show can be made robust against aliasing in an analogous manner. Building on the idea from the paper we define the operator

$$\begin{aligned} I^*_{t_p}\{f(t)\} &= \int_0^{t_p} f(t)dt - \int_{t_p}^{\frac{\pi}{2w_r}} f(t)dt \\ &\quad + \int_{\frac{\pi}{2w_r}}^{\frac{\pi}{2w_r}+t_p} f(t)dt - \int_{\frac{\pi}{2w_r}+t_p}^{\frac{\pi}{w_r}} f(t)dt \\ &\quad + \int_{\frac{\pi}{w_r}}^{\frac{\pi}{w_r}+t_p} f(t)dt - \int_{\frac{\pi}{w_r}+t_p}^{\frac{3\pi}{2w_r}} f(t)dt \\ &\quad + \int_{\frac{3\pi}{2w_r}}^{\frac{3\pi}{2w_r}+t_p} f(t)dt - \int_{\frac{3\pi}{2w_r}+t_p}^{\frac{2\pi}{w_r}} f(t)dt \end{aligned}$$

and note that

$$I^*_{t_p}\{H(t)\} = w\,(8t_p - \tau_r)$$

where $\tau_r = \frac{2\pi}{w_r}$ is the rotor period. From the methods presented in section III, It is clear that by appropriate selection of t_p any amount of aliasing can be suppressed in the complete description as well.

Appendix D

Piecewise Constant E_2 Bound

We calculate the 3rd order term in E_2 used in the proof of theorem 4.5.1. Recalling the definitions

$$\phi_k = \omega_0 t_k + a t_k^2/2 \qquad \omega_k = \omega_0 + a t_k$$

we calculate E_2 as follows

$$\begin{aligned}
E_2 &= \Big| \int_{t_k}^{t_{k+1}} (\omega\Omega_z + u_0 \cos\phi(t)\Omega_x + \sin\phi(t)\Omega_y) \\
&\qquad \int_{t_k}^{t} (\omega\Omega_z + u_0 \cos\phi(\tau)\Omega_x + \sin\phi(\tau)\Omega_y) d\tau dt \\
&\qquad\qquad - \frac{(\omega\Omega_z + u_k\Omega_x\Delta t + v_k\Omega_y\Delta t)^2}{2} \Big| \\
&= \Big| \int_0^{\Delta t} (\omega\Omega_z + u_0 \cos(\phi_k + w_k t + a t^2/2)\Omega_x + u_0 \sin(\phi_k + w_k t + a t^2/2)\Omega_y) \\
&\qquad \times \int_0^{t} (\omega\Omega_z + u_0 \cos(\phi_k + w_k\tau + a\tau^2/2)\Omega_x + u_0 \sin(\phi_k + w_k\tau + a\tau^2/2)\Omega_y) d\tau dt \\
&\qquad - \frac{(\omega\Omega_z + u_k\Omega_x\Delta t + v_k\Omega_y\Delta t)^2}{2} \Big|
\end{aligned}$$

$$
\begin{aligned}
E_2 &= \Big| \int_0^{\Delta t} (\omega\Omega_z + u_0 \cos\phi_k \Omega_x + u_0 \sin\phi_k + u_0\omega_k(\cos\phi_k\Omega_y - \sin\phi_k\Omega_x)t \\
&\quad + \frac{1}{2}(u_0((\omega_k^2\Omega_x - a\Omega_y)\cos\phi_k + (a\Omega_x + \omega_k^2\Omega_y)\sin(\phi_k))t^2) \\
&\quad \times \int_0^t (\omega\Omega_z + u_0\cos\phi_k\Omega_x + u_0\sin\phi_k + u_0\omega_k(\cos\phi_k\Omega_y - \sin\phi_k\Omega_x)\tau)d\tau dt \\
&\quad - \frac{(\omega\Omega_z + u_k\Omega_x\Delta t + v_k\Omega_y\Delta t)^2}{2}\Big| + O(\Delta t^4) \\
&= \Big| \int_0^{\Delta t} (\omega\Omega_z + u_0 \cos\phi_k \Omega_x + u_0 \sin\phi_k + u_0\omega_k(\cos\phi_k\Omega_y - \sin\phi_k\Omega_x)t \\
&\quad + \frac{1}{2}(u_0((\omega_k^2\Omega_x - a\Omega_y)\cos\phi_k + (a\Omega_x + \omega_k^2\Omega_y)\sin(\phi_k))t^2) \\
&\quad \times \frac{1}{2}t(2\omega\Omega_z + u_0(2\Omega_x + t\omega_k\Omega_y)\cos\phi_k + u_0(2\Omega_y - t\omega_k\Omega_x)\sin\phi_k)dt \\
&\quad - \frac{(\omega\Omega_z + u_k\Omega_x\Delta t + v_k\Omega_y\Delta t)^2}{2}\Big| + O(\Delta t^4) \\
&= \Big| \int_0^{\Delta t} \frac{1}{4}t(2\omega\Omega_z + u_0(2\Omega_x + t\omega_k\Omega_y)\cos\phi_k + u_0(-t\omega_k\Omega_x + 2\Omega_y)\sin\phi_k) \\
&\quad \times (2\Omega_z + u_0((2 - t^2\omega_k^2)\Omega_x + t(at + 2\omega_k)\Omega_y)\cos\phi_k \\
&\qquad - u(-2\Omega_y + t(at\Omega_x + 2\omega_k\Omega_x + t\omega_k^2\Omega_y))\sin\phi_k)dt \\
&\quad - \frac{(\omega\Omega_z + u_k\Omega_x\Delta t + v_k\Omega_y\Delta t)^2}{2}\Big| + O(\Delta t^4) \\
&= \Big|\frac{1}{2}(\omega\Omega_z + u_0\cos\phi_k\Omega_x + u_0\sin\phi_k\Omega_y)^2\Delta t^2 \\
&\quad + \frac{1}{2}u_0\omega_k(\cos\phi_k\Omega_y - \sin\phi_k\Omega_x)(\omega\Omega_z + u_0\cos\phi_k\Omega_x + u_0\sin\phi_k\Omega_y)\Delta t^3 \\
&\quad - \frac{(\omega\Omega_z + u_k\Omega_x\Delta t + v_k\Omega_y\Delta t)^2}{2}\Big| + O(\Delta t^4) \\
&\leq u_0(u_0 + \omega)\omega_k O(\Delta t^3) \\
&\leq u_0 B^2 O(\Delta t^3)
\end{aligned}
$$

where the last follows from the adiabatic regime $\frac{u_0}{B} << 1$ and $\omega, \omega_k \leq B$.

Appendix E

Robust RF Pulse Generation Code

readme.rtf

Control of Inhomogeneous Ensembles on the Bloch Sphere
Code Repository for generating robust pulses
Philip Owrutsky
7/1/12

Generates controls using either known frequencies or using gradient descent to determine optimal frequencies.

To generate a pulse given known frequencies use the command

heuristicCont(nTerms,eL,eU,Basis,Freq,ampThresh)

where:
nTerms is the number of terms in the expansion
eL is the lower limit on epsilon, the dispersion in the controls
eH is the upper limit on epsilon, the dispersion in the controls
Basis set to 'Cos' for FSM and 'Sin' for delta modulation
Freq is the vector of frequencies for the controls in Degrees
ampThresh is a maximum amplitude threshold for the controls in degrees

For example:

heuristicCont(2,.5,1.5,'Sin',[90,270],9)

will generate a 2 term delta modulated controls with frequencies 90 and 270 for the range epsilon [.5,1.5]

To generate a pulse using gradient descent use the command

gradDescentCont(nTerms,eL,eU,Basis,k0,ampThresh)

where:
nTerms is the number of terms in the expansion
eL is the lower limit on epsilon, the dispersion in the controls
eH is the upper limit on epsilon, the dispersion in the controls
Basis set to 'Cos' for FSM and 'Sin' for delta modulation
k0 is a starting location for the frequencies for gradient descent in Degrees
ampThresh is a maximum amplitude threshold for the controls in degrees

For Example:

gradDescentCont(2,.5,1.5,'Sin',[90,270],9)

will generate a 2 term delta modulated control with frequencies obtained through gradient descent. Note that for nTerms>3 computation time can take a few moments.

```
function[] = heuristicCont(nTerms,eL,eU,Basis,Freq,ampThresh)
%Generates Robust Pi/2 Controls in the presence of multiplicative
%inhomogeneity given heuristically selected pulse frequencies
%
%Inputs:
%
%nTerms in the number of terms in Fourier Expansion
%eL is the lower limit on epsilon the dispersion in the Controls
%eU is the upper limit on epislon the dispersion in the controls
%Basis 'Cos' for FSM and 'Sin' for Δ modulation
%Freq is the vector of frequencies for the controls in Degrees
%ampThresh is a maximum amplitude threshold for controls
%
%
%Returns:
%Empty
%
%Philip Owrutsky
%6/1/12


%Set ampThresh to default 9 degrees (pi/20) if not input
if nargin<6
    ampThresh = 9;
end

%Convert Frequencies from Degrees to Radians
```

```
28 Freq = Freq*pi/180;
29
30 %Calculate Pulse Parameters
31 Amp = AmpFromFreq(nTerms,Freq,eL,eU,Basis);
32
33 %Calculate Resulting Fit Error
34 E = L2ErrorFit(Amp,Freq,eL,eU,Basis);
35
36 %Display Sequence and Plot
37 pulse2String(Amp,Freq,E,eL,eU,Basis,ampThresh);
```

```
function[] = gradDescentCont(nTerms,eL,eU,Basis,k0,ampThresh)
%Generates Robust Pi/2 Controls in the Presence of Multiplicative
%inhomogeneity
%
%Inputs:
%nTerms in the number of terms in Fourier Expansion
%eL is the lower limit on epsilon the dispersion in the Controls
%eU is the upper limit on epislon the dispersion in the controls
%Basis 'Cos' for FSM and 'Sin' for Δ modulation
%k0 (optional) is a starting location for the frequncies for gradient
%descent in degrees
%ampThresh is a maximum amplitude threshold for controls
%
%
%Returns:
%Empty
%
%Philip Owrutsky
%6/1/12


%Set ampThresh to default 9 degrees (pi/20) if not input
if nargin<6
    ampThresh = 9;
end

%Set default Starting point for gradient Descent if not input
```

```
28 if nargin<5
29     k0 = pi/2*(1:2:2*nTerms);
30 else
31     k0 = k0*pi/180;  %Convert from degrees to radians
32 end
33
34
35 %Calculate Pulse Parameters
36 [Freq,Amp,E] = calcControlsDescentHelper(nTerms,eL,eU,Basis,k0);
37
38 %Display Sequence and Plot
39 pulse2String(Amp,Freq,E,eL,eU,Basis,ampThresh);
```

```
function[kVec,BVec,E] = calcControlsFourier(nTerms,eL,eU,Basis,k0)
%Generates Pulse Amplitudes and Frequencies for Fourier Synthesis ...
    Method and Delta Modulation using Gradient Descent
%
%Inputs:
%nTerms in the number of terms in Fourier Expansion
%eL is the lower limit on epsilon the dispersion in the Controls
%eU is the upper limit on epislon the dispersion in the controls
%Basis 'Cos' for FSM and 'Sin' for Δ modulation
%k0 (optional) is a starting location for the frequncies for gradient
%descent in radians
%
%Returns:
%kVec the frequency components of the Pulse
%BVec the amplitude components of the Pulse
%E the L2 Error in the Expansion
%
%Philip Owrutsky
%6/1/12


%If k0 is not provided use a default value
if nargin<5
    k0 = pi/2*(1:2:2*nTerms);
end


```

```
27 %Construct L2 Error function of fit to be used as objective function
28 f=@(kVec)FourierError(nTerms,kVec,eL,eU,Basis);
29
30 %Reduce error tolerances in gradient descent method
31 opt = optimset('TolX',1e-10,'MaxIter',1e3,...
32     'MaxFunEval',1e3,'LargeScale','Off');
33
34 %Calculate Optimal Frequencies Using Gradient Descent through Matlabs
35 %fminunc Function
36 kVec=fminunc(f,k0,opt);
37
38 %Calculate Corresponding Optimal Pulse Amplitudes
39 BVec = AmpFromFreq(nTerms,kVec,eL,eU,Basis);
40
41 %Calculate Resulting Fit Error
42 E = L2ErrorFit(BVec,kVec,eL,eU,Basis);
```

```
function[B] = AmpFromFreq(nTerms,kVec,eL,eU,Basis)
%Calculates Amplitutes from Frequncies
%
%Inputs:
%nTerms is the number of terms in the expansion
%kVec is a vector of frequencies in radians
%eL is the lower limit on epsilon the dispersion in the Controls
%eU is the upper limit on epislon the dispersion in the controls
%Basis 'Cos' for FSM and 'Sin' for Δ modulation
%
%Returns:
%B a vector of amplitude coefficients
%
%Philip Owrutsky
%6/1/12

%Calculate Matrix of Inner Products
[Phi,V] = Phi_Four(nTerms,kVec,eL,eU,Basis);

%Invert to Solve for Amplitudes
B = Phi\V;
```

```
function[f] = calcTargetf(Basis)
%Calculate Target Function for a pi/2 robust pulse

if(strcmp(Basis,'Sin'))
            f = @(e)pi/2;
elseif(strcmp(Basis,'Cos'))
            f = @(e)pi./(2*e);
else
            error('Not a Valid Basis');
end
```

```
function[f]=calcFit(BVec,kVec,Basis)
%Constructs expansion function
%
%Inputs:
%BVec a vector of amplitudes
%kVec a vector of frequencies in radians
%eL is the lower limit on epsilon the dispersion in the Controls
%eU is the upper limit on epislon the dispersion in the controls
%Basis 'Cos' for FSM and 'Sin' for ∆ modulation
%
%Returns:
%f the expansion as a function of epsilon (e)
%
%Philip Owrutsky
%6/1/12


%Initialize f
f = @(e)0;

%Loop through Amplitude Frequency Pairs Constructing expansion
for i=1:length(BVec)

    if strcmp(Basis,'Sin')
        %Delta Modulation
        f = @(e)(f(e)+BVec(i)*sin(kVec(i).*e));
    else
```

```
28          %Fourier Synthesis
29          f = @(e)(f(e)+BVec(i)*cos(kVec(i).*e));
30      end
31  end
```

```
function[BVec,kVec] = dilateCont(BVec0,kVec0,ampThresh)
%Reduces maximum flip angle to ampThresh by repeating elements ...
    with smaller
%amplitudes
%
%Inputs:
%BVec0 is a vector of amplitudes
%kVec0 is corresponding vector of frequencies
%ampThresh (optional) is a threshold value for the amplitudes in ...
    radians
%
%Returns:
%BVec the new amplitudes
%kVec the new frequencies
%
%Philip Owrutsky
%6/1/12


%Set ampThresh to default pi/20 if not input
if nargin<3
    ampThresh = pi/20;
end

%Check that Input Vectors are the Same Length
if length(BVec0) ~= length(kVec0)
    error('Amplitude and Frequency Vectors are Not the Same Length');
```

```
26 end
27
28 %Calculate Number of Repetitions for Each Pulse Element
29 nVec = ceil(abs(BVec0)./ampThresh);
30
31 %Preallocate Output Vectors
32 BVec = zeros(sum(nVec),1);
33 kVec = zeros(sum(nVec),1);
34
35 %Calculate map of indices in input vectors to those in outputs
36 cnVec = [0; cumsum(nVec)];
37
38 %Loop through input Amplitude/Frequency elements to calculate outputs
39 for i=1:length(BVec0)
40
41     %Calculate output indices corresponding to input index i
42     in = (cnVec(i)+1):cnVec(i+1);
43
44     %Reduce Amplitude by the number of repetitions and repeat ...
          frequencies
45     %accordingly
46     BVec(in) = BVec0(i)/nVec(i);
47     kVec(in) = kVec0(i)*ones(size(in))';
48
49 end
```

```
function[E] = FourierError(nTerms,kVec,eL,eU,Basis)
%Calculates Error in Expansion
%
%Inputs:
%nTerms is the number of terms in the expansion
%kVec is a vector of frequencies in radians
%eL is the lower limit on epsilon the dispersion in the Controls
%eU is the upper limit on epislon the dispersion in the controls
%Basis 'Cos' for FSM and 'Sin' for Δ modulation
%
%Returns:
%E the L2 Error of the Expansion
%
%Philip Owrutsky
%6/1/12

%Calculate Amplitudes
BVec = AmpFromFreq(nTerms,kVec,eL,eU,Basis);

%Calculate Corresponding L2 Error
E = L2ErrorFit(BVec,kVec,eL,eU,Basis);
```

```
function[E] = L2ErrorFit(BVec,kVec,eL,eU,Basis)
%Calculates L2 Error of fit
%
%Inputs:
%BVec a vector of amplitudes
%kVec a vector of frequencies in radians
%eL is the lower limit on epsilon the dispersion in the Controls
%eU is the upper limit on epislon the dispersion in the controls
%Basis 'Cos' for FSM and 'Sin' for Δ modulation
%
%Returns:
%E the L2 Error in the Expansion
%
%Philip Owrutsky
%6/1/12

%Function of epsilon (e) to evaluate expansion
f = calcFit(BVec,kVec,Basis);

%Target function
target = calcTargetf(Basis);

%L2 Error between expansion and Target
E = sqrt( quad(@(e)((f(e)-target(e)).^2),eL,eU,1e-10) );
```

```
function[Phi,V] = Phi_Four(nTerms,kVec,eL,eU,Basis)
%Calculates Phi matrix and V for control calc

%Calculate Phi and V
f = calcTargetf(Basis);
Phi = zeros(nTerms);
V = zeros(nTerms,1);
for i=1:nTerms
    for j=1:nTerms
        %Calculate f depending on Fourier or Mod Fourier
        if(strcmp(Basis,'Sin'))
            fi = @(e)sin(kVec(i).*e);
            fj = @(e)sin(kVec(j).*e);
        else
            fi = @(e)cos(kVec(i).*e);
            fj = @(e)cos(kVec(j).*e);
        end
        Phi(i,j) = quad(@(e)(fi(e).*fj(e)),eL,eU,1e-10);
    end
    V(i) = quad(@(e)(fi(e).*f(e)),eL,eU,1e-10);
end
```

```
function[] = pulse2String(Amp,Freq,E,eL,eU,Basis,ampThresh)
%Display Pulse and Plot Resulting Magnetization
%
%Inputs:
%Amp vector of control amplitudes
%Freq vector of control frequencies in radians
%E Error returned from control calculation
%eL is the lower limit on epsilon the dispersion in the Controls
%eU is the upper limit on epislon the dispersion in the controls
%Basis 'Cos' for FSM and 'Sin' for Δ modulation
%
%Returns:
%
%Philip Owrutsky
%6/1/12


if nargin<6
    ampThresh = 9;
end

%% Display Pulse Sequence

%Convert to degrees
AmpDeg = Amp*180/pi;
FreqDeg = Freq*180/pi;

```

```
28 fprintf('Generated Pulse is: \n');
29
30 for i=1:length(Amp)
31
32     n = ceil(abs(AmpDeg(i))/ampThresh);
33     A = AmpDeg(i)/n;
34     F = FreqDeg(i);
35
36     if strcmp(Basis,'Sin')
37         %Delta Modulation
38         fprintf('[(%3.1f) %3.1f (%3.1f) %3.1f (%3.1f) %3.1f]^%d  ...
               ',...
39             F,0,2*F,180-A/2,F,0,n);
40     else
41         %Fourier Synthesis
42         fprintf('[(%3.1f) 0 (%3.1f) 90 (%3.1f) 180 (%3.1f) 90 ...
               (%3.1f) 0]^%d  ', ...
43         F,A/2,2*F,A/2,F,n);
44     end
45
46 end
47 fprintf('\n \n');
48
49
50 %% Plot Resulting Magnetization
51
52
```

```
53 eVec = linspace(eL,eU,101);                                %Vector of ...
       Epsilon Values
54 [AmpD,FreqD] = dilateCont(Amp,Freq,ampThresh*pi/180); %Reduce ...
       Large Amplitudes
55 xF = simFour(eVec,AmpD,FreqD,Basis);                       %Simulate ...
       Using Calculated Controls
56
57 %Calculate and Display Error
58 E_L2 = sqrt( sum( sum( (xF-repmat([1;0;0],1,length(eVec)) ).^2 ) ...
       )/length(eVec) );
59 fprintf('L2 Error is %1.4f \n \n',E_L2);
60
61 %Plot
62 figure; set(gca,'FontSize',20);
63 plot(eVec, xF,'LineWidth',5);
64 title('Resulting Magnetization Vs. Epsilon');
65 xlabel('Epsilon (\epsilon)');  ylabel('Magnetization');
66 legend('x','y','z');
67
68
69 %% Calculate and Display Flip Angle
70
71 if strcmp(Basis,'Sin')
72     FA = 4*sum(FreqD);
73 else
74     FA = 4*sum(FreqD) + sum(AmpD);
75 end
76
```

```
77 fprintf('Total Flip Angle in Degrees is: %7.1f \n',FA*180/pi);
```

```
function[xF] = simFour(eVec,BVec,kVec,Basis)
%Simulate Fourier Methods using Matrix Exponentials
%
%Inputs:
%eVec a vector of epsilon values
%BVec a vector of control amplitudes
%kVec a vector of frequencies in radians
%Basis 'Cos' for FSM and 'Sin' for Δ modulation
%
%Returns:
%xF the resulting magnetization (x,y,z)' for each epsilon in eVec
%
%Philip Owrutsky
%6/1/12


%Define Rotation Matrices
Ox = [0 0 0; 0 0 -1; 0 1 0];
Oy = [0 0 1; 0 0 0; -1 0 0];

x0 = [0;0;1];                       %Initial Mag along Z-axis
xF = repmat(x0,1,length(eVec));     %Pre-allocate output vector

%Loop through multilicative dispersions (epsilon)
for i=1:length(eVec)
    e = eVec(i);

```

```
28      %Loop through pulse sequence
29      for j=1:length(BVec)
30          k = kVec(j);  B=BVec(j);
31
32          %Delta Modulation
33          if strcmp(Basis,'Sin')
34              xF(:,i) = expm(-k*e*Ox)*xF(:,i);
35              xF(:,i) = expm(2*k*e*(cos(B/2)*Ox+sin(B/2)*Oy))*xF(:,i);
36              xF(:,i) = expm(-k*e*Ox)*xF(:,i);
37
38          %Fourier Synthesis
39          else
40              xF(:,i) = expm(-k*e*Ox)*expm(B/2*e*Oy)*expm(2*k*e*Ox)*...
41                  expm(B/2*e*Oy)*expm(-k*e*Ox)*xF(:,i);
42          end
43      end
44  end
```